เอกสารอ้างอิง

1. Gerhard Ziegler. Numerical Differential Protection. 2nd. Erlangen : Publicis Corporate Poblishing, 2005.
2. Working Group of GEC T&D Protection & Control. Protective Relay & Application Guide. 3rd. London & Peterborough : Blading + Mansell plc, 1995.
3. W.A. Elmore. Pilot Protective Relaying. 1st. New York-Basel : Marcel Dekker Inc, 2000.
4. Working Group of the IEEE PES Power System Relaying Committee. "Relay performance considerations with low ratio CTs and high fault currents." Power Delivery, IEEE Transactions on. Vol.8 (1993) : 884-897.
5. D.A. Bradley, C.B. Gray and D. O'Kelly. "Transient Compensation of Current Transformers." IEEE Transactions on Power Apparatus and Systems. Vol.PAS-97 (1978) : 1264-1271.
6. B. Kasztenny and D. Finney. "Generator protection and CT-saturation problems and solutions." Industry Applications, IEEE Transactions on. Vol.41 (2005) : 1452-1457.
7. Y.C. Kang, et al. "Development and hardware implementation of a compensating algorithm for the secondary current of current transformers." Electric Power Applications, IEE Proceedings. Vol.143 (1996) : 41-49.
8. Y.C. Kang, et al. "An algorithm for compensating secondary currents of current transformers." Power Delivery, IEEE Transactions on. Vol.12 (1997) : 116-124.
9. Y.C. Kang, et al. "Compensation of the distortion in the secondary current caused by saturation and remanence in a CT." Power Delivery, IEEE Transactions on. Vol.19 (2004) : 1642-1649.
10. Y.C. Kang, U.J. Lim and S.H. Kang. "Compensating algorithm suitable for use with measurement-type current transformers for protection." Generation, Transmission and Distribution, IEE Proceedings. Vol.152 (2005) : 880-890.
11. Y.C. Kang, et al. "Busbar differential protection in conjunction with a current transformer compensating." Generation, Transmission & Distribution, IET. Vol.2 (2008) : 100-109.

12. F. Li, Y. Li and R.K. Aggarwal. "Combined wavelet transform and regression technique for secondary current compensation of current transformer." Generation, Transmission and Distribution, IEE Proceedings. Vol.149 (2002) : 497-503.

13. Z. Lu, J.S. Smith and Q.H. Wu. "Morphological Lifting Scheme for Current Transformer Saturation Detection and Compensation." Circuits and Systems I: Regular Papers, IEEE Transactions on. Vol.55 (2008) : 3349-3357.

14. K.M. El-Naggar and M.I. Gilany. "A discrete dynamic filter for detecting and compensating CT saturation." Electric Power Systems Research. Vol.77 (2007) : 527-533.

15. A. Wiszniewski, W. Rebizant and L. Schiel. "Correction of Current Transformer Transient Performance." Power Delivery, IEEE Transactions on. Vol.23 (2008) : 624-632.

16. K. Erenturk. "ANFIS-Based Compensation Algorithm for Current-Transformer Saturation Effects." Power Delivery, IEEE Transactions on. Vol. 24 (2009) : 195-201.

17. H. Khorashadi-Zadeh and M. Sanaye-Pasand. "Correction of saturated current transformers secondary current using ANNs." Power Delivery, IEEE Transactions on. Vol.21 (2006) : 73-79.

18. N. Locci and C. Muscas. "A digital compensation method for improving current transformer accuracy." Power Delivery, IEEE Transactions on. Vol.15 (2000) : 1104-1109.

19. T. Bunyagul, P. Crossley and P. Gale. "Overcurrent protection using signals derived from saturated measurement CTs." Power Engineering Society Summer Meeting. [n.p. : n.p.], 2001 : (103-108).

20. T. Bunyagul, P.A. Crossley and P. Gale. "Design and evaluation of an overcurrent relay suitable for operation with measurement current transformers." Developments in Power System Protection, 2001. Seventh International Conference on (IEE). [n.p. : n.p.], 2001 : (201-204).

21. F.J. Evans and G. Wells. "Use of a Sampling Scheme to Detect Transient Saturation in Protective Current Transformers." Instrumentation and Measurement, IEEE Transactions on. Vol.19 (1970) : 144-147.

22. Y.C. Kang, S.H. Kang and P.A. Crossley. "Design, evaluation and implementation of a busbar differential protection relay immune to the effects of current transformer saturation." Generation, Transmission and Distribution, IEE Proceedings-. Vol.151 (2004) : 305-312.

23. Y.C. Kang, et al. "Design and evaluation of an algorithm for detecting current transformer saturation." Generation, Transmission and Distribution, IEE Proceedings-. Vol.151 (2004) : 27-35.

24. L. Xiangning, et al. "A series multiresolution morphological gradient-based criterion to identify CT saturation." Power Delivery, IEEE Transactions on. Vol.21 (2006) : 1169-1175.

25. K. Yong-Cheol, O. Seung-Hun and K. Sang-Hee. "A CT saturation detection algorithm." Power Delivery, IEEE Transactions on. Vol.19 (2004) : 78-85.

26. Z. Yongbin and L. Yuping. "The theory of CT saturation detection based on virtual impedance in bus-bar differential protection." Power India Conference. [n.p. : n.p.], 2006.

27. C. Fernandez. "An impedance-based CT saturation detection algorithm for busbar differential protection." Power Delivery, IEEE Transactions on. Vol.16 (2001) : 468-472.

28. W. Rebizant and D. Bejmert. "Current-Transformer Saturation Detection With Genetically Optimized Neural Networks." Power Delivery, IEEE Transactions on. Vol.22 (2007) : 820-827.

29. Ya-lun Chou. Statistical Analysis. 1st. [n.p] : Holt International, 1975.

30. J. Holbach. "Comparison between high impedance and low impedance bus differential protection." Power Systems Conference, 2009. [n.p. : n.p.], 2009 : (1-16).

31. Noppadol Charbkaew, Teratam Bunyagul and Yotaka Chompusri. "Experience on Stray Flux Interference of CT (Case Study of A Power Plant in Thailand)." The IET 9th International Conference on DEVELOPMENT IN POWER SYSTEM PROTECTION. [n.p. : n.p.], 2008.

32. Pflaum, M., et al. "New aspects of the reliability of high voltage circuitbreakers." Cigre' Session Paper Ref.13-07. [n.p. : n.p.], 1997.

33. Fawdrey, CA. "The application of development and diagnostic techniquesto circuit breaker reliability." Cigre' Session Paper Ref. 13-02. [n.p. : n.p.], 1978.

34. Runde, M., et al. "Acoustic diagnosis of high voltage circuit-breakers." Power Delivery, IEEE Transactions on. Vol.7 (1992) : 1306-1315.

35. Demjanenko, V., et al. "A noninvasive diagnostic instrument for power circuit breakers." Power Delivery, IEEE Transactions on. Vol.7 (1992) : 656-663.

36. Goto K., et al. "On-line monitoring and diagnostics of gas circuit breakers." Power Delivery, IEEE Transactions on. Vol.4 (1989) : 375-381.

37. Hess DP, et al. "Noninvasive condition assessment and event timing for power circuit breakers." Power Delivery, IEEE Transactions on. Vol.7 (1992) : 353-360.

38. Lai ML, et al. "Mechanical failure detection of circuit breakers." PowerDelivery,IEEE Transactions on. Vol.3 (1988) : 1724-1731.

39. Landry, M., et al. "An Improved Vibration Analysis Algorithm as a Diagnostic Tool for Detecting Mechanical Anomalies on Power Circuit Breakers." Power Delivery, IEEE Transactions on. Vol.23 (2008) : 1986-1994.

40. Lee DSS, et al. "New fault diagnosis of circuit breakers." Power Delivery, IEEE Transactions on. Vol.18 (2003) : 454-459.

41. Ohshita, Y., et al. "A diagnostic technique to detect abnormal conditionsof contacts measuring vibrations in metal enclosures of gas insulated switchgear." Power Delivery, IEEE Transactions on. Vol.4 (1989) : 2090-2094.

42. Runde, M., et al. "Vibration analysis for diagnostic testing of circuit-breakers." Power Delivery, IEEE Transactions on. Vol.11 (1996) : 1816-1823.

ภาคผนวก ก

ผลการทดสอบของอัลกอริธึมโดยใช้สัญญาณกระแสจากเครื่องกำเนิดไฟฟ้า ในกรณีที่ความผิดพร่องไม่ได้เกิดขึ้นแต่สัญญาณกระแสมีความผิดเพี้ยน

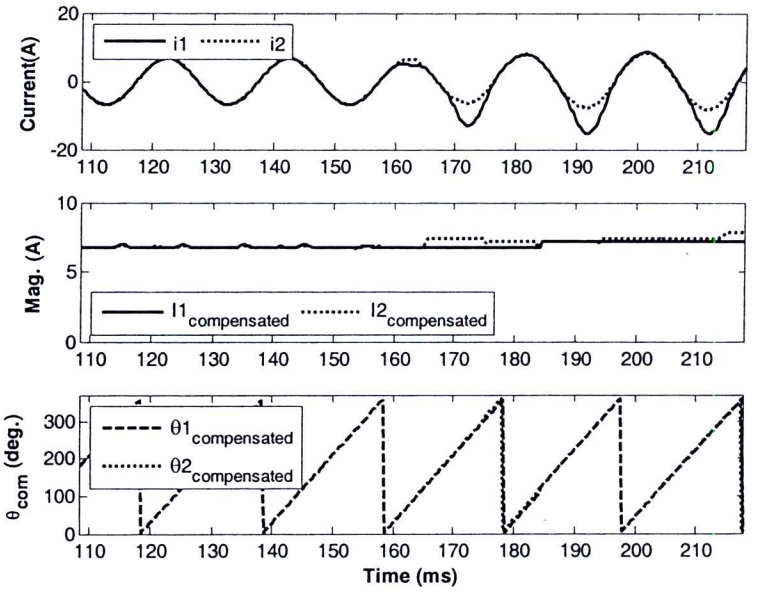

ภาพที่ ก-1 ผลการคำนวณค่าขนาดและมุมในกรณีที่ใช้สัญญาณทดสอบหมายเลข 1

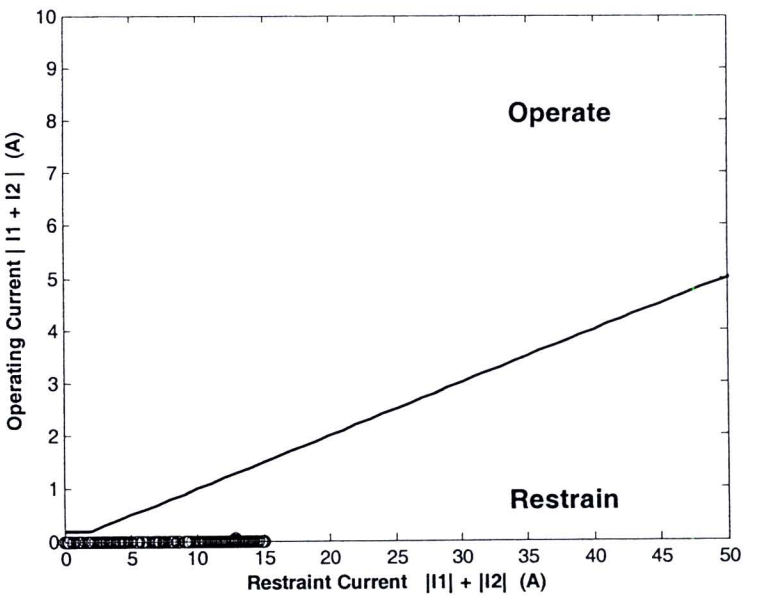

ภาพที่ ก-2 การตัดสินใจของรีเลย์ผลต่างในกรณีที่ใช้สัญญาณทดสอบหมายเลข 1

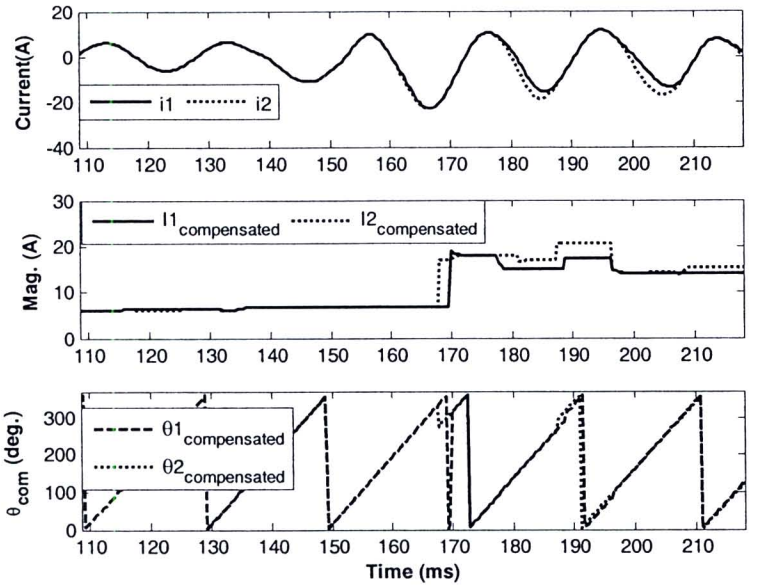

ภาพที่ ก-3 ผลการคำนวณค่าขนาดและมุมในกรณีที่ใช้สัญญาณทดสอบหมายเลข 2

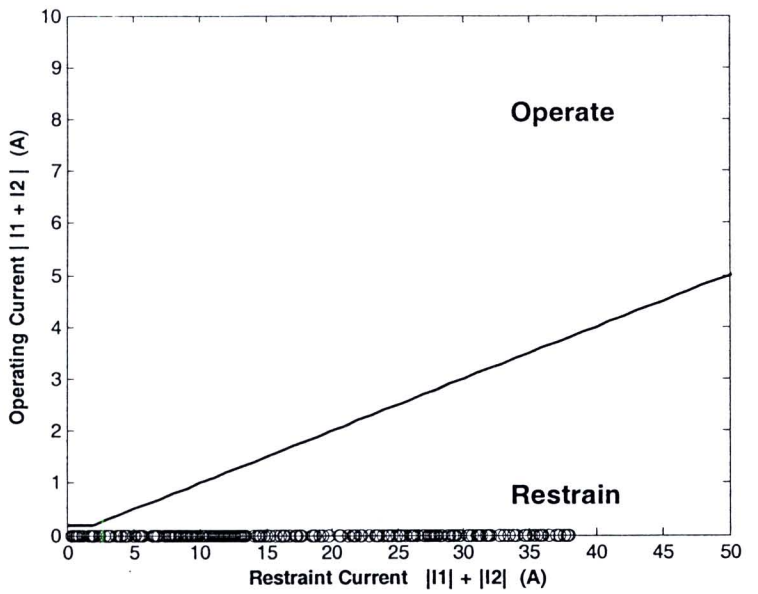

ภาพที่ ก-4 การตัดสินใจของรีเลย์ผลต่างในกรณีที่ใช้สัญญาณทดสอบหมายเลข 2

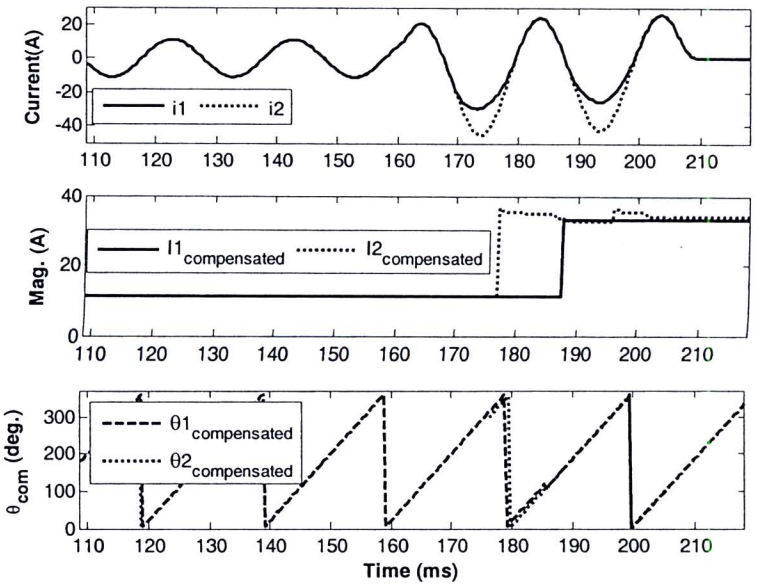

ภาพที่ ก-5 ผลการคำนวณค่าขนาดและมุมในกรณีที่ใช้สัญญาณทดสอบหมายเลข 3

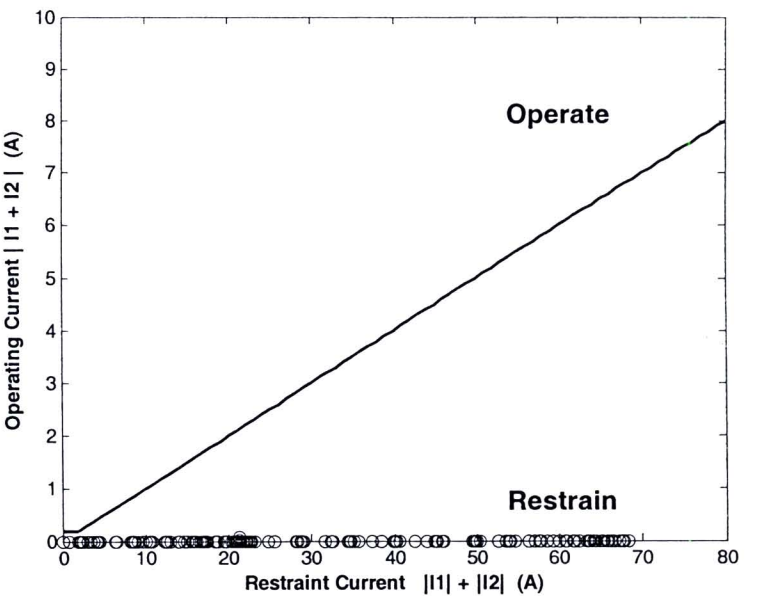

ภาพที่ ก-6 การตัดสินใจของรีเลย์ผลต่างในกรณีที่ใช้สัญญาณทดสอบหมายเลข 3

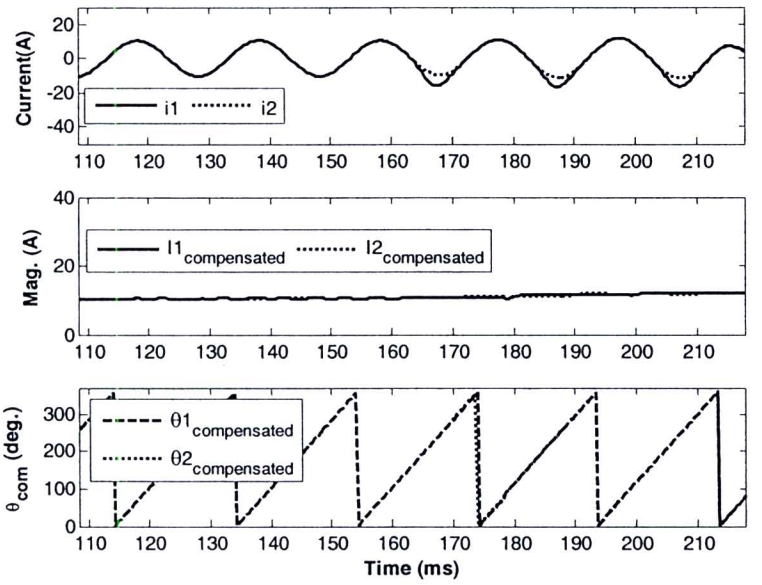

ภาพที่ ก-7 ผลการคำนวณค่าขนาดและมุมในกรณีที่ใช้สัญญาณทดสอบหมายเลข 4

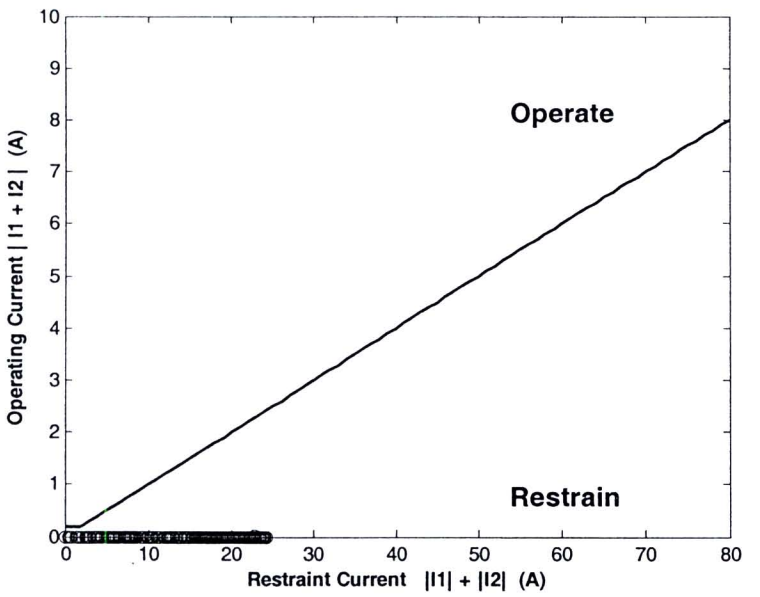

ภาพที่ ก-8 การตัดสินใจของรีเลย์ผลต่างในกรณีที่ใช้สัญญาณทดสอบหมายเลข 4

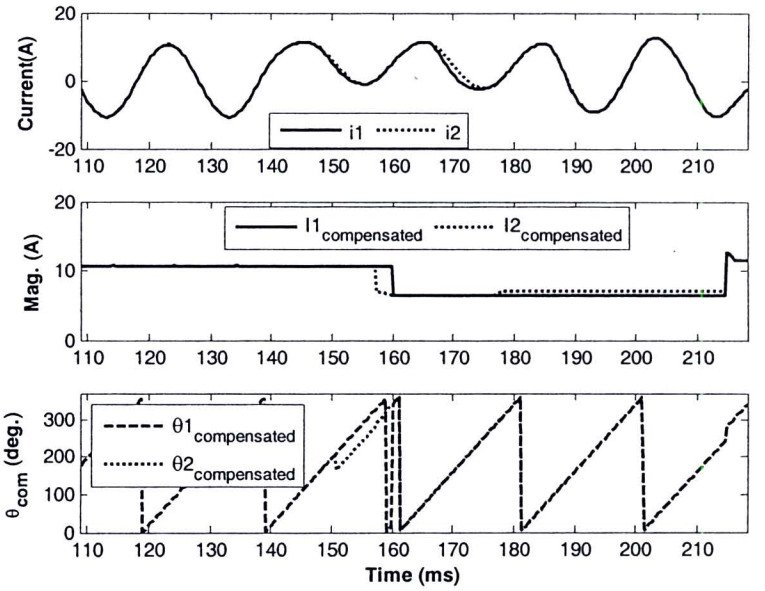

ภาพที่ ก-9 ผลการคำนวณค่าขนาดและมุมในกรณีที่ใช้สัญญาณทดสอบหมายเลข 5

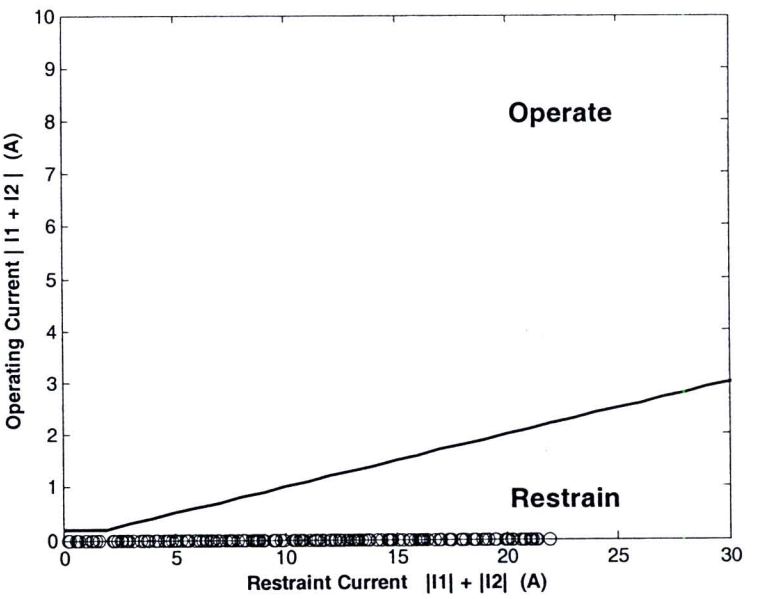

ภาพที่ ก-10 การตัดสินใจของรีเลย์ผลต่างในกรณีที่ใช้สัญญาณทดสอบหมายเลข 5

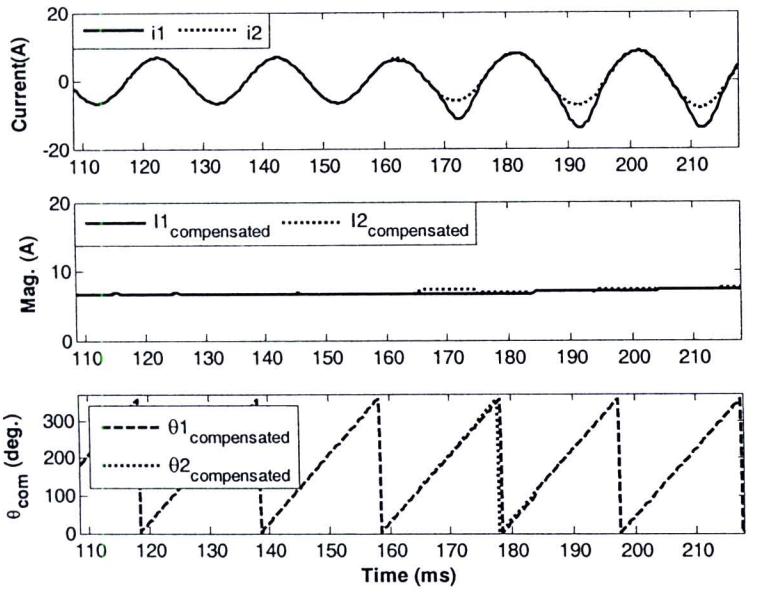

ภาพที่ ก-11 ผลการคำนวณค่าขนาดและมุมในกรณีที่ใช้สัญญาณทดสอบหมายเลข 6

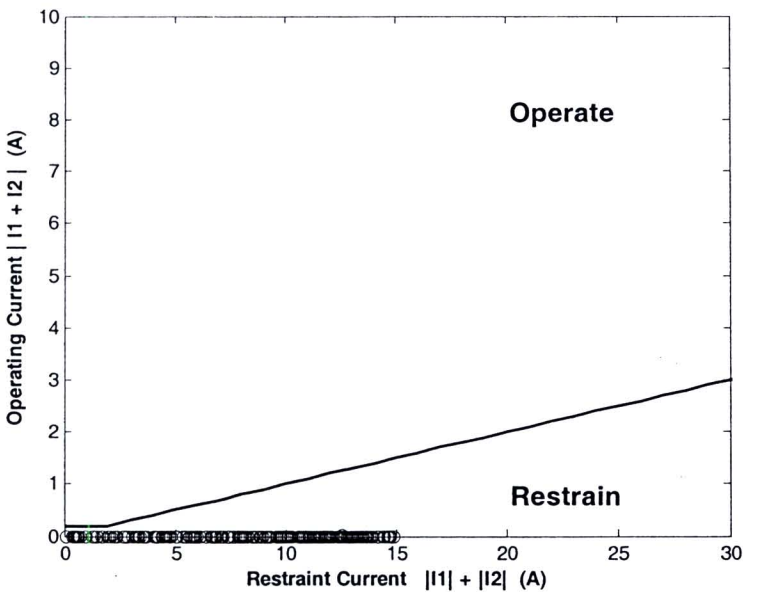

ภาพที่ ก-12 การตัดสินใจของรีเลย์ผลต่างในกรณีที่ใช้สัญญาณทดสอบหมายเลข 6

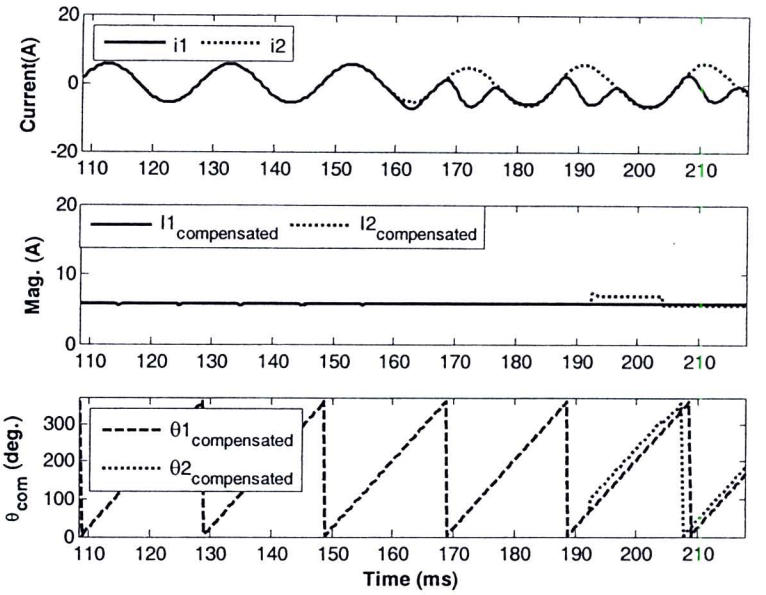

ภาพที่ ก-13 ผลการคำนวณค่าขนาดและมุมในกรณีที่ใช้สัญญาณทดสอบหมายเลข 7

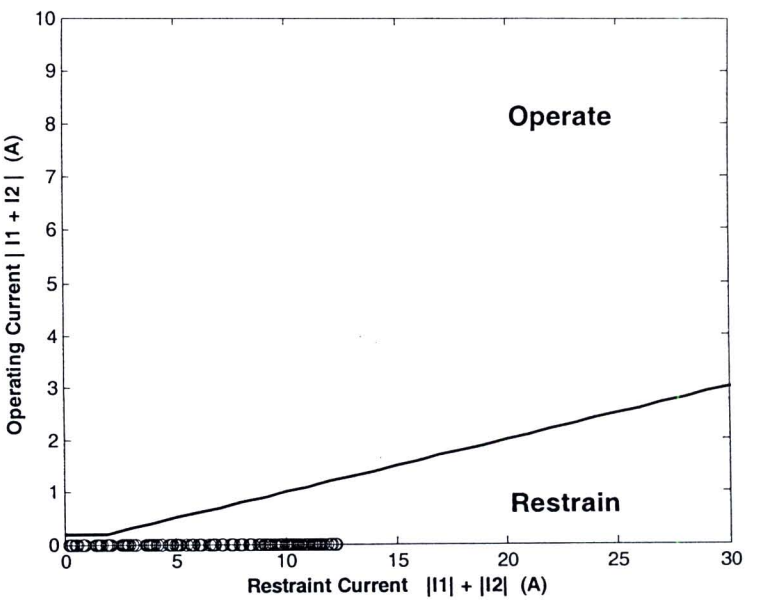

ภาพที่ ก-14 การตัดสินใจของรีเลย์ผลต่างในกรณีที่ใช้สัญญาณทดสอบหมายเลข 7

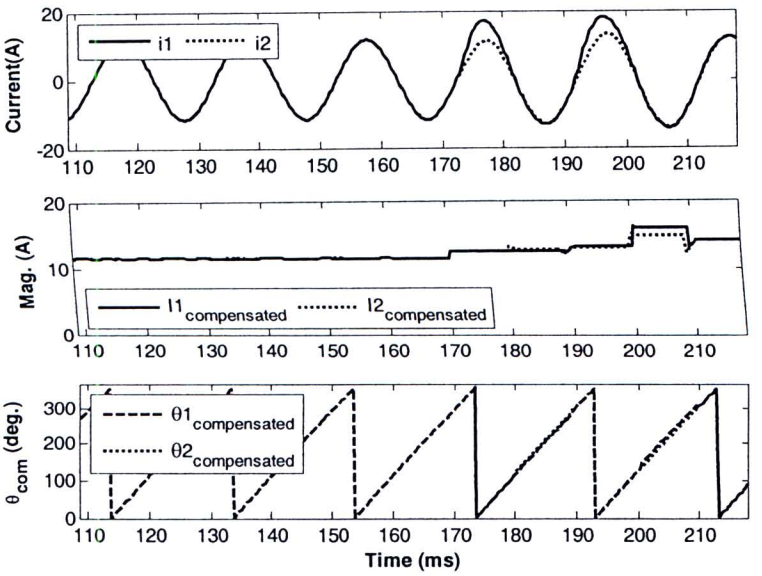

ภาพที่ ก-15 ผลการคำนวณค่าขนาดและมุมในกรณีที่ใช้สัญญาณทดสอบหมายเลข 8

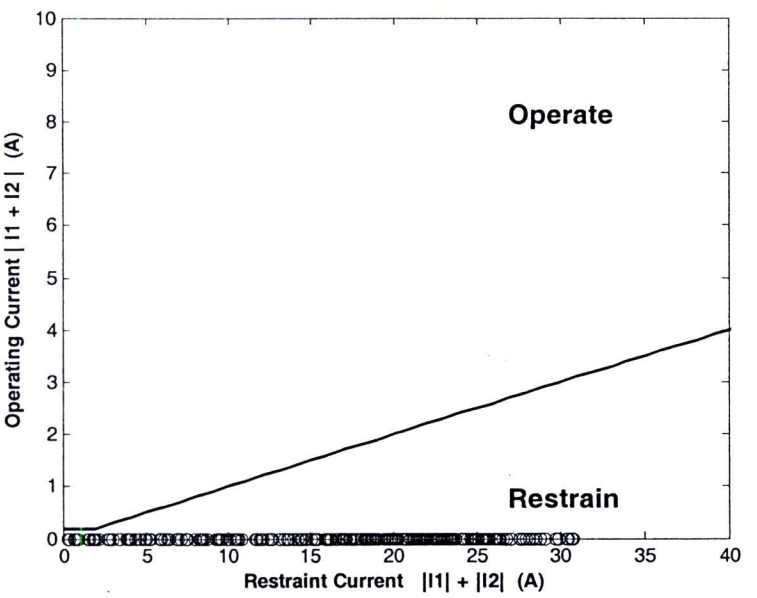

ภาพที่ ก-16 การตัดสินใจของรีเลย์ผลต่างในกรณีที่ใช้สัญญาณทดสอบหมายเลข 8

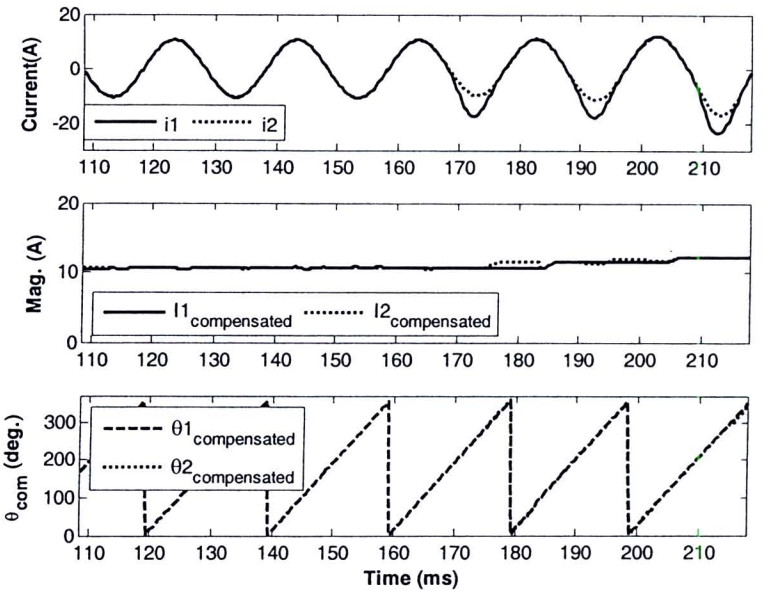

ภาพที่ ก-17 ผลการคำนวณค่าขนาดและมุมในกรณีที่ใช้สัญญาณทดสอบหมายเลข 9

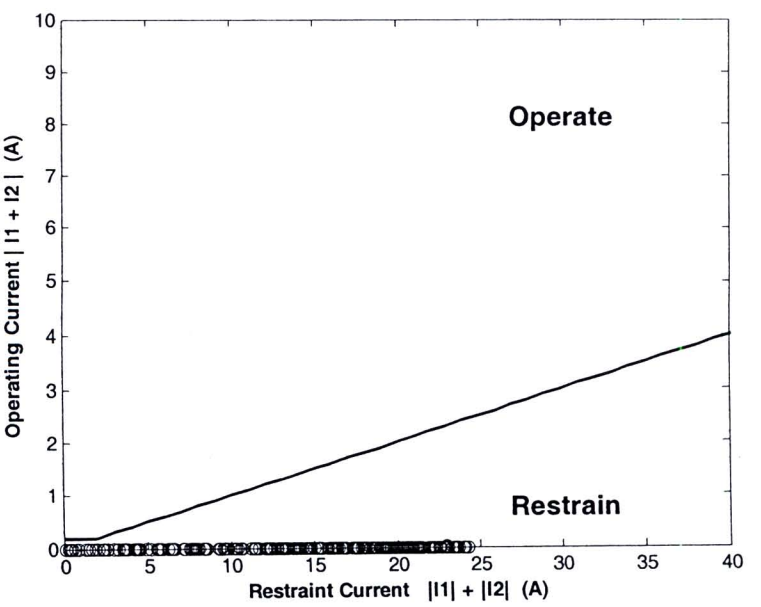

ภาพที่ ก-18 การตัดสินใจของรีเลย์ผลต่างในกรณีที่ใช้สัญญาณทดสอบหมายเลข 9

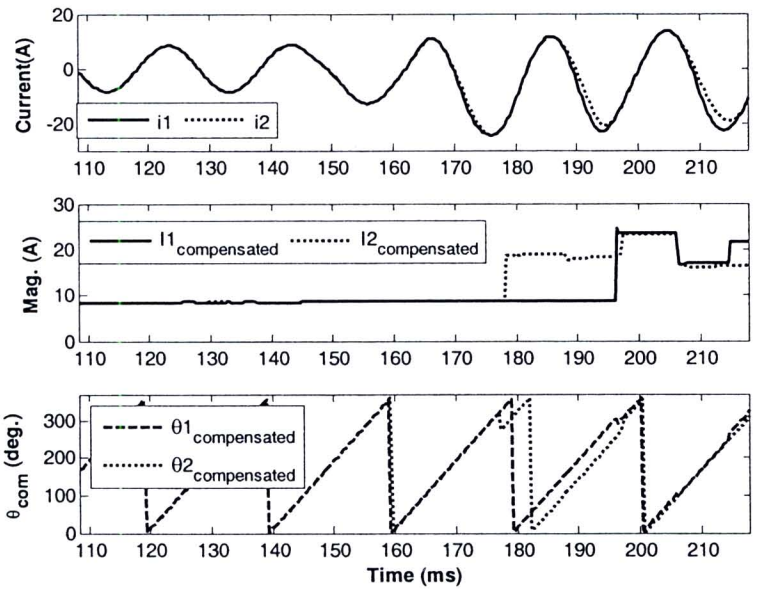

ภาพที่ ก-19 ผลการคำนวณค่าขนาดและมุมในกรณีที่ใช้สัญญาณทดสอบหมายเลข 10

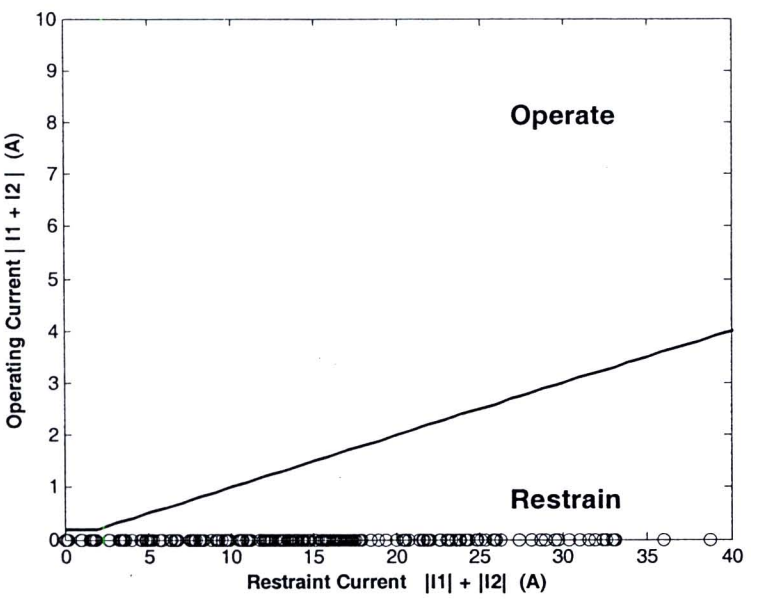

ภาพที่ ก-20 การตัดสินใจของรีเลย์ผลต่างในกรณีที่ใช้สัญญาณทดสอบหมายเลข 10

ภาคผนวก ข

ผลการทดสอบของอัลกอริธึมโดยใช้สัญญาณกระแสจากเครื่องกำเนิดไฟฟ้า ในกรณีที่เกิดความผิดพร่องภายนอก สัญญาณกระแสไม่มีความผิดเพี้ยน

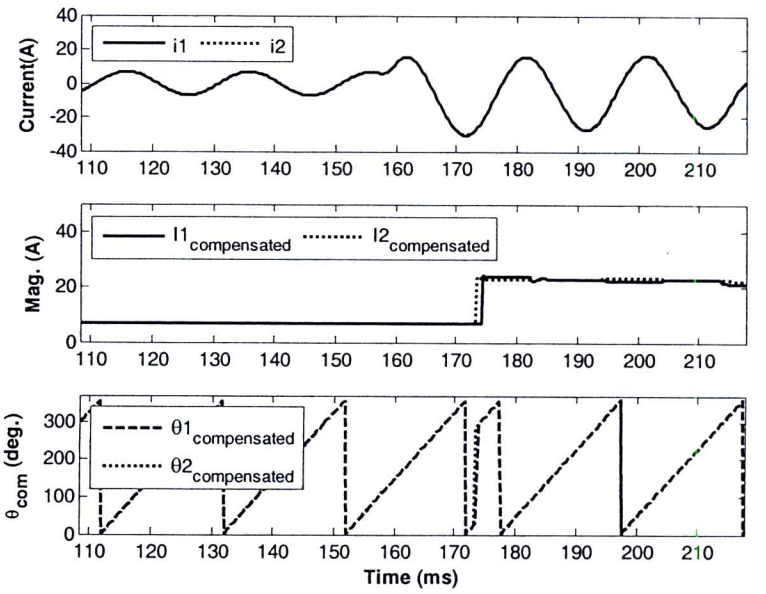

ภาพที่ ข-1 ผลการคำนวณค่าขนาดและมุมในกรณีที่ใช้สัญญาณทดสอบหมายเลข 1

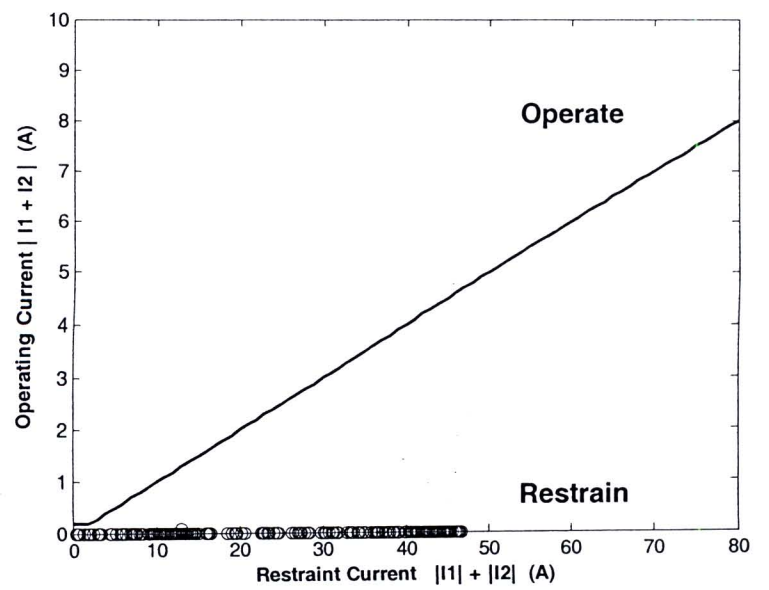

ภาพที่ ข-2 การตัดสินใจของรีเลย์ผลต่างในกรณีที่ใช้สัญญาณทดสอบหมายเลข 1

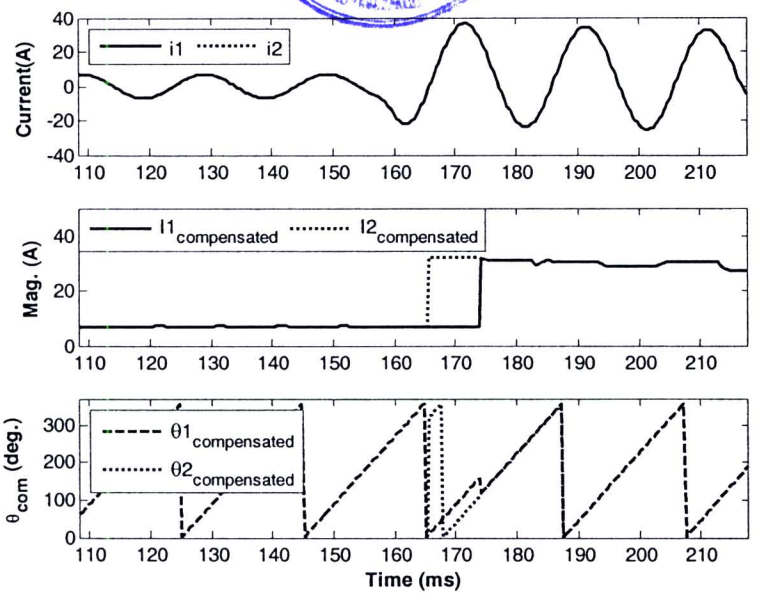

ภาพที่ ข-3 ผลการคำนวณค่าขนาดและมุมในกรณีที่ใช้สัญญาณทดสอบหมายเลข 2

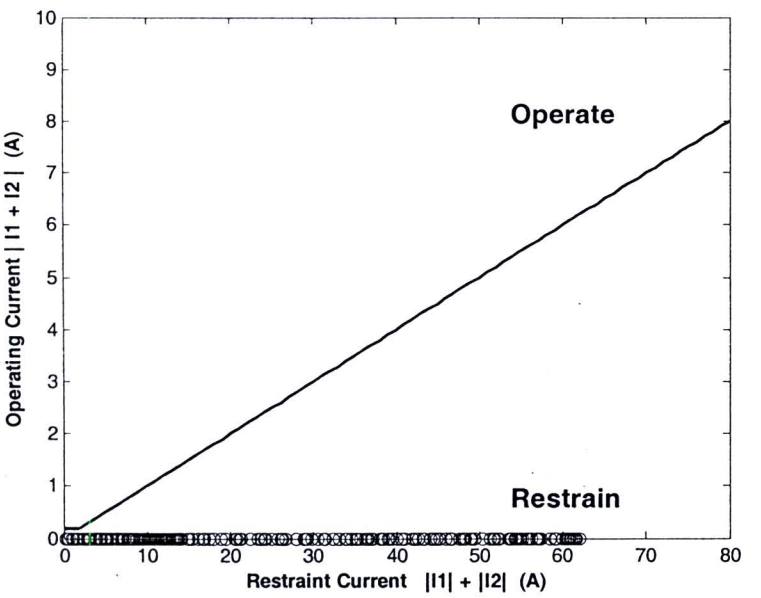

ภาพที่ ข-4 การตัดสินใจของรีเลย์ผลต่างในกรณีที่ใช้สัญญาณทดสอบหมายเลข 2

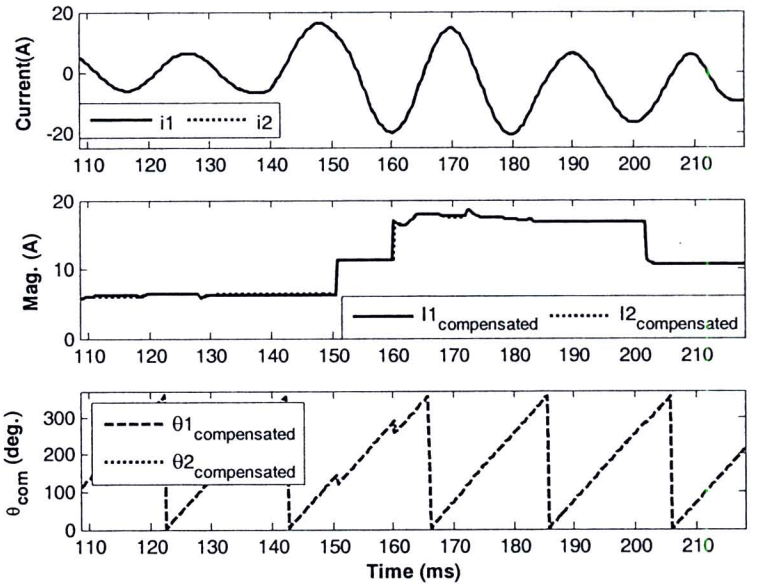

ภาพที่ ข-5 ผลการคำนวณค่าขนาดและมุมในกรณีที่ใช้สัญญาณทดสอบหมายเลข 3

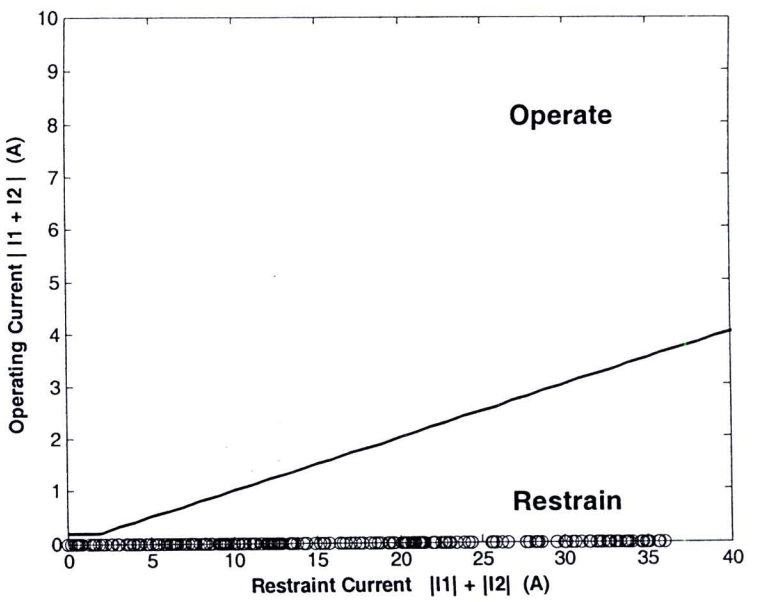

ภาพที่ ข-6 การตัดสินใจของรีเลย์ผลต่างในกรณีที่ใช้สัญญาณทดสอบหมายเลข 3

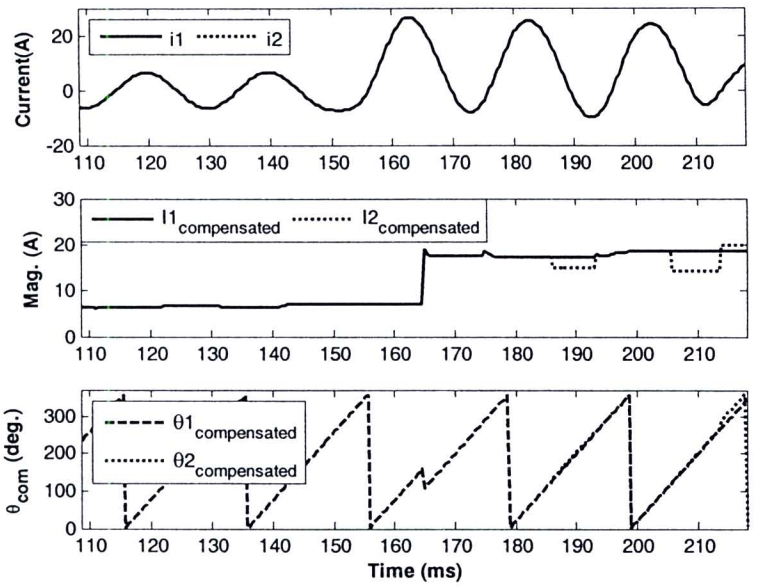

ภาพที่ ข-7 ผลการคำนวณค่าขนาดและมุมในกรณีที่ใช้สัญญาณทดสอบหมายเลข 4

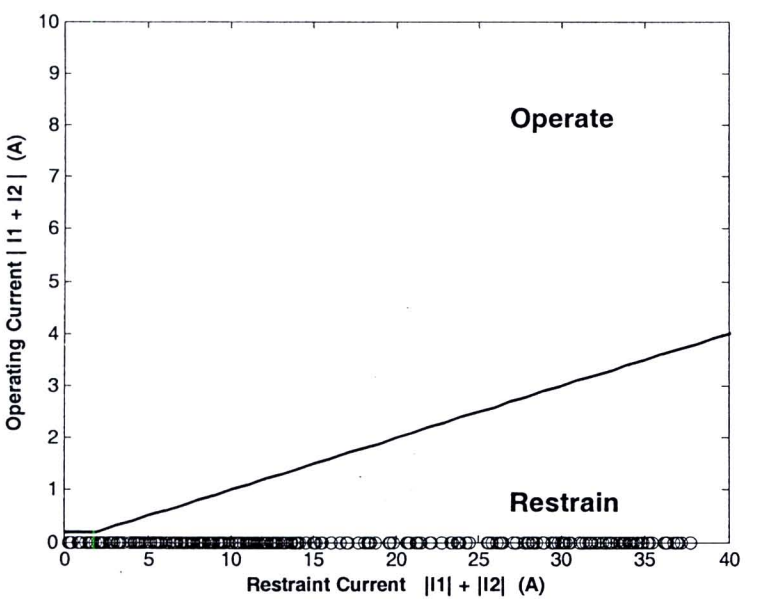

ภาพที่ ข-8 การตัดสินใจของรีเลย์ผลต่างในกรณีที่ใช้สัญญาณทดสอบหมายเลข 4

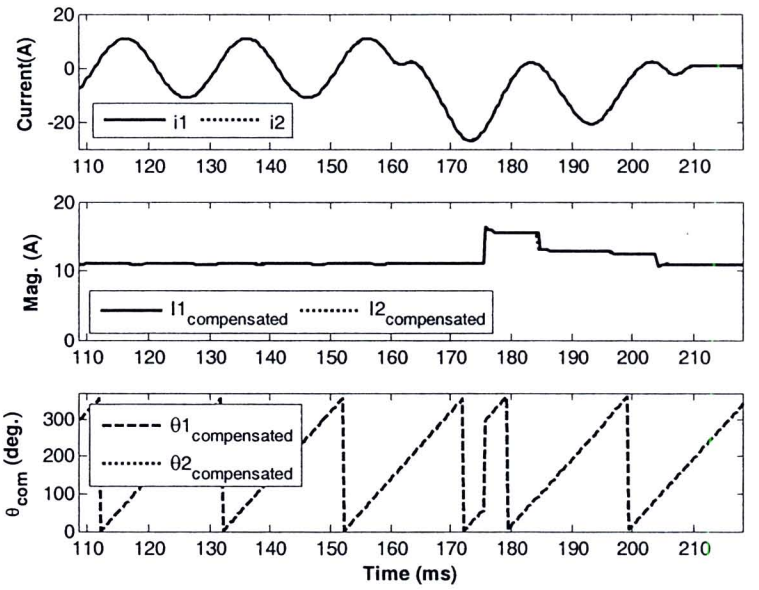

ภาพที่ ข-9 ผลการคำนวณค่าขนาดและมุมในกรณีที่ใช้สัญญาณทดสอบหมายเลข 5

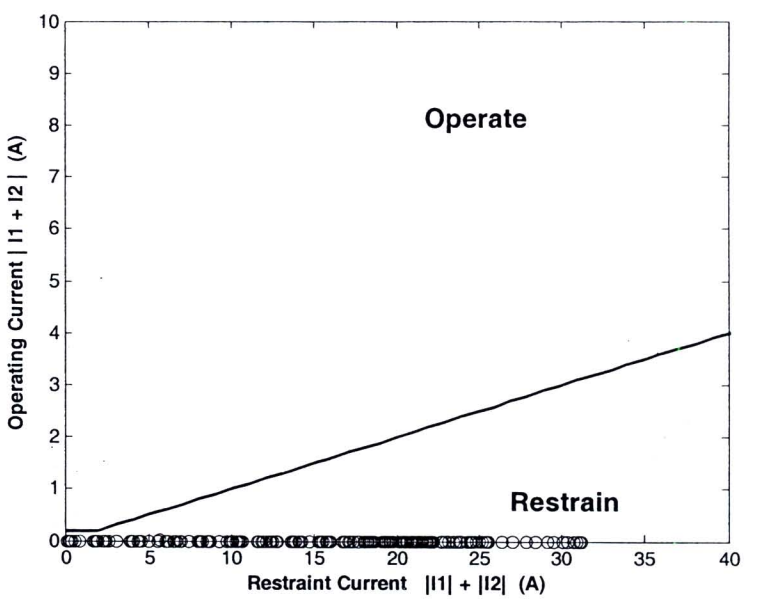

ภาพที่ ข-10 การตัดสินใจของรีเลย์ผลต่างในกรณีที่ใช้สัญญาณทดสอบหมายเลข 5

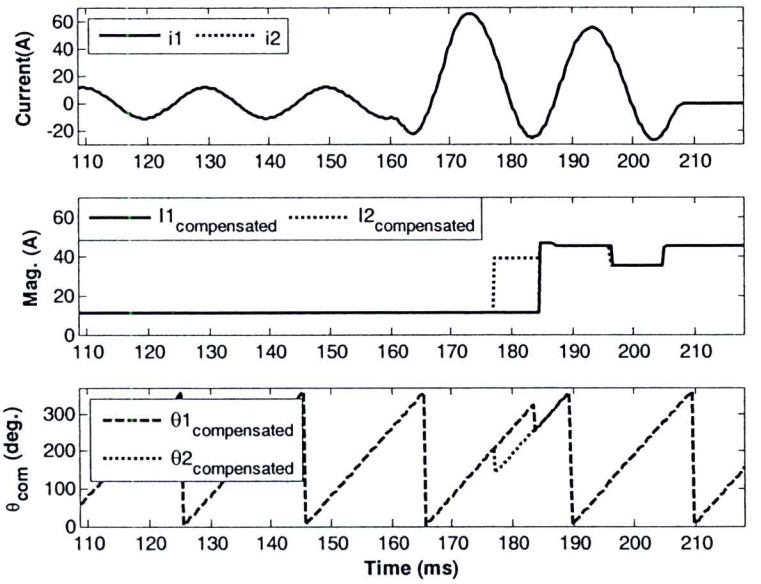

ภาพที่ ข-11 ผลการคำนวณค่าขนาดและมุมในกรณีที่ใช้สัญญาณทดสอบหมายเลข 6

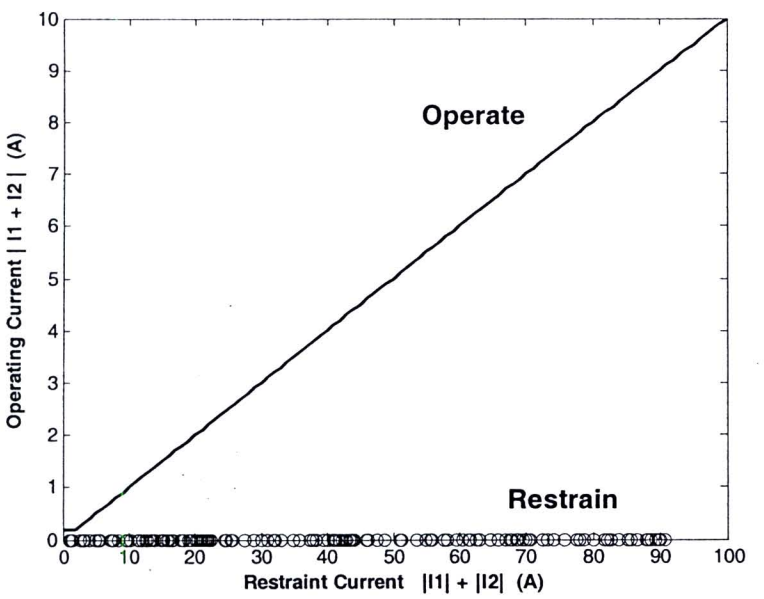

ภาพที่ ข-12 การตัดสินใจของรีเลย์ผลต่างในกรณีที่ใช้สัญญาณทดสอบหมายเลข 6

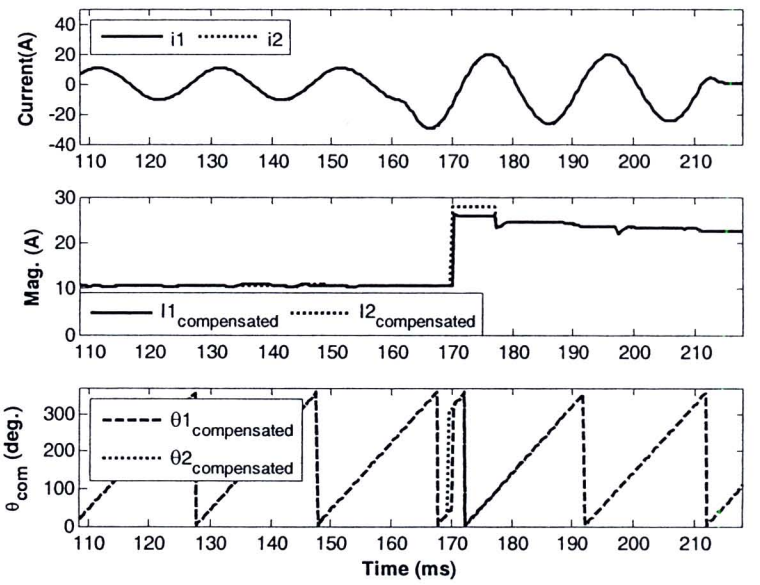

ภาพที่ ข-13 ผลการคำนวณค่าขนาดและมุมในกรณีที่ใช้สัญญาณทดสอบหมายเลข 7

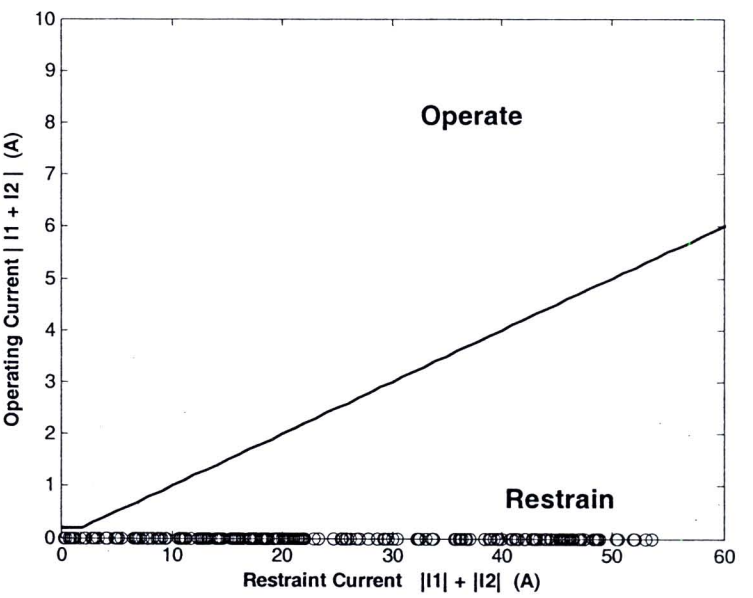

ภาพที่ ข-14 การตัดสินใจของรีเลย์ผลต่างในกรณีที่ใช้สัญญาณทดสอบหมายเลข 7

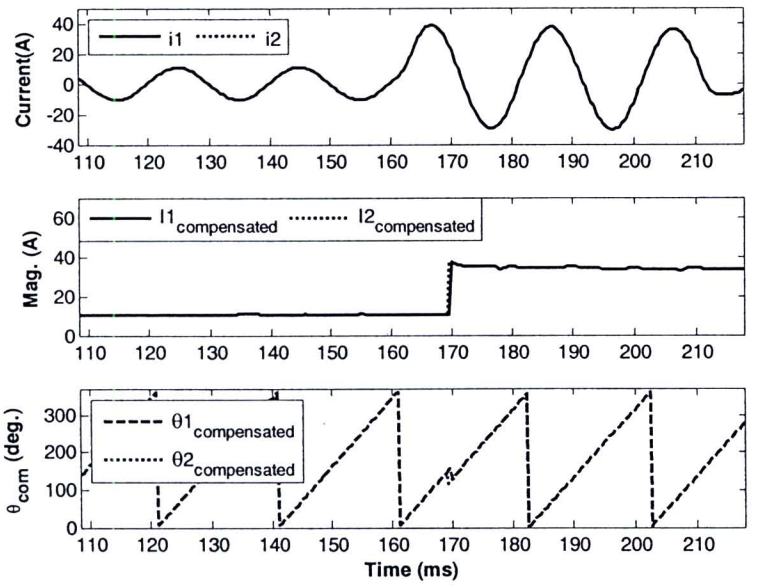

ภาพที่ ข-15 ผลการคำนวณค่าขนาดและมุมในกรณีที่ใช้สัญญาณทดสอบหมายเลข 8

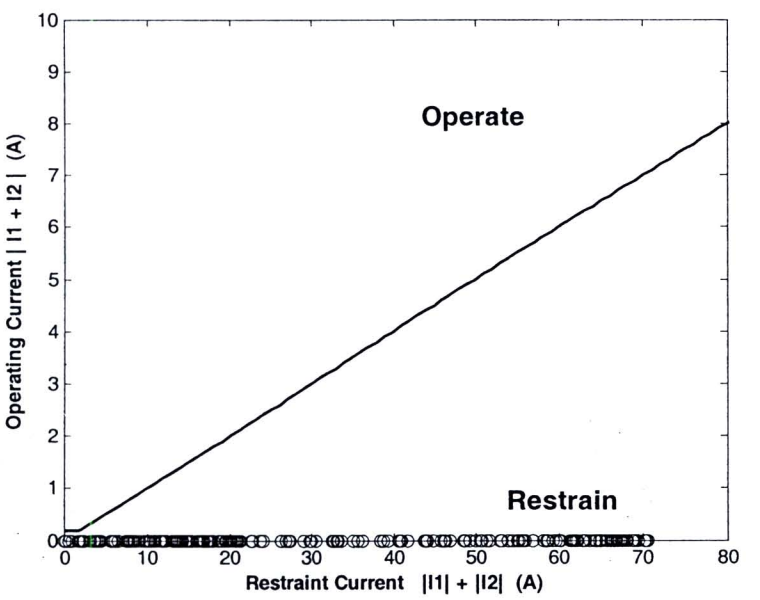

ภาพที่ ข-16 การตัดสินใจของรีเลย์ผลต่างในกรณีที่ใช้สัญญาณทดสอบหมายเลข 8

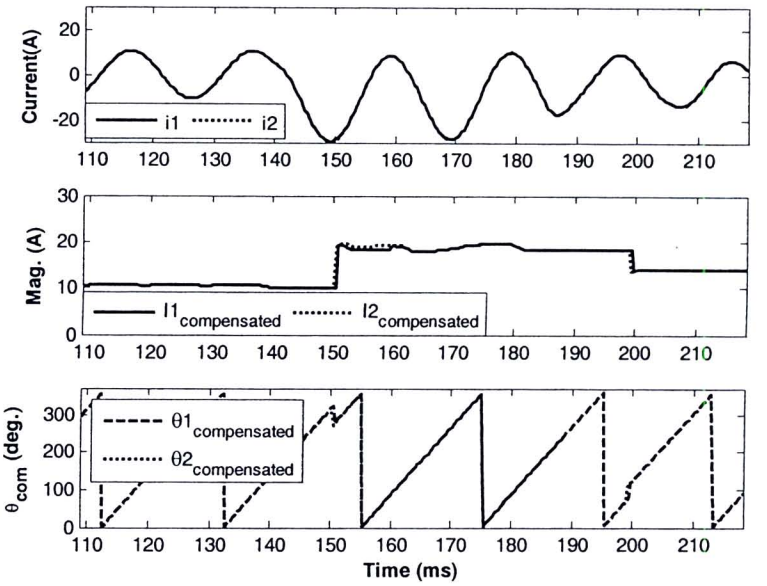

ภาพที่ ข-17 ผลการคำนวณค่าขนาดและมุมในกรณีที่ใช้สัญญาณทดสอบหมายเลข 9

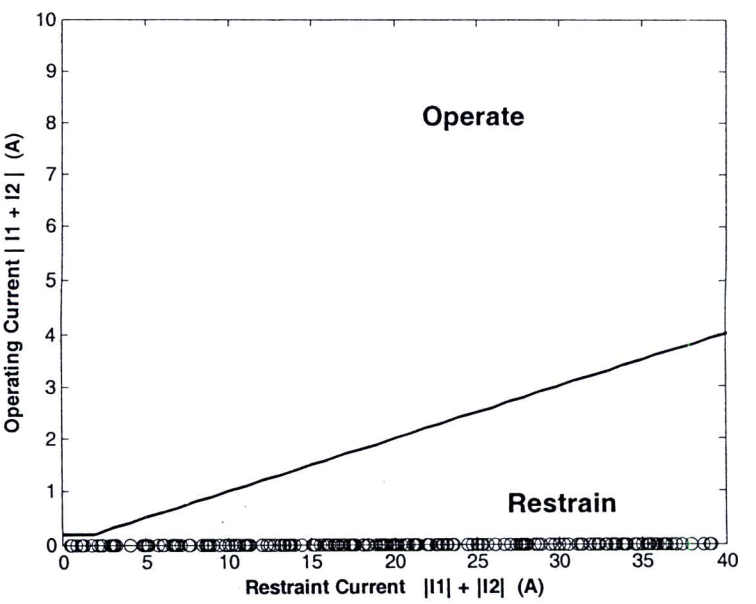

ภาพที่ ข-18 การตัดสินใจของรีเลย์ผลต่างในกรณีที่ใช้สัญญาณทดสอบหมายเลข 9

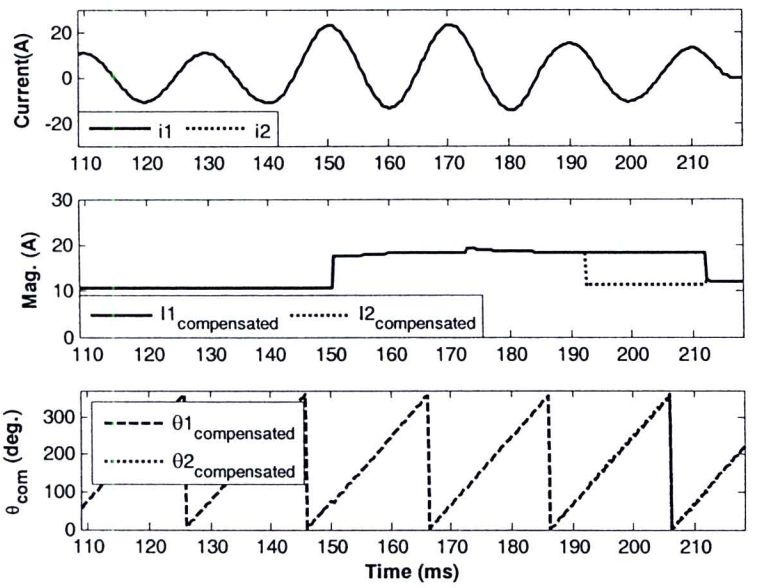

ภาพที่ ข-19 ผลการคำนวณค่าขนาดและมุมในกรณีที่ใช้สัญญาณทดสอบหมายเลข 10

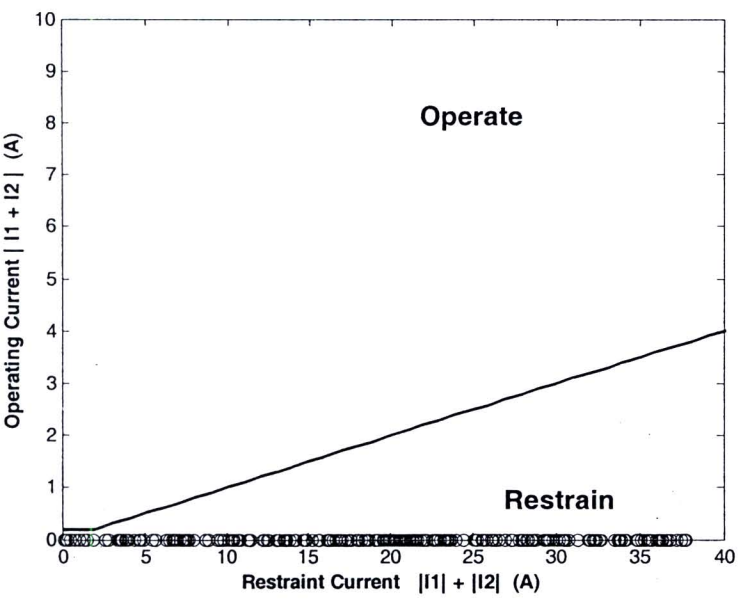

ภาพที่ ข-20 การตัดสินใจของรีเลย์ผลต่างในกรณีที่ใช้สัญญาณทดสอบหมายเลข 10

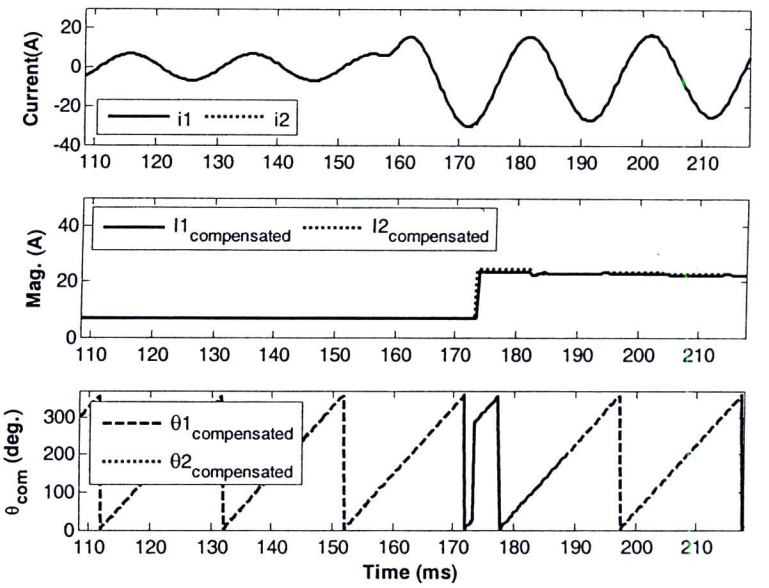

ภาพที่ ข-21 ผลการคำนวณค่าขนาดและมุมในกรณีที่ใช้สัญญาณทดสอบหมายเลข 11

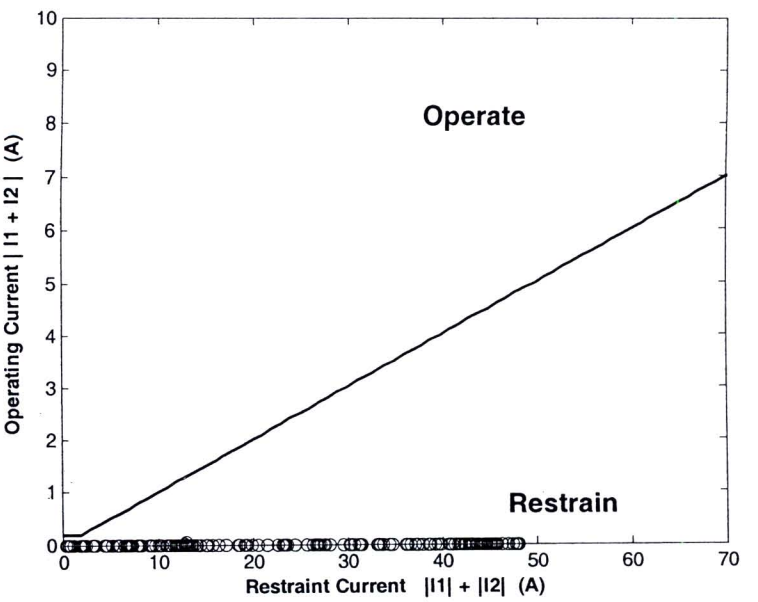

ภาพที่ ข-22 การตัดสินใจของรีเลย์ผลต่างในกรณีที่ใช้สัญญาณทดสอบหมายเลข 11

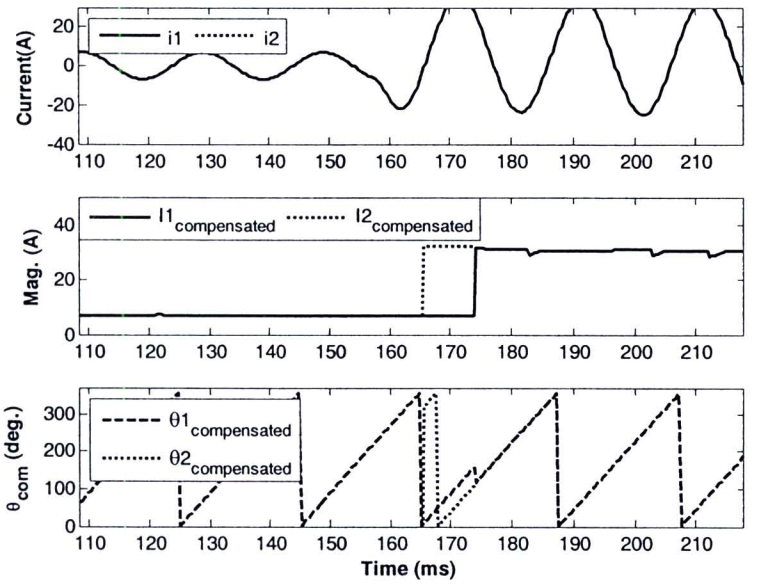

ภาพที่ ข-23 ผลการคำนวณค่าขนาดและมุมในกรณีที่ใช้สัญญาณทดสอบหมายเลข 12

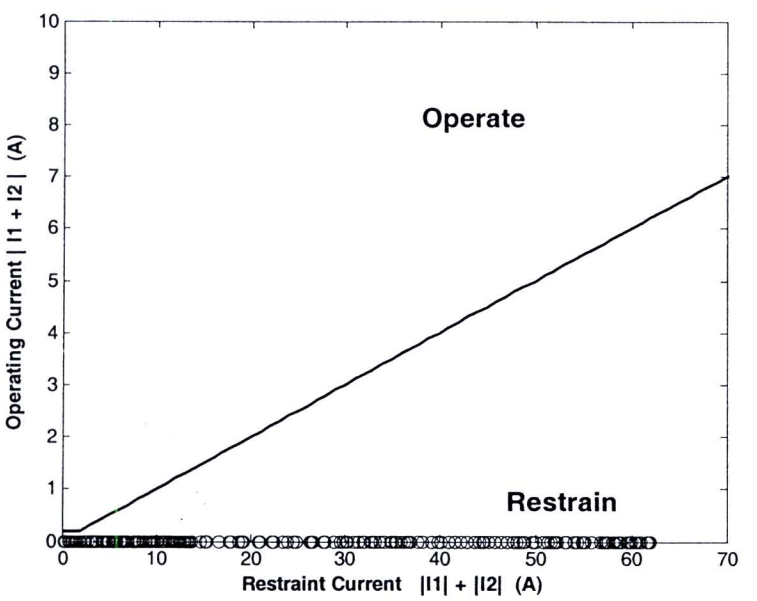

ภาพที่ ข-24 การตัดสินใจของรีเลย์ผลต่างในกรณีที่ใช้สัญญาณทดสอบหมายเลข 12

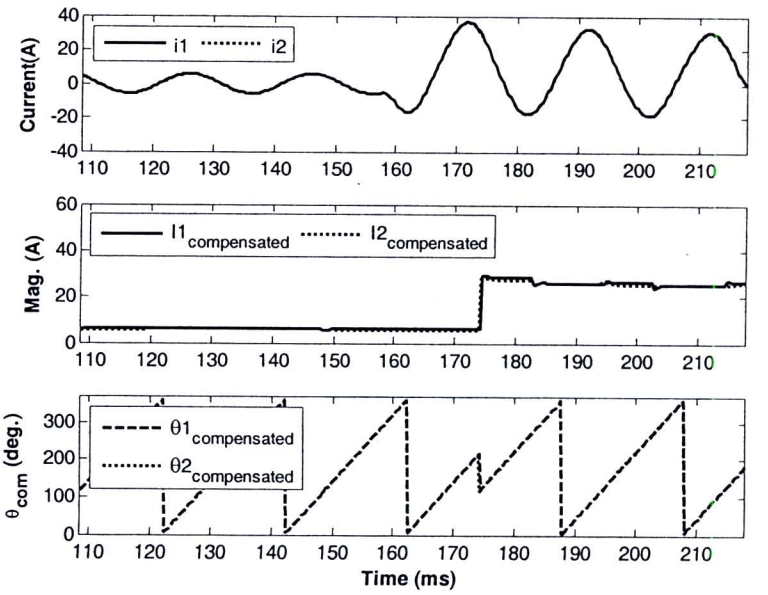

ภาพที่ ข-25 ผลการคำนวณค่าขนาดและมุมในกรณีที่ใช้สัญญาณทดสอบหมายเลข 13

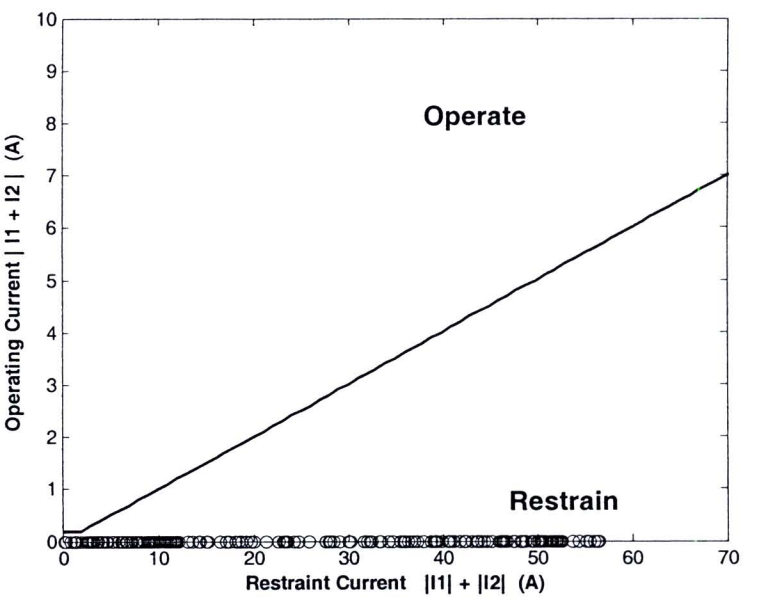

ภาพที่ ข-26 การตัดสินใจของรีเลย์ผลต่างในกรณีที่ใช้สัญญาณทดสอบหมายเลข 13

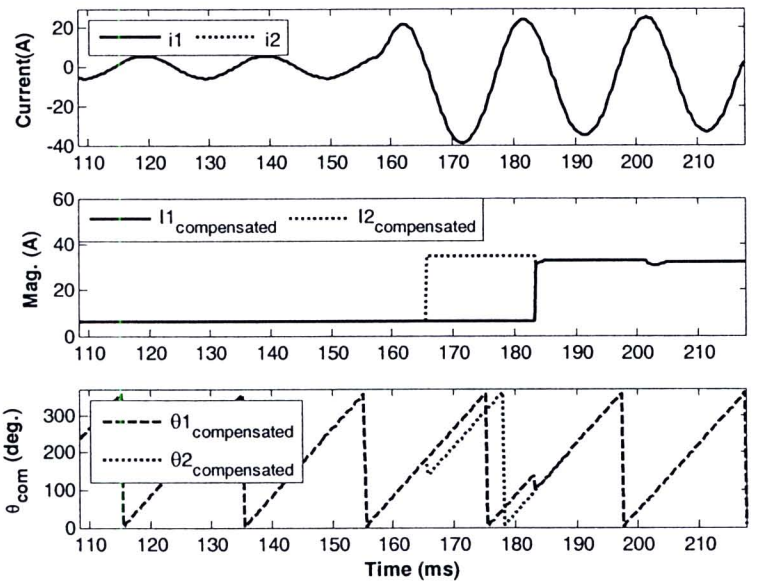

ภาพที่ ข-27 ผลการคำนวณค่าขนาดและมุมในกรณีที่ใช้สัญญาณทดสอบหมายเลข 14

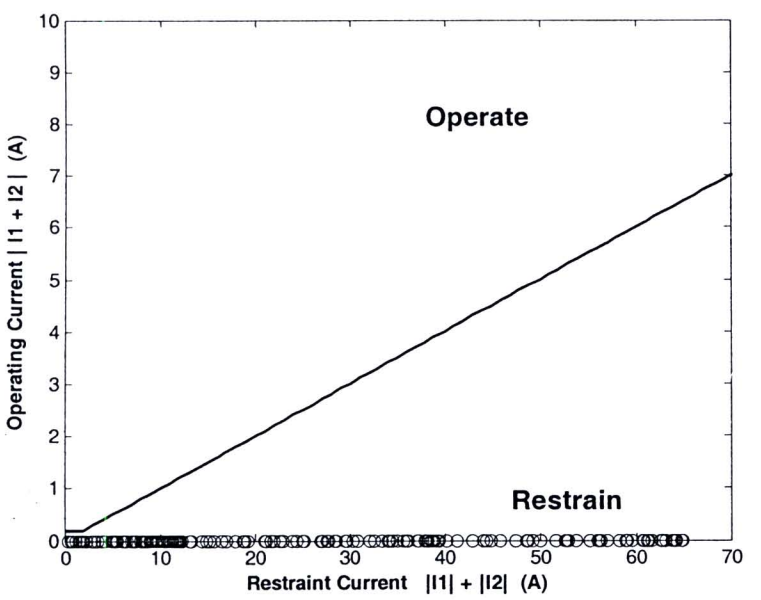

ภาพที่ ข-28 การตัดสินใจของรีเลย์ผลต่างในกรณีที่ใช้สัญญาณทดสอบหมายเลข 14

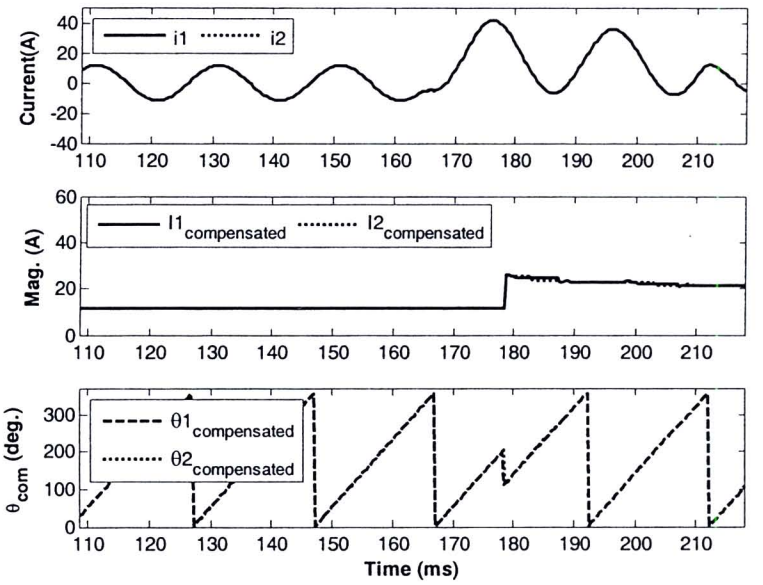

ภาพที่ ข-29 ผลการคำนวณค่าขนาดและมุมในกรณีที่ใช้สัญญาณทดสอบหมายเลข 15

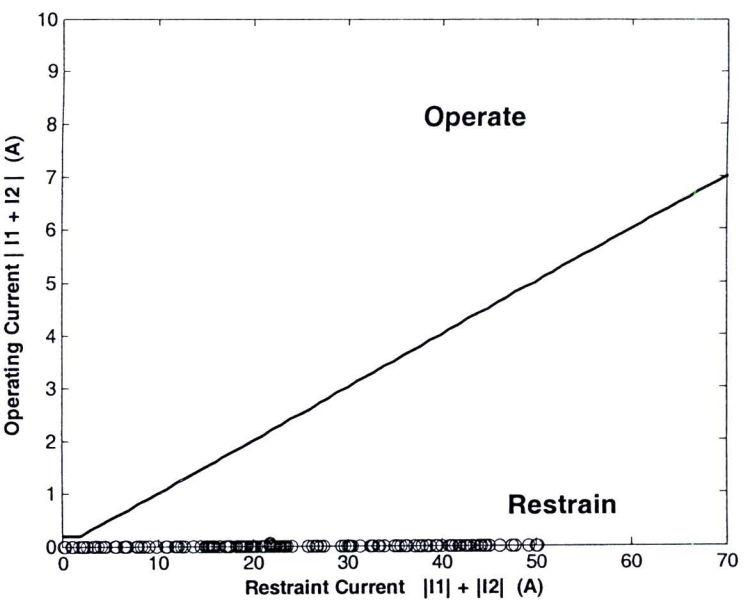

ภาพที่ ข-30 การตัดสินใจของรีเลย์ผลต่างในกรณีที่ใช้สัญญาณทดสอบหมายเลข 15

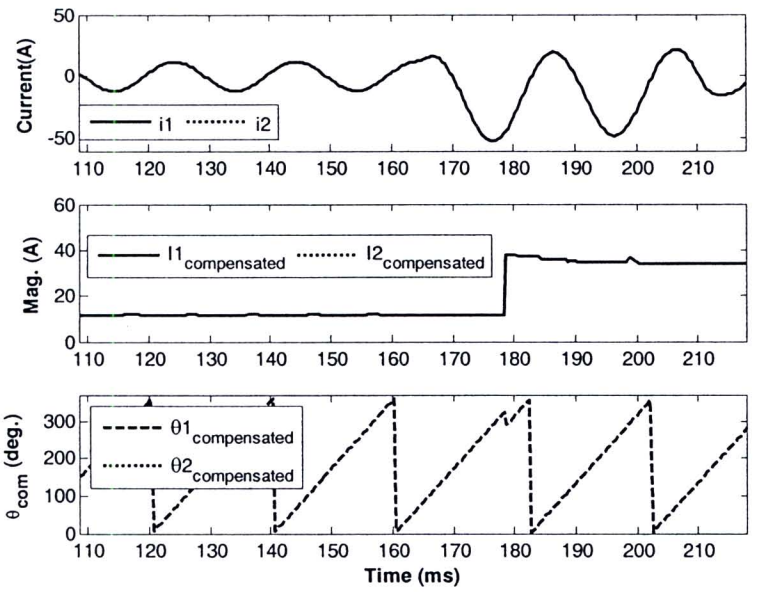

ภาพที่ ข-31 ผลการคำนวณค่าขนาดและมุมในกรณีที่ใช้สัญญาณทดสอบหมายเลข 16

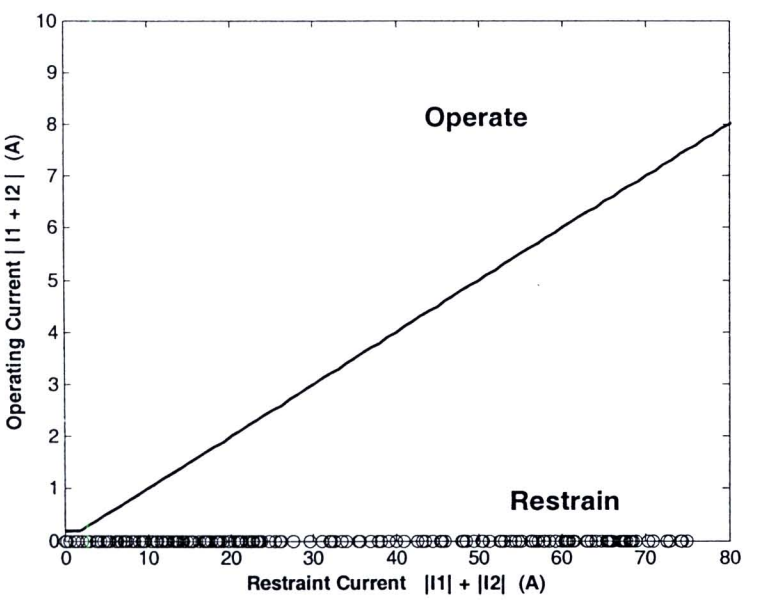

ภาพที่ ข-32 การตัดสินใจของรีเลย์ผลต่างในกรณีที่ใช้สัญญาณทดสอบหมายเลข 16

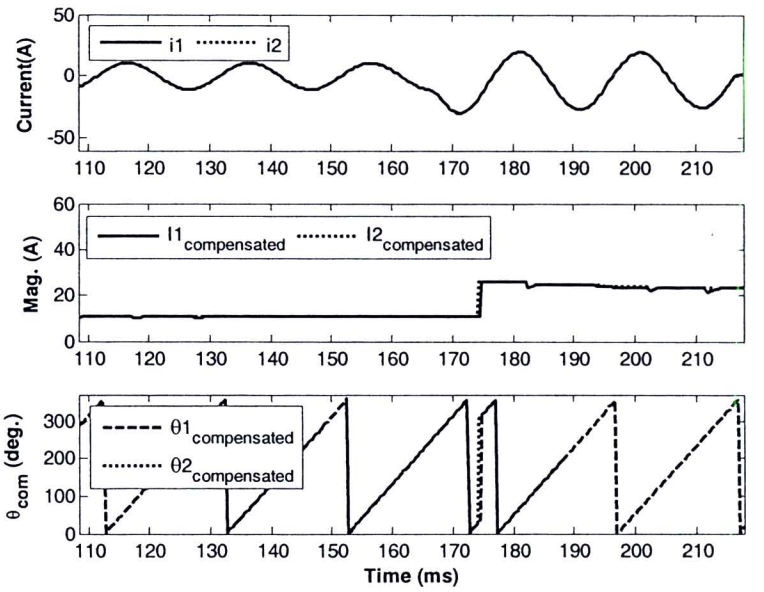

ภาพที่ ข-33 ผลการคำนวณค่าขนาดและมุมในกรณีที่ใช้สัญญาณทดสอบหมายเลข 17

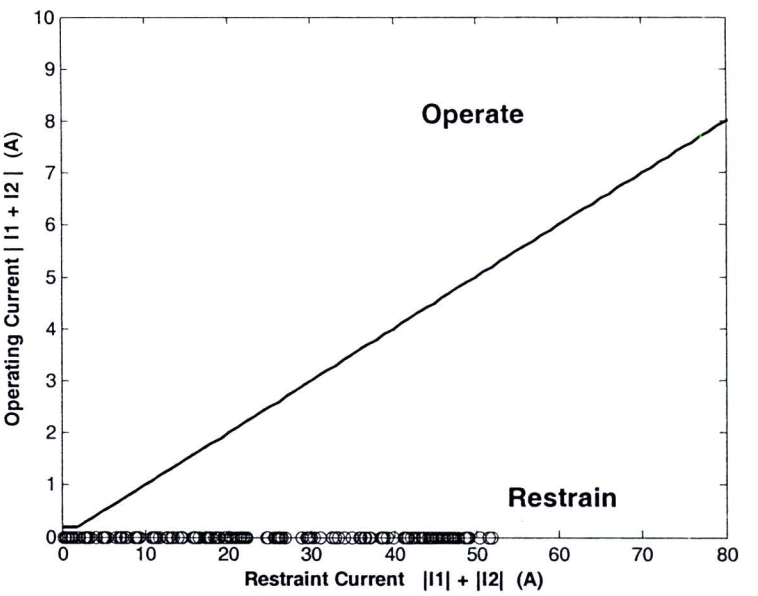

ภาพที่ ข-34 การตัดสินใจของรีเลย์ผลต่างในกรณีที่ใช้สัญญาณทดสอบหมายเลข 17

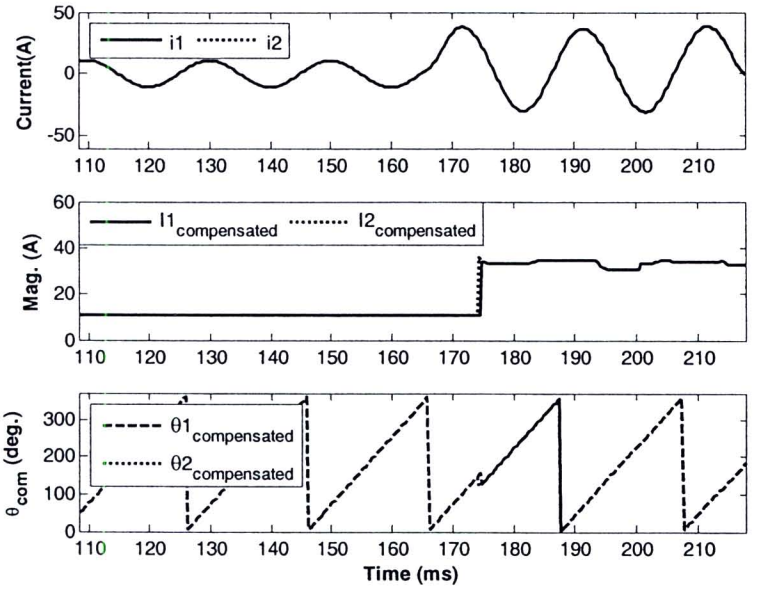

ภาพที่ ข-35 ผลการคำนวณค่าขนาดและมุมในกรณีที่ใช้สัญญาณทดสอบหมายเลข 18

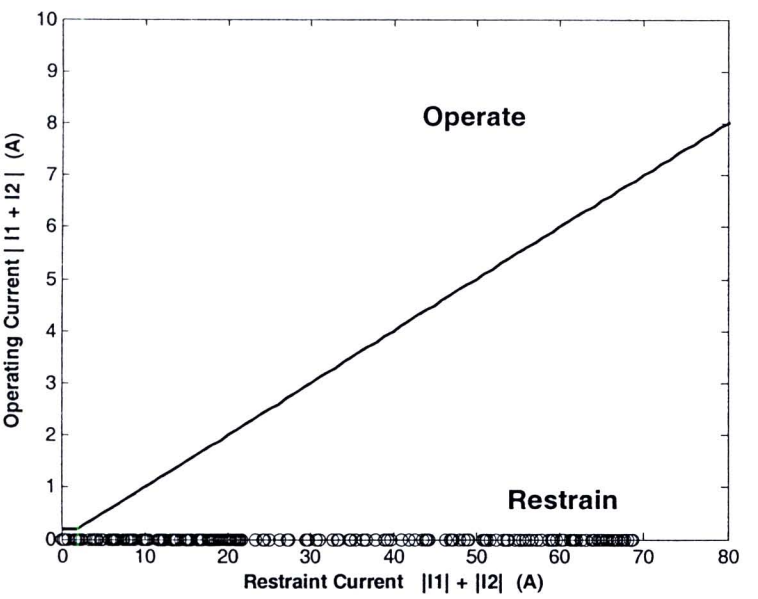

ภาพที่ ข-36 การตัดสินใจของรีเลย์ผลต่างในกรณีที่ใช้สัญญาณทดสอบหมายเลข 18

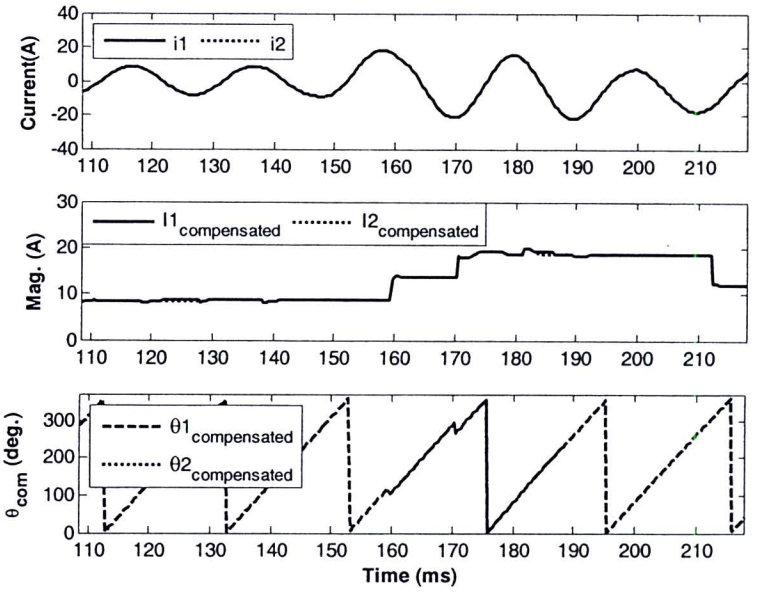

ภาพที่ ข-37 ผลการคำนวณค่าขนาดและมุมในกรณีที่ใช้สัญญาณทดสอบหมายเลข 19

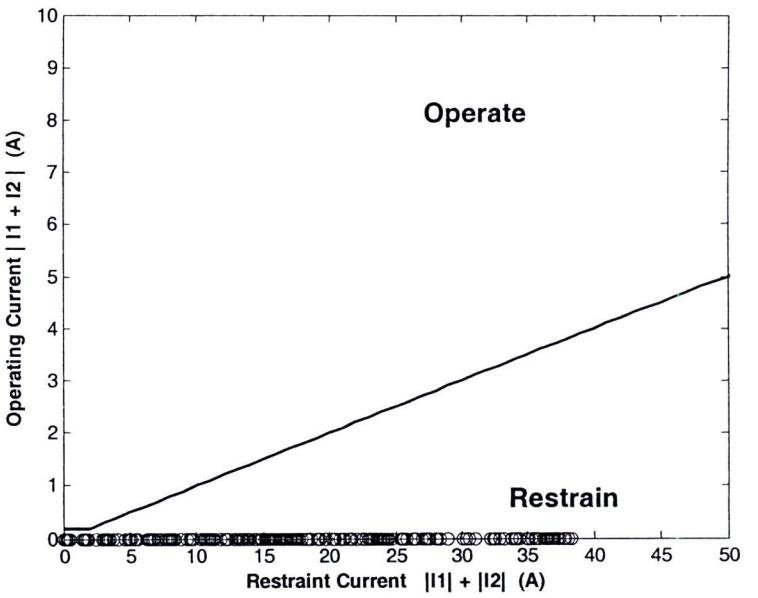

ภาพที่ ข-38 การตัดสินใจของรีเลย์ผลต่างในกรณีที่ใช้สัญญาณทดสอบหมายเลข 19

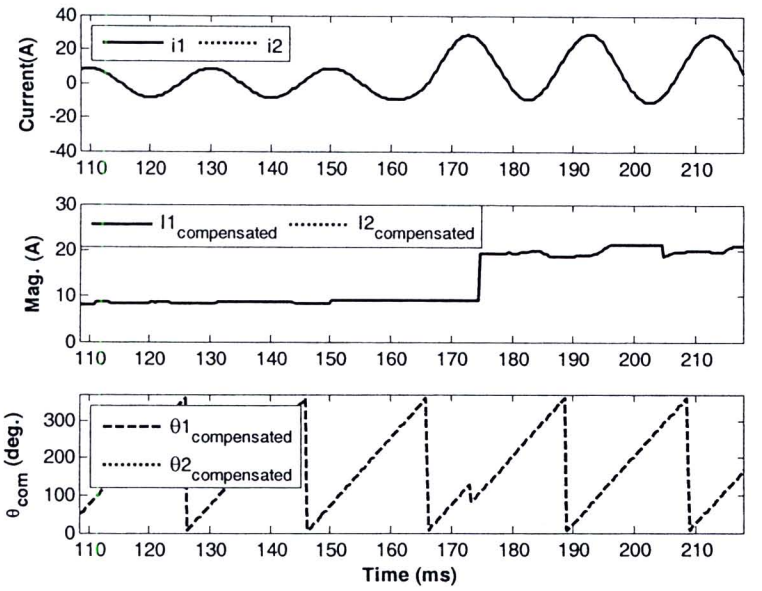

ภาพที่ ข-39 ผลการคำนวณค่าขนาดและมุมในกรณีที่ใช้สัญญาณทดสอบหมายเลข 20

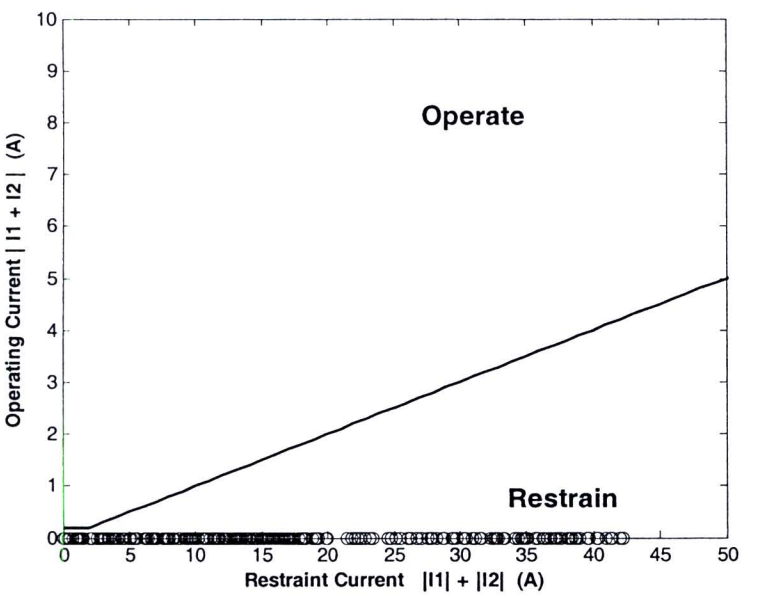

ภาพที่ ข-40 การตัดสินใจของรีเลย์ผลต่างในกรณีที่ใช้สัญญาณทดสอบหมายเลข 20

ภาคผนวก ค

ผลงานที่ได้รับการเผยแพร่

1. Adaptive Compensated Synchronous Switching of Shunt Capacitor Bank by Using Wavelet Transform

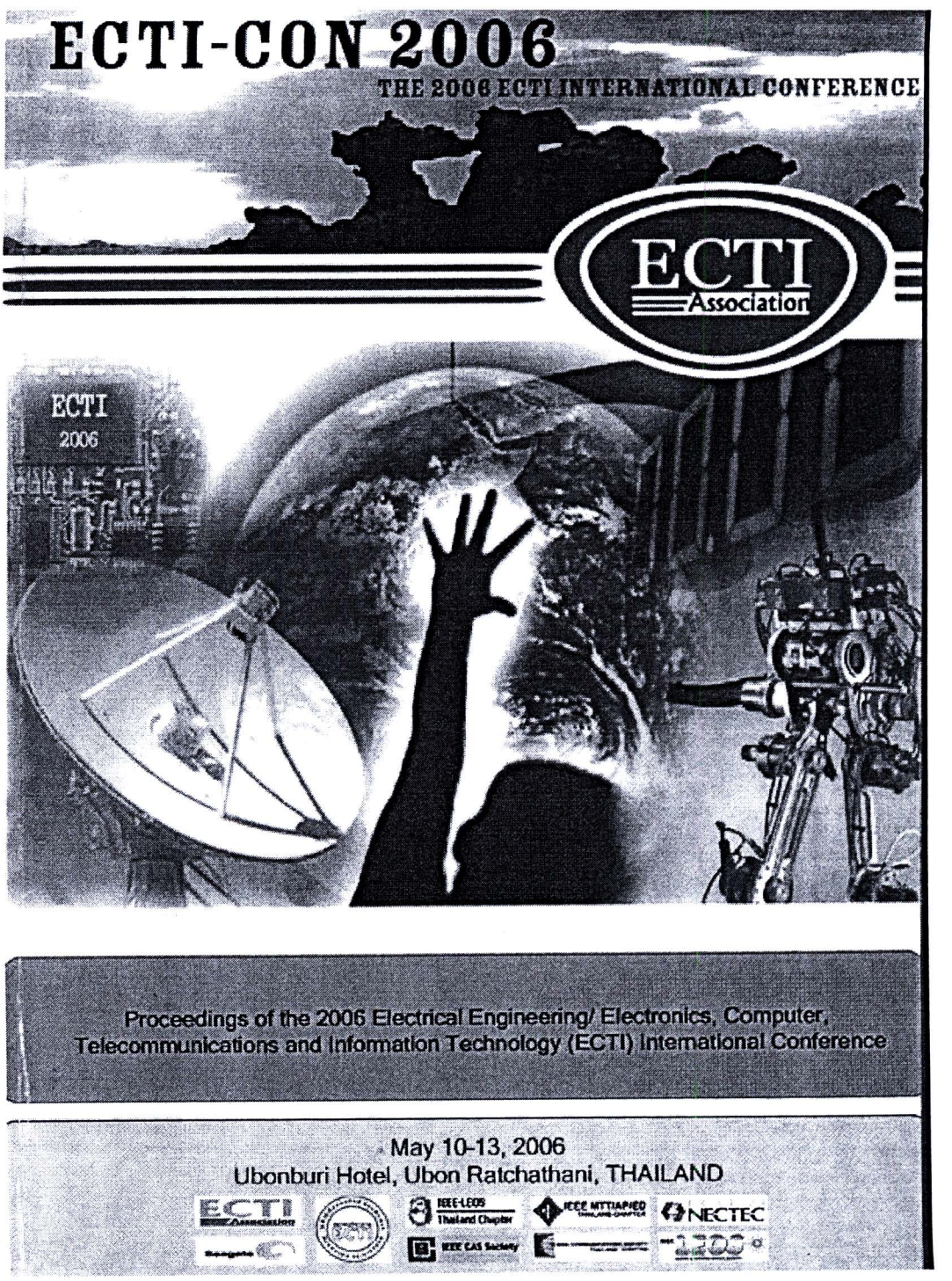

Adaptive Compensated Synchronous Switching of Shunt Capacitor Bank by Using Wavelet Transform

Noppadol Charbkaew*, Teratam Bunyagul*,
Chanin Chaonirattisai, Praditpong Suksirithawornkul*****

*Department of Electrical Engineering, Faculty of Engineering, KMITNB, Thailand
Email: noppadolc@kmitnb.ac.th, teratam@kmitnb.ac.th
**Control and Protection System Division, EGAT Public Company Limited, Bangkok Thailand
*** Department of Electrical Engineer, Faculty of Engineering, Thonburi College of Technology, Thailand

ABSTRACT

A shunt capacitor is widely used in a power system for supporting the line voltage and compensating the reactive power. Its energization causes switching transient which leads to problems in the system e.g. over voltage, ferroresonance, voltage magnification, transient over-swing trip of adjustable speed drives. These problems can be mitigated by switch the capacitor bank at the appropriate time (zero voltage target point). The switching target point is determined by a synchronous switching controller (SSC) that sends a close signal to a circuit breaker (CB). The calculation of the switching target point has to include the circuit breaker closing time. However the circuit breaker closing time changes due to its age, number of operations and environment. It is very important to be aware of the change of the CB closing time in designing the SSC.

The paper discusses the basic concept of the SSC or point on wave controller. The paper also offers the technique that can compensate the deviation of the circuit breaker closing time affected by the number of operations. This advantage of the technique is achieved by an adaptive algorithm to compensate closing time change. The SSC applied with the new adaptive algorithm utilize the signal from a voltage transformer without additional signal from a current transformer. The algorithm using Wavelet transforms and noise mitigation technique. The signals from PSCAD/EMTDC were used to test the algorithm in MATLAB. The results show that the algorithm was able to compensate the closing time changes of the CB following its deviation with robustness to noise.

Keywords: Synchronous switching, Capacitor bank, point on wave, Wavelet transform, Circuit breaker, Rate of decrease of dielectric strength(RDDS)

1. INTRODUCTION

Capacitor bank energization causes severe switching surge problems [1-8]. There are three most common practices to minimize the switching surge to an acceptable level. These methods are surge arrestor installation, impedance pre-insertion and synchronous controlled switching [3-5]. Prior to 1990's the synchronous controlled switching was difficult to use because the circuit breakers (CB) had a long closing time with wide deviation. The impedance pre-insertion was the predominant method although it employed a complex mechanism. Since then the development of CBs have provided faster closing time with smaller deviation. This has encouraged the use of synchronous controlled switching. The small deviation of the CB closing time can be compensated by an algorithm in the microprocessor based Synchronous Switching Controller (SSC) [1,2,6].

Inrush current and voltage surge occur during capacitor bank energization. The severity of the surge depends on voltage across CB at the instant of switching [4,7]. Fig.1 shows a simple model of the capacitor energization. The CB was switched at the zero and 90 degree points on the voltage to obtain the inrush current magnitude at different switching points. Fig. 2 shows that the minimum inrush current magnitude occurs when the voltage is at zero degree. This means in theory we should switch a CB to energize a capacitor bank when the voltage across the CB is zero [6-7].

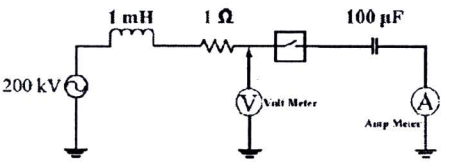

Fig.1: simple model of the capacitor energization

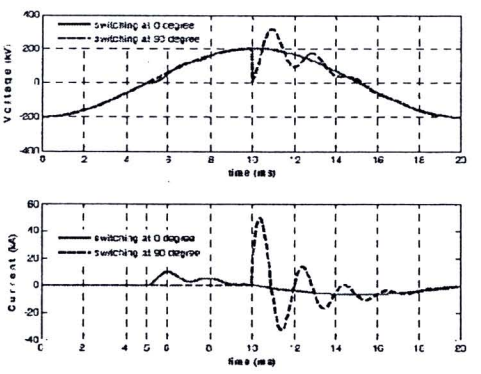

Fig.2: Bus voltages and capacitor inrush currents at the 0 and 90 electrical degree switching of V_{bus}

2. CAPACITOR BANK CONTROLLED SWITCHING

The capacitor bank should be switched at the zero degree point on voltage across CB. The closing instant can be controlled by SSC. The SSC is a device that receives the closing command form the command center and predicts the CB trigger point. The SSC trigs the CB that makes the CB to close near to the zero degree point on voltage (target point). Fig.3 shows that after the closing command arrives, the SSC seeks the reference point (zero crossing). Next, the SCC waits for the calculated trigger point. Then it trigs the CB and the CB closes at the target point [1,4,7]. The procedures require a precise CB closing time. However the CB closing time is not exact. The closing time is deviated by number of operations, ambient temperature, age, changing of Rate of Decrease of Dielectric Strength (RDDS), idle time, etc [4,6,7].

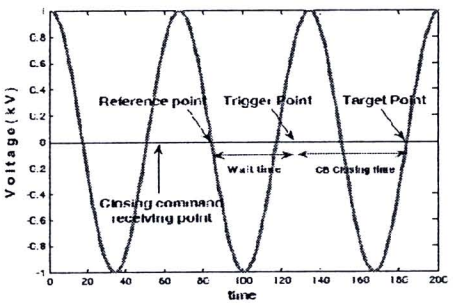

Fig.3: Capacitor bank controlled switching timing

The paper presents an adaptive technique to compensate the deviation of CB closing time. The compensation technique focuses on the deviation affected by age and number of operations. These cause the changes in mechanical characteristic. The variation of the closing time of CB tends to increase following the number of operations as illustrated in Fig.4

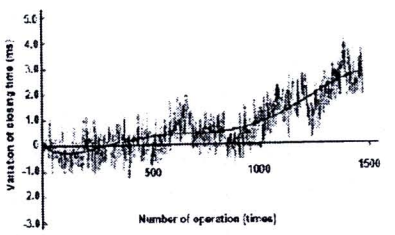

Fig. 4:Variation of the closing times following a number of consecutive operations [1]

The adaptive compensation is the effective method to compensate the closing time variation due to the number of operations. The technique detects the previous closing instant and adapts the wait time accordingly. The technique does not require a special sensor to detect the closing instant. This is unlike traditional SSCs that determine the closing instant by using additional CT to detect the instant flow of capacitor current [1, 3-4, 6-7]. It is important to note that the technique is CB and network independent.

3. WAVELET TRANSFORM

Wavelet Transform (WT) is a mathematical tool that transforms the signal in time domain to time-frequency domain. Its concept is similar to Short Time Fourier Transform (STFT). STFT decomposes the original signal to a set of 'sinusoidal signals' with different frequencies. The coefficients of STFT are proportional to the correlation coefficients of the original signal with the unit complex sinusoidal in each frequency.

WT decomposes the original signal to a set of wave like signals, called 'wavelet'. These wavelet signals are the scaled (dilated) and shifted forms of mother wavelet, as shown in Fig.5.

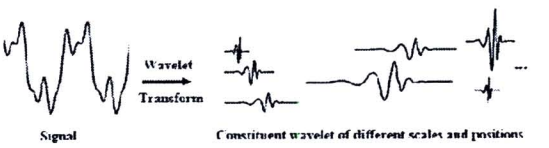

Fig.5: Signal decomposition using wavelet transformation [2]

The WT coefficient can be calculated by following expression.

$$C(a,b) = \int_{-\infty}^{\infty} f(t) \frac{1}{\sqrt{a}} \psi\left(\frac{t-b}{a}\right) dt \qquad (1)$$

Where, ψ is the wavelet function and its shape varied by variables **a** (dilation) and **b** (position). Fig. 6 shows the example of the mother wavelet, dilated wavelet (a = 2) and position shifted wavelet (b = 10). The observation can be made that the smaller the dilation means the higher the frequency. The greater the position shifted means the longer the delay.

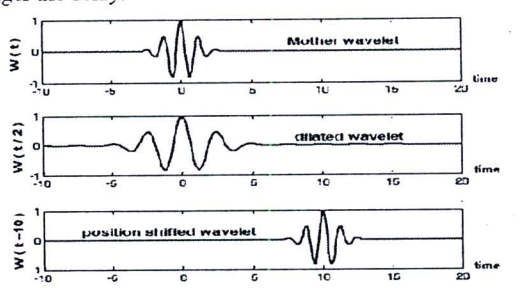

Fig.6: mother wavelet, dilated wavelet (a=2) and position shifted wavelet (b= 10)

The great advantage of WT is the ability to analyze transient signals. This is because it is able to decompose the selected frequency component at any time instant. Even a small discontinuity barely visible can still be detected [9].

4. VOLTAGE DISCONTINUTY DETECTION

The capacitor bank energization switching causes sudden change of the bus voltage [4]. The discontinuity appears on the voltage waveform. This can be demonstrated by a simple RLC circuit as shown in Fig.1.

The model was simulated in PSCAD/EMTDC to generate the signals for testing the algorithm. CB closing points were varied from 19.0 to 22.6 ms (-18° to 46.8°) in a step of 0.2 ms.

Fig. 7 shows the comparison of switching points at 0 and 46.8 electrical degrees or at 20 and 22.6 ms respectively. Switching at the exact zero degree point causes the smallest voltage signal fluctuation and it is the most difficult switching point to detect. For this reason, the 'zero switching signals' are used for algorithm performance testing, although in the practice 'zero point' is not used to be the switching target [8].

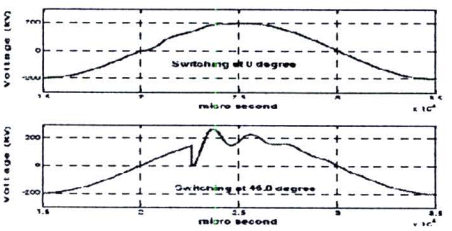

Fig.7: comparison of bus voltage that are switched at 0 and 46.8 degree (at 20 and 22.6 ms respectively)

The voltage signal is suddenly changed at the switching point. The fast changing of signal (abruption) reflects the local high frequency signal. That means the switching point can be detected by seeking the local high frequency of the signal.

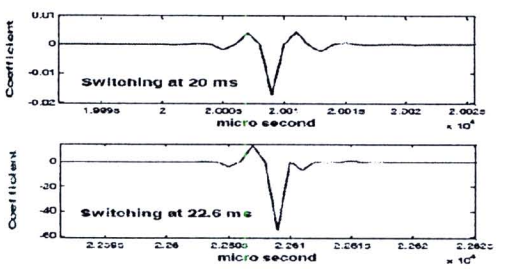

Fig.8: Detail signals of switching at 0° and 46.8° (20 & 22.6 ms respectively)

A low dilated wavelet called 'unit scale fifth order Coiflets wavelet' extracts the high frequency component from the signal as shown in Fig.8. The switching point can be obtained by evaluating the absolute maximum the signal in Fig.8. This causes a delay of approx. 10 microseconds that is negligible. The lowest spike magnitude occur when apply the zero voltage switching point. It confirms that switching at zero voltage point is the most difficult to detect. The spike magnitude of switching at 46.8° is much higher and easier to detect.

4.1 Effects of Noise and Its Mitigation

The noises may interfere with the measured signals. In the experiment, noises were added to the voltage signal as shown in Fig.9. Then let the algorithm determined the switching point again.

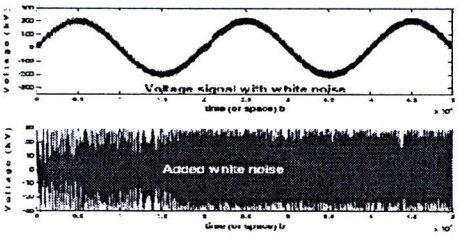

Fig.9: The voltage signal with white noise interference and the added white noise

The detail signals which are received from wavelet transform are shown in Fig.10. The algorithm miscalculated the switching point near the zero voltage. The near peak voltage switching could be correctly detected. That means the single scale detection algorithm is not robust to the noise interferences.

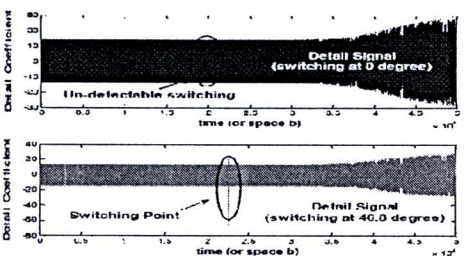

Fig.10: comparison of bus voltage that are switched at 0 and 46.8 degree (with noise interference)

4.2 The Long Frequency Line Algorithm

The algorithm is called Long Frequency Line. This is because the algorithm detects the switching instant by using the property of abruption. The discontinuous point was decomposed to a wide range of frequency signals. This method is robust to noises. Fig.11 shows the wavelet coefficient plot of zero point switching **without noise** interference.

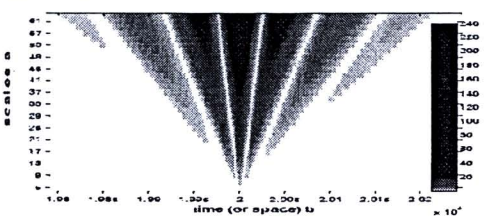

Fig.11: Spectrogram of zero point switching without noise

The switching instant (at about 2 ms) has the highest coefficient and longest continuous vertical line as seen in

Fig.11. It illustrates that the switching point has the widest frequency components. The switching point can be detected by the method of calculating the sum of long vertical line's coefficient that reaches the maximum. The highest score point is determined by summing all coefficients that have the same b value as the following expression.

$$score(b) = \sum_{a=1}^{n} C(a,b) \qquad (2)$$

Where a is the scale (dilation). Fig.12 is the gray-scale coefficient plot of zero point switching (at b= $2*10^4$ or 20 ms) **with strong noise** signal. The result of algorithm show that the position of maximum score is at about b= $1*10^4$ (1 ms). The detection was incorrect because there are very high coefficient in the region A. Therefore, the maximum score is no longer reflex the switching point.

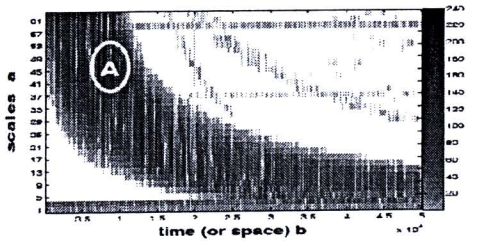

Fig.12: Gray-scale spectrogram of zero point switching with noise

To solve the incorrect detection, the gray-scale coefficient plot must be converted to a black and white plot by using threshold comparator. The threshold was determined by using Otsu's method [10]. The coefficient is higher than the threshold will be converted to 1 and the lower to 0, as shown in Fig.13. Then let the algorithm determined the switching point again.

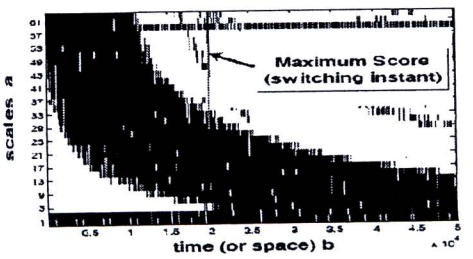

Fig.13: Black & White spectrogram of zero point switching with noise

After applying the algorithm, it is detected the correct switching point, b= $2*10^4$ (2 ms). This can be observed by a summation of vertical lines length (2) that reaches the maximum value at 2ms.

5. WAIT TIME ADAPTING

After acquiring the switching instant, the SSC will know whether the wait time is too long or too short. The SSC will calculate the new adapted value then subtract it with the previous wait time. The adapted value is not the closing error, but it is the closing error multiply with creep factor (c), creep factor is used for the convergent adaptive reason [4].

$$WaitTime_{new} = WaitTime_{old} - (error * c) \qquad (3)$$

The selected c value will be high or low depending on the performance of the CB, RDDS, scattering of closing time. The value of c is always less than one.

6. CONCLUDSION & FURTHER WORK

The wavelet transform can be used for transient analysis, finding the switching instant. By using Long Frequency Line algorithm can detect the switching point with more robustness to noise. The technique can compensate the deviation of the circuit breaker closing time. The SSC applied with the adaptive algorithm utilize the signal from a voltage transformer without additional signal from a current transformer. The next step is to implement this algorithm on a DSP controller then test with a digital real-time simulator (HYPERSIM).

7. REFERENCES

[1] H. Tsutada, T. Hirai, H. Kohyama, H. Ito and K. Sasaki, "Development of Synchronous Switching Controller for Gas Circuit Breakers" Transmission and Distribution Conference and Exhibition 2002: Asia Pacific. IEEE/PES Volume 2

[2] E.P. Dick, D. Fischer, R. Marttila, C. Mulkins, "Point-On-Wave Capacitor Switching and Adjustable Speed Drive", IEEE Transaction on Power Delivery, Vol. 11, No. 3, July 1996

[3] C.D. Tsirekis, N.D. Hatziargyriou, "Control of Shunt Capacitor and Shunt Reactors Energization", IPST 2003 in New Orleans, USA

[4] "Understanding High Voltage Circuit Breaker", Chapter 7, ABB Switchgear, 2003

[5] Liuling Li, Y. QIU, "Controlled Switching of Circuit Breaker and Its Site Measurement in Power Distribution System", ISEIM 2001, Page(s):777 - 780

[6] H. Ito, "Controlled Switching Technologies, State-of-the-Art", Transmission and Distribution Conference and Exhibition 2002: Asia Pacific. IEEE/PES

[7] "Control Switching Buyer's Guide", 2004-2005,ABB

[8] H. Kohyama, K. Wada, H. Ito, M. Hidaka, S. Billings, T. Sugiyama, H. Yamamoto, "Development of 550kV and 362kV Synchronous Switching Gas CirCuit Breakers" IEEE, 2001

[9] M. Misiti, Y. Misiti, G. Oppenheim, J. Poggi, "Wavelet Toolbox for Use with MATLAB user guide", MathWorks, Inc.,1996

[10] Otsu, N., "A Threshold Selection Method from Gray-Level Histograms," IEEE Transactions on Systems, Man, and Cybernetics, Vol. 9, No.1, 1979

2. Wavelet based Capacitor Bank Adaptive Controlled Switching and its Application to RDDS Approximation for already installed Circuit Breaker

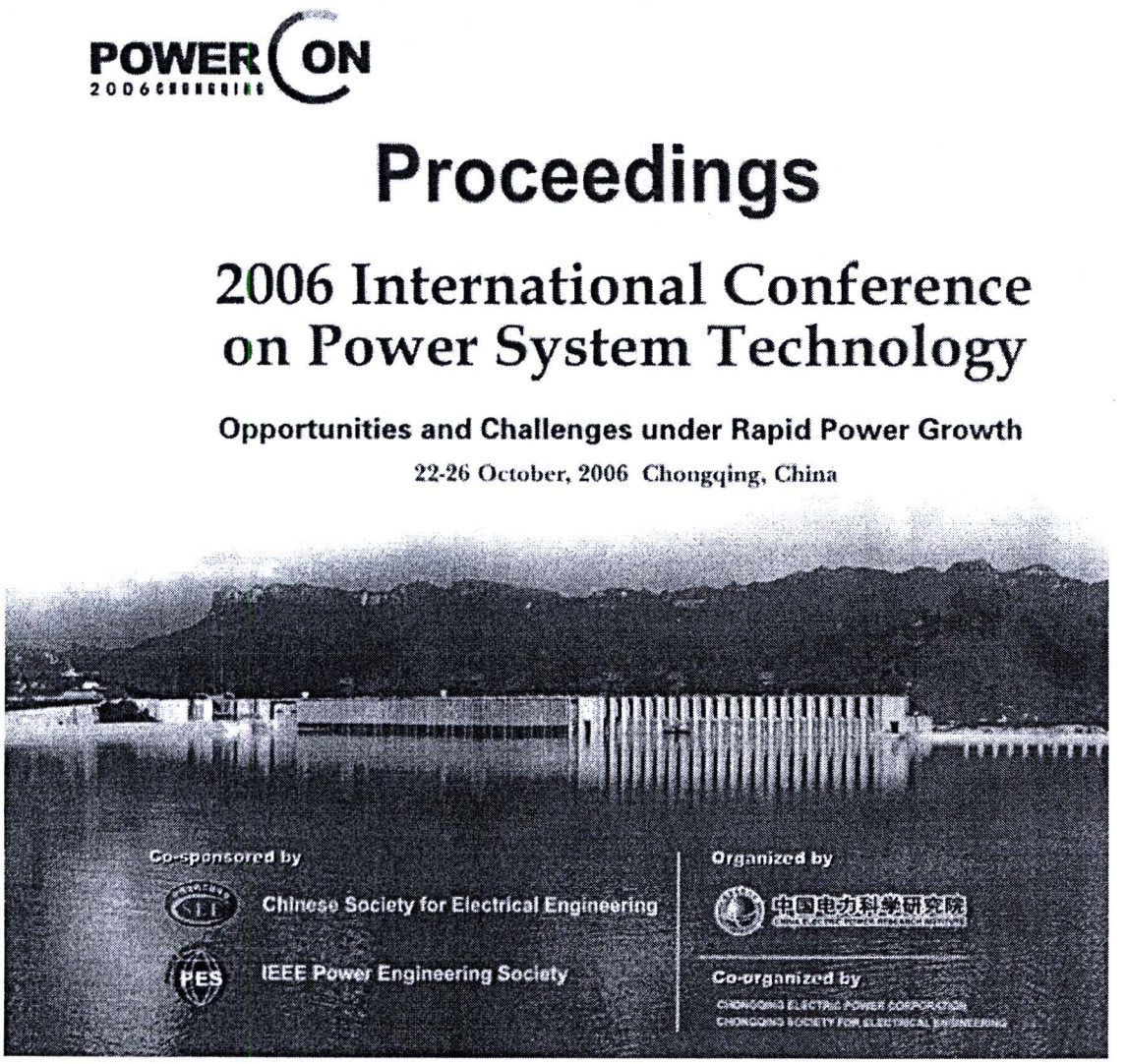

Wavelet based Capacitor Bank Adaptive Controlled Switching and its Application to RDDS Approximation for already installed Circuit Breaker

Noppadol Charbkaew and Teratam Bunyagul, *Member, IEEE*

Abstract-- **The conventional adaptive compensation of capacitor bank synchronous switching requires additional current transformers for detection of circuit breaker's making point, resulting in increased costs and installation time. This led to invention of a new algorithm that is adaptively compensates for variation in closing time. The new algorithm removes the need for current transformers or special sensors. It uses only phase voltage signals. The algorithm can be used with any circuit breaker model and independent from network's R, L, C properties. Using wavelet transform and 'Widest Frequency Band algorithm', the making point can be detected with robust to noise interference.**

A method is also developed to approximate the rate of decrease of dielectric strength (RDDS), which enables faster compensation adapting

Index Terms-- **Capacitor Bank, Circuit Breaker, Point on Wave, Rate of Decrease of Dielectric Strength (RDDS), Switching Transients, Synchronous Switching, Wavelet Transforms, Widest Frequency Band Algorithm**

I. Nomenclature

Closing Time: Time from energizing the closing coil until contact touch in the circuit breaker.

Closing Point: The instant of contact touch in the circuit breaker.

Make Point: The instant of current starts to flow in the circuit breaker.

Wait time: Time from the reference point (zero crossing) until the circuit breaker trigger point.

II. Introduction

Shunt capacitor is widely used in a power system for compensating the reactive power and controlling the line voltage. Its energization lead to severe switching transient e.g. over voltage, voltage magnification, transient over-swing trip of adjustable speed drives [1]-[8]. There are many ways to control the switching surge to be in acceptable level. Such as installing of surge arrestor, pre-insertion impedance and synchronous controlled switching [3]-[5]. Prior to 1990's the synchronous controlled switching was rarely used because the circuit breakers (CB) had not good enough performance and the computing technology at that time was not support for the synchronous controlled switching technology. Since then the development of CBs have provided faster closing operation with smaller deviation. The small deviation of the CB operation can be compensated by microprocessor based Synchronous Switching Controller (SSC) [1], [2], [6].

The severity of the switching surge extremely depends on switching point on voltage wave [4], [7]. Fig. 1, shows a simple model of the capacitor switching. The CB was closed at the zero and 90 degree points on the voltage to obtain the inrush current magnitude at different switching points. Fig. 2, shows that the minimum inrush current magnitude occurs when making point is at the zero degree. This means in theory we should switch a CB to energize a capacitor bank when the voltage across the CB is zero [6], [7].

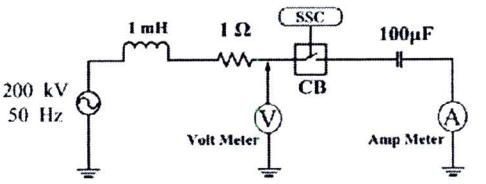

Fig. 1. Simple model of the capacitor energization that is used for simulation

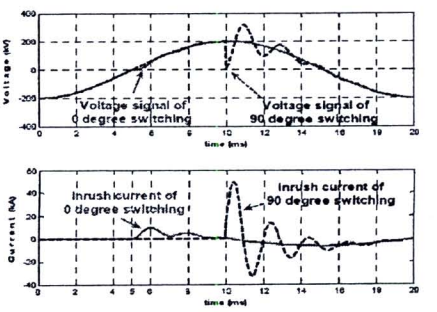

Fig. 2. Bus voltages and capacitor inrush currents at the 0 and 90 electrical degree switching

III. Capacitor Bank Controlled Switching

Theoretically, the target of the capacitor bank switching is at the zero degree point on voltage across CB. The making

This work was supported in simulation tools by Control and Protection System Division, Electric Generation Authority of Thailand.

Noppadol Charbkaew and Teratam Bunyagul are with Department of Electrical Engineering, Faculty of Engineering, King Mongkut's Institute of Technology North Bangkok, Bangkok, Thailand
(email: noppadolc@kmitnb.ac.th , teratam@kmitnb.ac.th)

instant can be controlled by SSC. After the closing command arrive, the SSC will seek for the reference point and waits for the calculated trigger point then trig the CB. By these mechanism, the CB making point will occur at the target point, as shown in Fig. 3, [1], [4], [7]. However the CB closing time is not exact. The CB closing time is deviated by many factors, such as number of operation, ambient temperature, changing of RDDS, etc [4], [6], [7].

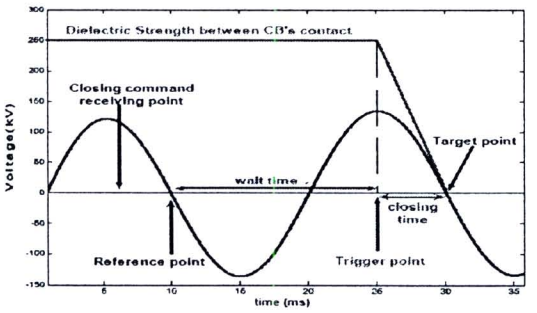

Fig. 3. Capacitor bank synchronous controlled switching timing

The research is focused on the compensation of CB closing time deviation that depends on its age and number of operations. Many times of CB operation cycles cause the mechanical characteristic change. The variation of the CB closing time tends to increase as illustrated in Fig. 4,. The adaptive compensation is an effective method for mitigate this problem.

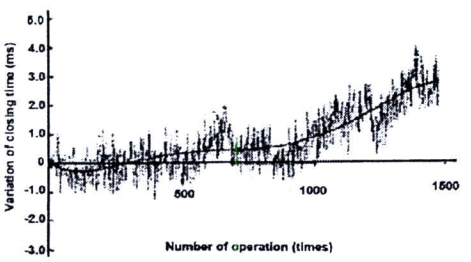

Fig. 4. Variation of the closing times following a number of consecutive operations [1]

The adaptive technique uses the previous making instant for adapting the new wait time accordingly. The novel technique does not require a special sensor to detect the making instant. This is unlike conventional SSCs that determine the making instant by using additional CT to detect the instant flow of capacitor current [1], [3], [4], [6], [7]. It is important to note that this new technique is CB and network independent.

IV. Wavelet Transform

In this work, Wavelet Transform (WT) is used for the making point detection. WT is a mathematical tool that transforms the signal in time domain to time-frequency domain. Its concept is similar to Short Time Fourier Transform (STFT). STFT decomposes the original signal to a set of 'sinusoidal signals' with different frequencies. The coefficients of STFT are proportional to the correlation coefficients of the original signal with the unit complex sinusoidal in each frequency.

WT decomposes the original signal to a set of wave like signals, called 'wavelet'. These wavelet signals are the scaled (dilated) and shifted forms of mother wavelet, as shown in Fig. 5,.

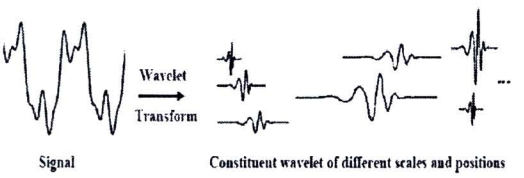

Fig. 5. Signal decomposition using wavelet transformation [2]

The WT coefficient can be calculated by following expression.

$$C(a,b) = \int_{-\infty}^{\infty} f(t)\frac{1}{\sqrt{a}}\psi(\frac{t-b}{a})\,dt \qquad (1)$$

Where, ψ is the wavelet function and its shape varied by variables **a** (dilation) and **b** (position). Fig. 6, shows the example of the mother wavelet, dilated wavelet (a = 2) and position shifted wavelet (b = 10). The observation can be made that the smaller the dilation means the higher the frequency. The greater the position shifted means the longer the delay.

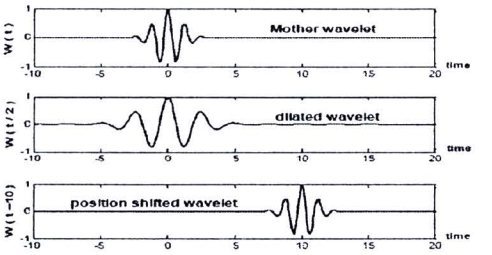

Fig. 6. Mother wavelet, dilated wavelet (a=2) and position shifted wavelet (b= 10)

The great advantage of WT is the ability to analyze transient signals. This is because it is able to decompose the selected frequency component at any time instant. Even a small discontinuity barely visible can still be detected [9].

V. Making Point Detection

The capacitor bank energization switching causes sudden change of the bus voltage [4]. The discontinuity appears on the voltage waveform. This can be demonstrated by a simple RLC circuit as shown in Fig. 1,.

The model was simulated in PSCAD/EMTDC to generate

the signals for testing the algorithm. CB making points were varied from 19.0 to 22.6 ms (-18° to 46.8°) in a step of 0.2 ms.

Fig. 7., shows the comparison of switching points at 0 and 46.8 electrical degrees or at 20 and 22.6 ms respectively. Switching at the exact zero degree point causes the smallest voltage signal fluctuation and it is the most difficult making point detection. For this reason, the 'zero switching signals' are used for algorithm performance testing, although in the practice 'zero point' is not used to be the switching target [8].

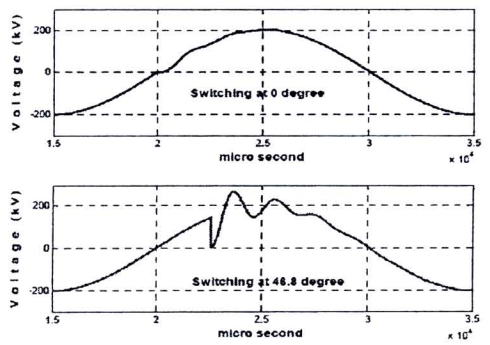

Fig. 7. Comparison of bus voltage that are switched at 0 and 46.8 degree (at 20 and 22.6 ms respectively)

The voltage signal is suddenly changed at the making point. The fast changing of signal (abruption) reflects the local high frequency signal. That means the switching point can be detected by seeking the local high frequency of the signal.

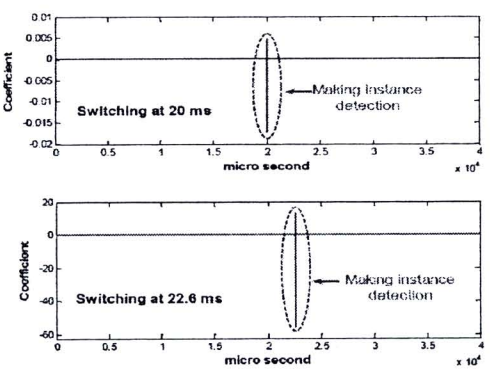

Fig. 8. Detail signals of switching at 0° and 46.8° (20 & 22.6 ms respectively)

A low dilated wavelet called 'unit scale fifth order Coiflets wavelet' extracts the high frequency component from the signal as shown in Fig. 8,. The making point can be obtained by evaluating the absolute maximum the signal in Fig. 8,. The lowest spike magnitude occur when apply the zero voltage switching point. It confirms that switching at zero voltage point is the most difficult to detect. The spike magnitude of switching at 46.8° is much higher and easier to detect.

A. Mitigation of noise problem

The noises may interfere with the measured signals. In the experiment, noises were added to the voltage signal as shown in Fig. 9,. Then let the algorithm determined the switching point again.

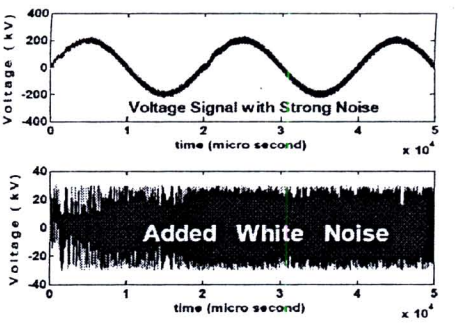

Fig. 9. The voltage signal with white noise interference and the added white noise

The detail signals which are received from wavelet transform are shown in Fig. 10,. The algorithm miscalculated the making point of near the zero voltage switching. The near peak voltage switching could be correctly detected. That means the single scale detection algorithm is not robust to the noise interferences.

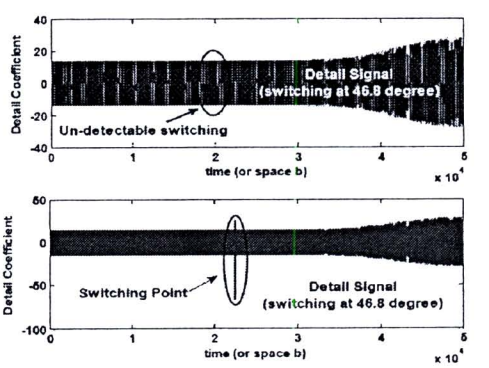

Fig. 10. Comparison of making point detection of switching at 0 and 46.8 degree (with noise interference)

B. The Widest Frequency Band Algorithm

The algorithm is called Widest Frequency Band. This is because the algorithm detects the making instant by using the property of abruption. The discontinuous point was decomposed to a wide range of frequency signals. This method is robust to noises. Fig. 11, shows the wavelet coefficient plot of zero point switching without noise interference.

The switching instant (at about 20 ms) has the highest

coefficient and widest frequency band as seen in Fig. 11,.

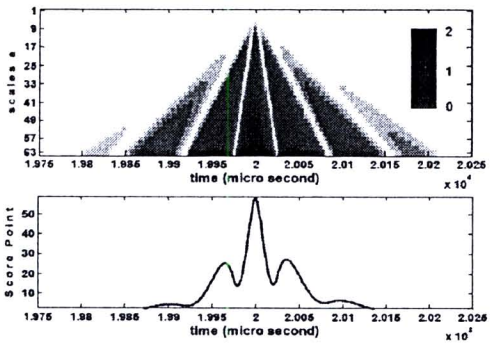

Fig. 11. Spectrogram of zero point switching without noise and the instantaneous score point

It illustrates that the making point has the widest frequency components. The making point can be detected by the method of calculating the sum along the vertical line's coefficient that reaches the maximum. The highest score point is determined by summing all coefficients that have the same b value as the following expression.

$$score(b) = \sum_{a=1}^{n} C(a,b) \qquad (2)$$

Where a is the scale (dilation). Fig. 12, is the color-scale coefficient plot of zero point switching (at b= $2*10^4$ or 20 ms) with strong noise signal. The result of algorithm show that the position of maximum score is at about b= $1*10^4$ (1 ms). The detection was incorrect because there are very high coefficient at that region. Therefore, the maximum score is no longer reflex the making point.

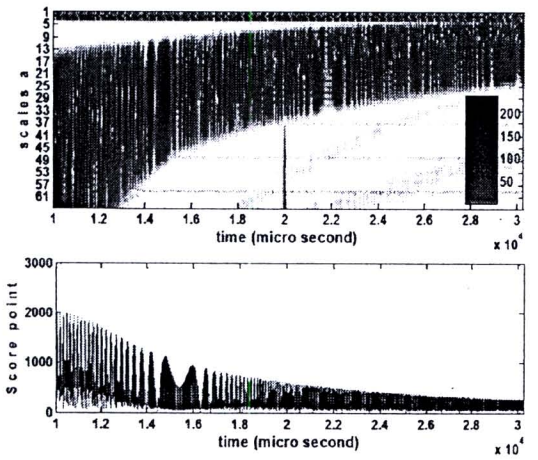

Fig. 12. Color-scale spectrogram and the instantaneous score point of zero point switching with noise interference

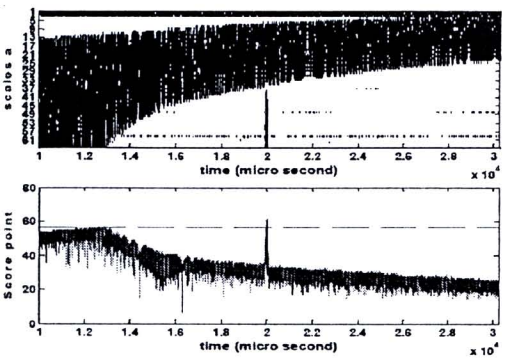

Fig. 13. Black & White spectrogram and the instantaneous score point of zero point switching with noise

After applying the algorithm, it is detected the correct switching point, b= $2*10^4$ (2 ms). This can be observed by a summation of vertical lines that reaches the maximum value at 2ms.

VI. RDDS Approximation

Using SSC, the making instant can be detected. As Fig. 14 shows two CB switching, the making instant of the first and the second switching occur at point A and C respectively. Also the shifting of closing target can be controlled. That means the length between point A and B also can be controlled.(in Fig. 14, length AB is 3 ms) The RDDS (slope of line BC) can be determine by the follow equation.

$$RDDS = \left(\frac{L_{CD}}{L_{DB}} \right) \qquad (3)$$

Where L_{CD} and L_{DB} are the length of line CD and line DB respectively.

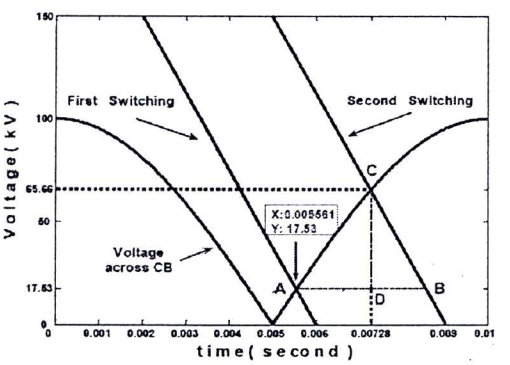

Fig. 14. The RDDS approximation using twice CB switching

From Fig. 14, the length of line CD and line DB can be determine by follow

$$L_{CD} = 65.66\text{-}17.53\text{=}48.13 \text{ kV}$$

$$L_{DB} = L_{AB}\text{-}L_{AD}$$

$$= 0.003\text{-}(0.00728\text{-}.005561)$$

$$= 0.00128 \text{ s}$$

$$RDDS = \left(\frac{L_{CD}}{L_{DB}}\right)$$

$$= \frac{48.13}{0.001281}$$

$$= 37572 \quad kV/s$$

VII. Wait Time Adapting

For the conventional SSCs, after acquiring the making instant, the SSC will know whether the making instant is too late or too early. But it can not detect the error of its closing point. The SSC will calculate the new adapted value then subtract it with the previous wait time. The adapted value is not the closing error, but it is the switching error multiply with creep factor (c), as below

$$WaitTime_{new} = WaitTime_{old} - (making\_error * c) \quad (4)$$

Creep factor is used because the error that was observed by conventional SSCs is the making instant error not the closing contact error. The selected c value will be high or low depending on the performance of the CB, RDDS, scattering of closing time and the type of switching error. If the switching is too late, c will greater than one, vice versa the selected c is less than one. This adapting method uses more than one switching cycle to reach the desired target.

The approximate able of RDDS value lead to the new wait time adapting method. The closing instant can be determined by the follow equation.

$$t_{closing} = \frac{V_{make}}{RDDS} + t_{make} \quad (5)$$

Where $t_{closing}$, t_{make} and V_{make} are the closing point, making point and making voltage (pre-arcing voltage) respectively. After the closing point error is acquired, the new adaptive method can be done by the following

$$WaitTime_{new} = WaitTime_{old} - (closing\_error) \quad (6)$$

Using new method, the target can be reached by only single switching cycle.

VIII. Adaptive Algorithm Testing

The algorithm with and without RDDS approximation were done by simulated on PSCAD/EMTDC. The capacitor bank, SSC and CB with adjustable RDDS were modeled. The capacitor bank was switched 10 cycles with controlling of SSC. Every end of switching cycle, the PSCAD/EMTDC will send the voltage signal to the adaptive compensation module that ran on MATLAB. The module will detect the making instant. Then the new wait time was determined and sent back to the SSC in PSCAD/EMTDC and the next switching cycle will start again, as shown in Fig. 15,.

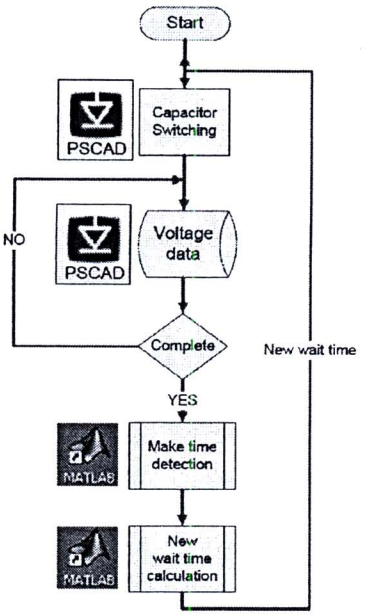

Fig. 15. The adaptive algorithm testing process which implemented on PSCAD/EMTDC and MATLAB

In the simulation, initial value of wait time is 8 ms, the RDDS is 400*2π*50 kV/s and the creep factor in (4) is one. The target point is set at the zero point. The result, switching error in each switching cycle is illustrated in Fig. 16,.

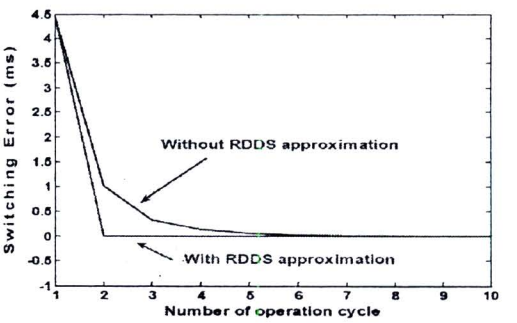

Fig. 16. Comparison the switching error between with and without RDDS approximation.

The result shows that without RDDS approximation, the target point can be reached but it takes about 6 adapting cycle.

While the adaptive algorithm with RDDS approximation can reach the target with only single adapting cycle.

IX. Discussion and Conclusion

The RDDS approximation technique can compensate the deviation of the circuit breaker closing time with only single adapting cycle. Acquiring of RDDS also can be used for monitoring the health of CB. The 'wavelet based widest frequency band' was applied with the adaptive algorithm. It can work without additional signal from a current transformer and robust to noise interference.

The approximation of RDDS is sensitive with the scattering of CB closing time. This problem can be reduced by use the average values of multiple switching. The RDDS approximation method has the limitation that it can use only when the system voltage magnitude and system envelopment in each switching must be nearly the same value.

. The next working step is to implement this algorithm with a FPGA target and also on DSP controller then test them with a digital real-time simulator (HYPERSIM).

X. References

[1] H. Tsutada, T. Hirai, H. Kohyama, H. Ito and K. Sasaki, "Development of Synchronous Switching Controller for Gas Circuit Breakers" Transmission and Distribution Conference and Exhibition 2002: Asia Pacific. IEEE/PES Volume 2

[2] E.P. Dick, D. Fischer, R. Marttila, C. Mulkins, "Point-On-Wave Capacitor Switching and Adjustable Speed Drive", IEEE Transaction on Power Delivery, Vol. 11, No. 3, July 1996

[3] C.D. Tsirekis, N.D. Hatziargyriou, "Control of Shunt Capacitor and Shunt Reactors Energization", IPST 2003 in New Orleans, USA

[4] "Understanding High Voltage Circuit Breaker", Chapter 7, ABB Switchgear, 2003

[5] Liuling Li, Y. QIU, "Controlled Switching of Circuit Breaker and Its Site Measurement in Power Distribution System", ISEIM 2001, Page(s):777 - 780

[6] H. Ito, "Controlled Switching Technologies, State-of-the-Art", Transmission and Distribution Conference and Exhibition 2002: Asia Pacific. IEEE/PES

[7] "Control Switching Buyer's Guide", 2004-2005,ABB

[8] H. Kohyama, K. Wada, H, Ito, M. Hidaka, S. Billings, T. Sugiyama, H. Yamamoto, "Development of 550kV and 362kV Synchronous Switching Gas CirCuit Breakers" IEEE, 2001

[9] M. Misiti, Y. Misiti, G. Oppenheim, J. Poggi, "Wavelet Toolbox for Use with MATLAB user guide", MathWorks, Inc.,1996

[10] Otsu, N., "A Threshold Selection Method from Gray-Level Histograms," IEEE Transactions on Systems, Man, and Cybernetics, Vol. 9, No.1, 1979

XI. Biographies

Noppadol Charbkaew graduated with B.Eng in electrical engineering from King Mongkut's Institute of Technology North Bangkok (KMITNB), Thailand in 2001 and M.Eng in Elektro- and Informationtechnik from Rosenheim University of applied sciences, Germany in 2003. He is currently working toward Ph.D. degree at KMITNB. His research activities and interests are implementation of signal processing in power system protection, control and monitoring.

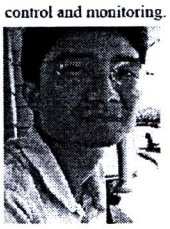

Teratam Bunyagul received BEng (second class honor) degree in electrical engineering from King Mongkut's Institute of Technology North Bangkok (KMITNB) in 1995. He obtained his M.Sc and Ph.D degrees from University of Manchester Institute of Science and Technology (UMIST), UK in 1998 and 2003 respectively.

He currently holds the position Head of Power System Laboratory for the department of electrical engineering at KMITNB. His main activity during academic career has involved research into new techniques in power system protection and control, the design and development of new types of protection relays and control systems

3. Controlled Switching based RDDS Approximation of Capacitor Bank Gas CircuitBreaker by Different Voltage Method

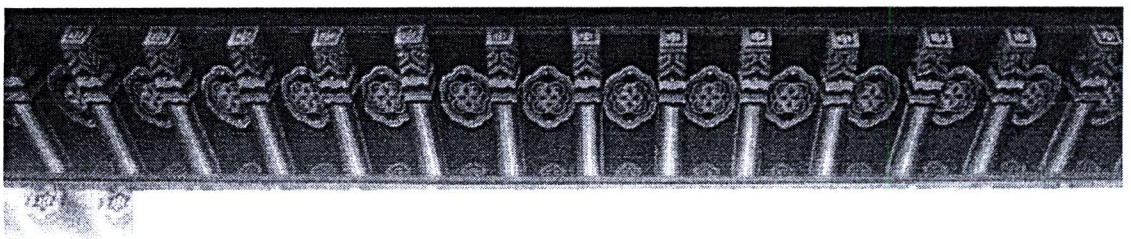

Proceedings of International Conference on Advanced Power System Automation and Protection

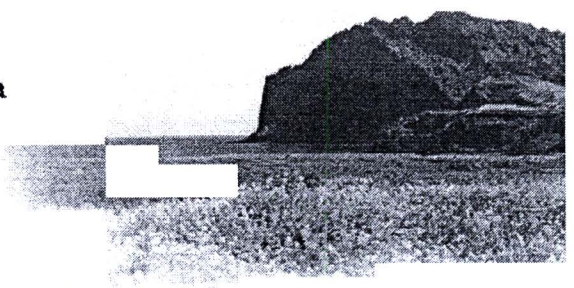

Ramada Plaza Jeju Hotel, Jeju, Korea
April 24-27, 2007

Organized by :
- Next-generation Power Technology Center **(NPTC)**
- The New Power System Technologies Group(2nd **BK21**), Myongji Uni

Technically Sponsored by :
- The Korea Institute of Electrical Engineers **(KIEE)**
- The Institute of Electrical Engineers of Japan **(IEEJ)**
- International Council on Large Electric System **(CIGRE)**

Sponsored by :
- Ministry of Science and Technology, Korea **(MOST)**
- Korea Science and Engineering Foundation **(KOSEF)**
- Korea Electric Power Corporation **(KEPCO)**

APAP 2007

Controlled Switching based RDDS Approximation of Capacitor Bank Gas Circuit Breaker by Different Voltage Method

Noppadol Charbkaew, Teratam Bunyagul and Yotaka Chompusri

Abstract—**A shunt capacitor is widely used in a power system for supporting the line voltage and compensating the reactive power. Its energization causes switching transient which leads to problems in the system e.g. over voltage, voltage magnification, transient over-swing trip of adjustable speed drives. These problems can be mitigated by switch the capacitor bank at the appropriate time (zero voltage target point). The switching target point is determined by a synchronous switching controller (SSC) that controls the close signal of a circuit breaker (CB). The calculation of the switching target point has to include the circuit breaker closing time. However the circuit breaker closing time changes due to its age, number of operations and environment. It is very important to be aware of the change of the CB closing time in designing the SSC.**

The paper presents a novel algorithm to estimate the gas circuit breaker (GCB) closing time using Rate of Decrease of Dielectric Strength (RDDS) value. As a result the SSC will have an ability to automatically adapt switching point to suit any GCB. It is important to note that RDDS can commonly be measured from a type test process on an off-line GCB. This paper also proposes a different voltage technique to calculate the RDDS of an ungrounded capacitor bank GCB using on-line monitoring.

Index Terms– **Capacitor Bank, Gas Circuit Breaker, Point on Wave, Rate of Decrease of Dielectric Strength, RDDS, Switching Transients, Synchronous Switching**

I. Nomenclature

Closing Time: Time from energizing the closing coil until contact touch in the circuit breaker.

Closing Point: The instant of contact touch in the circuit breaker.

Make Point: The instant of current starts to flow in the circuit breaker.

Pre-arcing time: Time duration from the instant of pre-strike to contact touching.

This work was supported by Faculty of Engineering, King Mongkut's Institute of Technology North Bangkok

N. Charbkaew and T. Bunyagul are with Department of Electrical Engineering, Faculty of Engineering, King Mongkut's Institute of Technology North Bangkok, Bangkok, Thailand
(email: noppadolc@kmitnb.ac.th , teratam@kmitnb.ac.th)

Y. Chompusri is with Department of Industrial Electrical Technology, Faculty of Engineering, King Mongkut's Institute of Technology North Bangkok, Bangkok, Thailand (email: ycps@kmitnb.ac.th)

II. Introduction

THE sudden change of a capacitor bank terminal voltage when the capacitor is randomly switched into a power system may cause an inrush current. The high inrush current leads to many repercussions [1], for instance, over voltage and damage of the capacitor bank. These consequences can be decreased by reducing the sudden change of the capacitor bank terminal voltage when switching. There are common ways to solve the inrush current problem, for example, a pre-insertion impedance switching or a synchronous controlled switching. The pre-insertion impedance switching is simple, applies uncomplicated controller and can be used with any types of circuit breaker (CB). However, the inrush current remains high comparing with the steady state current. This is because there is still the difference at the terminal voltage of the capacitor bank while switching.

Fig. 1, illustrates a simple model in PSCAD/EMTDC to demonstrate the inrush current occurred when switching a capacitor bank with different techniques. The result currents from the switching are shown in Fig. 2.

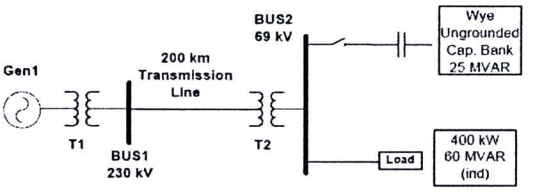

Fig. 1. Schematic of capacitor bank switching study

The top most of Fig. 2, shows that the direct switching results in very high inrush current of 2058A. It is about ten times of the steady state current. The maximum current of the pre-insertion switching is 640A as shown in the middle of Fig. 2,. The synchronous controlled switching yields minimum inrush current of 256A that almost equals to the steady state current.

The synchronous controlled switching has an advantage of very low to near zero inrush current. This is the result of precision control on the switching instance. To gain the advantage, the synchronous switching controller (SSC) requires the use of high specification circuit breaker. The circuit breaker also has to be able to close in single pole operation. The accuracy of the method depends heavily on the closing time of the circuit breaker. The closing time is

influenced by following operational parameters, the system voltage, control voltage, hydraulic oil pressure, ambient temperature and number of consecutive operation, etc [1]-[12].

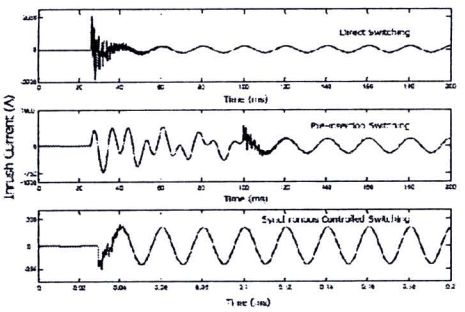

Fig. 2. Inrush current of capacitor bank switching

Although there are more conditions in using SSC than the pre-insertion impedance switching, modern high voltage substations prefer employing SSCs. This is because of the advantage of very low inrush current. The paper developed a new technique used in the synchronous switching controller. The technique was designed to adaptively compensate the circuit breaker operation parameters mentioned above to get more accurate switching instance.

III. CAPACITOR BANK CONTROLLED SWITCHING

The key point of the capacitor bank controlled switching is to control the make point of the circuit breaker to be at the zero point on the voltage waveform (zero point on wave). The procedures as shown in Fig.3, are as followed: Firstly the SSC receives a closing command. The SSC then seeks for a zero crossing point as a reference point. From the instance of the reference point the SSC wait for specific time delay. This specific delay is called 'wait time'. When the wait time is reached, the SSC trigs the circuit breaker. Consequently the circuit breaker closes on time for the closing point that is at the zero point on wave. In the ideal case the capacitor current will be conducted exactly at the zero point.

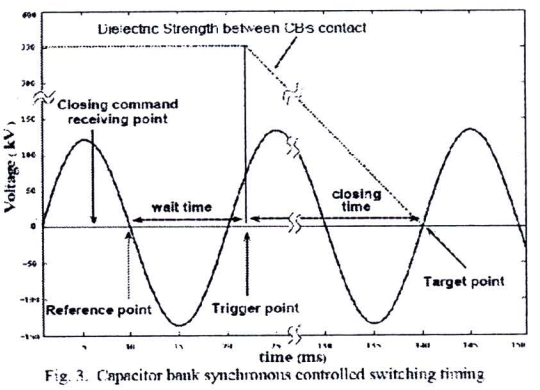

Fig. 3. Capacitor bank synchronous controlled switching timing

It is very important to note that the wait time will be calculated based on known closing time of the circuit breaker. If the closing time of the circuit breaker changes, the SSC has to be able to calculate a new wait time for the next closing operation.

The closing time of the circuit breaker tends to be longer for a number of consecutive operations. This is caused by the changes of friction or/and striking force of the circuit breaker moving parts [2] and other parameters as mentioned in the introduction. A close loop control is needed to calculate the new waiting time that is influenced by the closing time deviation of the circuit breaker. The capacitor current conduction point (make point) is normally used as a feedback signal. The make point can be detected using current transformers installed between the circuit breaker and capacitor bank as shown in Fig.4,. Hence the SSC can adapt the wait time using the information from the feedback signal.

It is also possible to detect the make point without using the current transformers. This is done by detecting abrupt change in voltage when the current conducts. The technique uses wavelet transform and Widest Frequency Brand Algorithm [3].

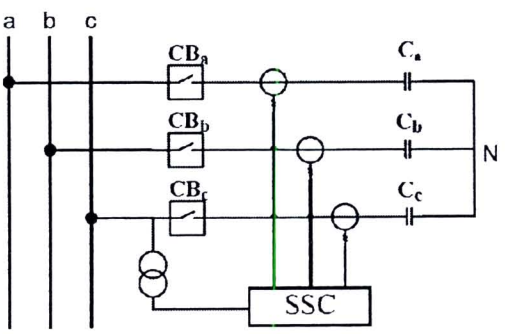

Fig. 4. Using of current transformer for making point detection

IV. EFFECT OF RDDS VALUE TO GCB CLOSING

Rate of Decrease of Dielectric Strength refers to the closing speed of the circuit breaker contacts. Fig. 5 illustrates the different RDDS values that affect the making points of the circuit breaker. The figure shows that CB1 has higher RDDS than of CB2. It is obvious that when these two circuit breakers start to close at the same time at about 6ms, they arrive at different making points. CB1 has higher RDDS hence it's dielectric strength decreases faster. From 11ms onwards CB1 has dielectric strength lower than its stress. At this point the CB1 starts conducting the current.

It is easier to control the making point of the circuit breaker that has high RDDS. This is because the slope of the dielectric strength will be very steep. Then the making point can be controlled to occur at very low stress (low voltage). Thus the high RDDS GCB is preferred for the synchronous controlled switching.

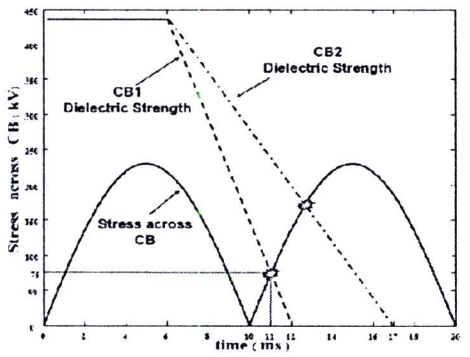

Fig. 5. Closing of different RDDS CBs

V. RDDS MEASUREMENT

It is common that RDDS can be acquired from the switching test. The test is carried out in an off-line condition. The pre-strike voltage and pre-arcing time are used to calculate RDDS as in (1) [2].

$$RDDS = \frac{pre\_strike\,voltage}{pre\_arcing\,time} \tag{1}$$

For example in Fig. 5, CB1 has RDDS as followed

$$RDDS_{CB1} = \frac{75kV}{(12-11)ms} = 75 \quad \frac{MV}{s} \tag{2}$$

It is worth mentioning that the pre-arcing time is difficult to measure. This is because it is difficult to detect the instance of the contacts touching. Although the auxiliary contacts are available, there will be some time variation from the main contacts [12].

VI. ONLINE RDDS APPROXIMATION

A typical SSC controls each pole of the GCB to be switched in sequences. For ungrounded capacitor bank in 50Hz system, the first two poles will be closed at the same time at the equal voltage point as shown in Fig. 6,. Then the third pole will be closed at 5ms later.

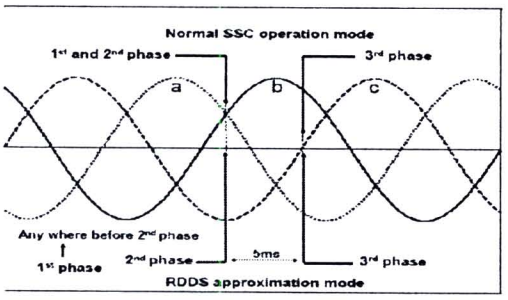

Fig. 6. CB closing sequence for normal SSC and for RDDS approximation

The paper propose the on-line RDDS approximation. The switching sequences are slightly different. The first pole (phase A shown as CB_a in Fig. 7,) can be switch at any time instance. Having switched the first pole, the pre-arcing does not occur because the capacitor circuit is still opened. After the first pole is closed, the stress on the remaining poles will increase to equal the line voltage. The second pole is then controlled to close at zero line voltage (V_{ab}=0). There will be a sudden change of the stress across the third pole (CB_c). The voltage across CB_c in Fig.7, can be defined by

$$V_{CBc} = V_c + \left(\frac{V_{ab}}{2} - V_a\right) \tag{3}$$

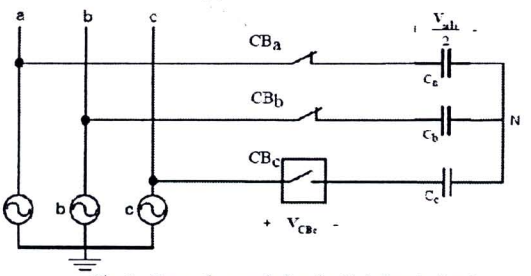

Fig. 7. Status of system before the third phase is closed

The phasor diagram in Fig. 8, shows that V_{CBc}=1.5xV_c

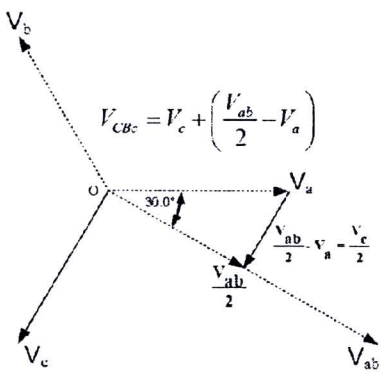

Fig. 8. Phasor diagram of voltage across CB_c in Fig. 7.

The operating sequences indicate that we can control the voltage across GCB to be 1.5 times or 1.732 times phase voltage. This depends on the switching sequences.

Fig. 9. illustrates that we can control the switching of GCB to give different voltages across one of GCB pole. The different of the voltages is 15.4 percent. By energizing the GCB two times in different occasions and different voltages, the dielectric strength will cut across two voltage levels from the first and second switching. The algorithm can detect the differences in voltages (V_1,V_2) and times (t_1,t_2). Therefore RDDS can be calculate by

$$RDDS = -\left(\frac{(V_2 - V_1)}{(t_2 - t_1)}\right) \tag{4}$$

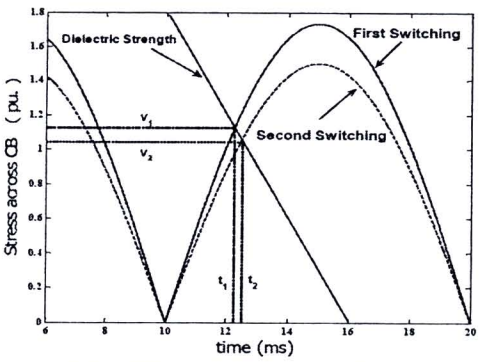

Fig. 9. RDDS approximation using twice CB switching

VII. WAIT TIME ADAPTING

For conventional SSCs, after acquiring the making point, SSC will know whether the making point is too late or too early. However it can not detect the closing point. The SSC will calculate the time to subtract with the previous wait time. The subtracted time is the error multiply with creep factor c [13].

$$WaitTime_{new} = WaitTime_{old} - (making\_error * c) \quad (5)$$

Creep factor is used because the error that was observed by conventional SSCs is the making point error not the closing contact error. The selected c value can be high or low depending on the performance of the GCB, RDDS, scattering of closing time and the sign of making point error. If the switching is too late, c will be greater than one. If the switching is too early, the selected c is less than one. This adaptive method uses more than one switching cycle to reach the desired target.

The approximation of RDDS value in this paper leads to the new wait time adapting method. The closing instant can be determined by

$$t_{\text{closing}} = \frac{V_{\text{make}}}{\text{RDDS}} + t_{\text{make}} \quad (6)$$

Where $t_{closing}$, t_{make} and V_{make} are the closing point, making point and making voltage (pre-arcing voltage) respectively. After the closing point error is acquired, the new adaptive method can be done by the following

$$WaitTime_{new} = WaitTime_{old} - (closing\_error) \quad (7)$$

Using the new method, the target can be reached by only single switching cycle.

VIII. ADAPTIVE ALGORITHM TESTING

The algorithm with and without RDDS approximation were simulated on PSCAD/EMTDC. The capacitor bank, SSC and GCB with adjustable RDDS were modeled. The capacitor bank was switched 10 cycles with controlling of SSC. Every ending of switching cycle, the PSCAD/EMTDC will send the voltage signal to the adaptive compensation module that run on MATLAB. The module will detect the making point. Then the new wait time is determined and sent back to the SSC in PSCAD/EMTDC and the next switching cycle will start again, as shown in Fig. 10,.

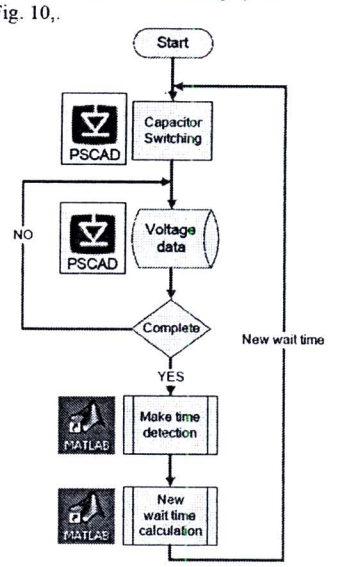

Fig. 10. The adaptive algorithm testing process which implemented on PSCAD/EMTDC and MATLAB

In the simulation, initial value of wait time is 8 ms, the RDDS is 400*2π*50 kV/s and the creep factor is one. The target point is set at the zero point. The result, switching error in each switching cycle is illustrated in Fig. 11,.

The result shows that without RDDS approximation, the target point can be reached at about 6 adapting cycle. While the adaptive algorithm with RDDS approximation can reach the target with only single adapting cycle.

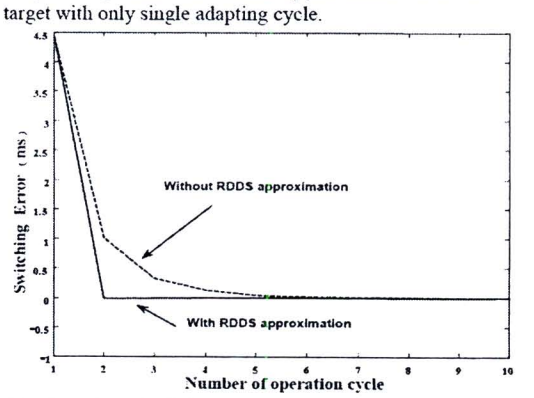

Fig. 11. Comparison of switching error between with and without RDDS approximation.

IX. Discussion and Conclusion

The ability of monitoring of RDDS value not only be used in the adaptive process of SSC, it can also be used for the CB condition assessment. If the RDDS value is not in the acceptable value, SSC will send warning signal.

The approximation of RDDS is sensitive with the scattering of CB closing time. This problem can be reduced by use the average values of multiple switching. The RDDS approximation with different voltage method has the limitation that it can use only with ungrounded capacitor bank. And it gives accurate RDDS when the system voltages in each switching are reasonably different.

The selection of RDDS approximation method depends on the CB operating type (single or three pole operation) and the system voltage at the second energization. The RDDS approximation with different voltage method can be applied only with single pole operation CB. If the system voltages of first and the second are nearly the same, the RDDS approximation by different target point method [3] is preferred. On the contrary, if the system voltages of each switching are different, the different voltage method is selected.

X. References

[1] H. Tsutada, T. Hirai, H. Kohyama, H. Ito and K. Sasaki, "Development of Synchronous Switching Controller for Gas Circuit Breakers" Transmission and Distribution Conference and Exhibition 2002: Asia Pacific. IEEE/PES Volume 2

[2] Bharat R. Naik, Rick G. Asche, Stan Billings, Haruhiko Kohyama, Hiroki Ito and Hiroshi Yamamoto, "Field Verification of Controlled Switching GCB",Power Engineering Society Summer Meeting,2002 IEEE Volume1

[3] N. Charbkaew and T. Bunyagul, "Wavelet based Capacitor Bank Adaptive ControlledSwitching and its Application to RDDS Approximation for already installed Circuit Breaker", 2006 International Conference on Power System Technology, Chongqing, China

[4] E.P. Dick, D. Fischer, R. Marttila, C. Mulkins, "Point-On-Wave Capacitor Switching and Adjustable Speed Drive", IEEE Transaction on Power Delivery, Vol. 11, No. 3, July 1996

[5] C.D. Tsirekis, N.D. Hatziargyriou, "Control of Shunt Capacitor and Shunt Reactors Energization", IPST 2003 in New Orleans, USA

[6] "Understanding High Voltage Circuit Breaker", Chapter 7, ABB Switchgear, 2003

[7] Linling Li, Y. QIU, "Controlled Switching of Circuit Breaker and Its Site Measurement in Power Distribution System", ISEIM 2001, Page(s):777 – 780

[8] H. Ito, "Controlled Switching Technologies, State-of-the-Art", Transmission and Distribution Conference and Exhibition 2002: Asia Pacific. IEEE/PES

[9] "Control Switching Buyer's Guide", 2004-2005,ABB

[10] H. Kohyama, K. Wada, H. Ito, M. Hidaka, S. Billings, T. Sugiyama, H. Yamamoto, "Development of 550kV and 362kV Synchronous Switching Gas CirCuit Breakers" IEEE, 2001

[11] M. Misiti, Y. Misiti, G. Oppenheim, J. Poggi, "Wavelet Toolbox for Use with MATLAB user guide", MathWorks, Inc.,1996

[12] T. Suwanasri," Investigation on HV puffer-type circuit breakers for condition monitoring parameter selection", 29th Electrical Engineering Conference 2006, Thailand

[13] "Understanding High Voltage Circuit Breaker", Chapter 7, ABB Switchgear, 2003

XI. Biographies

Noppadol Charbkaew graduated with B.Eng in electrical engineering from King Mongkut's Institute of Technology North Bangkok (KMITNB), Thailand in 2001 and M.Eng in Elektro- and Informationtechnik from Rosenheim University of applied sciences, Germany in 2003. He is currently working toward Ph.D. degree at KMITNB. His research activities and interests are implementation of signal processing in power system protection, control and monitoring.

Teratam Bunyagul received BEng (second class honor) degree in electrical engineering from King Mongkut's Institute of Technology North Bangkok (KMITNB) in 1995. He obtained his M.Sc and Ph.D degrees from University of Manchester Institute of Science and Technology (UMIST), UK in 1998 and 2003 respectively.

He currently holds the position Head of Power System Laboratory for the department of electrical engineering at KMITNB. His main activity during academic career has involved research into new techniques in power system protection and control, the design and development of new types of protection relays and control systems

Yotaka Chompusri received B.Eng degree from King Mongkut's Institute of Technology Ladkrabang , Thailand in 1998 and received M.Sc in EE degree from University of Southern California,USA in 2002. She is currently staff at Industrial Electrical Technology Department of King Mongkut's Institute of Technology North Bangkok, Thailand and works in area of signal processing of control system.

4. Vibration Signal Analysis for Condition Monitoring of High Voltage Circuit Breakers

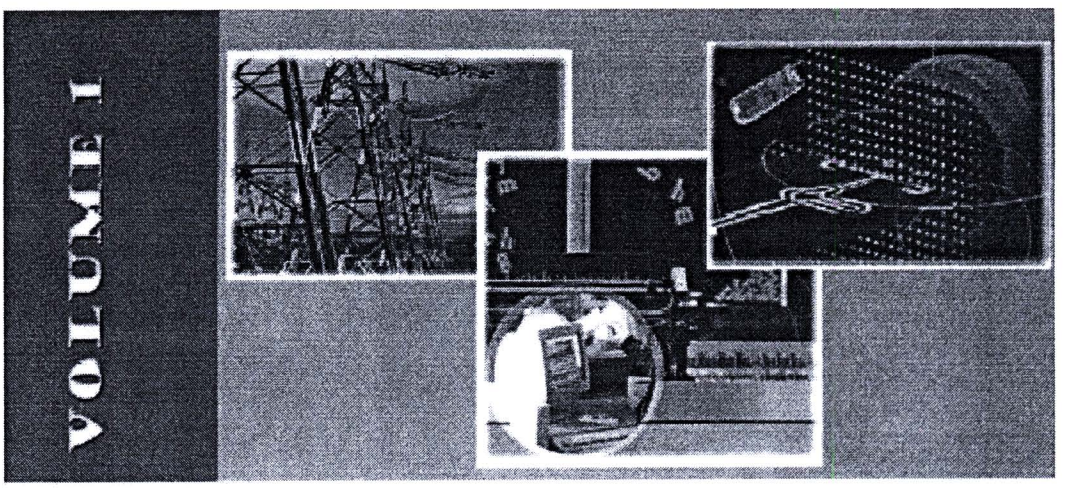

ECTI-CON 2007

Mae Fah Luang University, Chiang Rai, Thailand
May 9-12, 2007

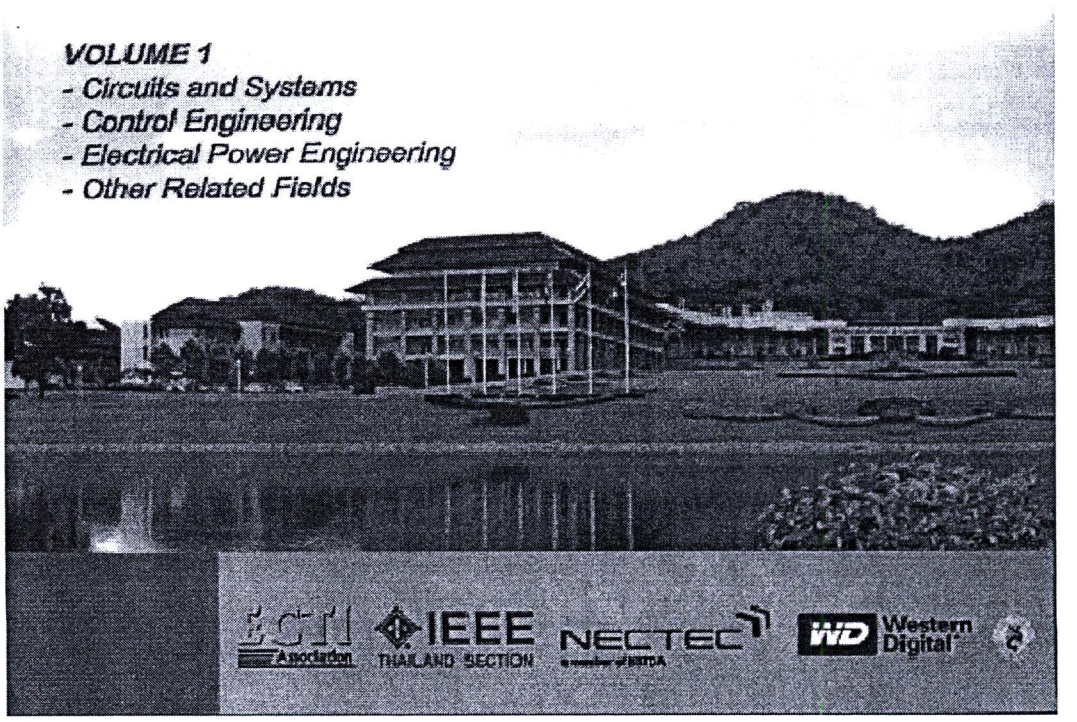

Vibration Signal Analysis for Condition Monitoring of High Voltage Circuit Breakers

T. Suwanasri[1], N. Charbkeaw[2], T. Bunyagul[2]
[1]The Sirindhorn International Thai-German Graduate School of Engineering
[2]Electrical Engineering Department, Faculty of Engineering
King Mongkut's Institute of Technology North Bangkok, Bangkok, 10800, Thailand

Abstract- **Nowadays, the goals of electrical supply utilities are to reduce equipment failures, to extend service life, to increase equipment reliability and to reduce their related operating and maintenance costs. High voltage circuit breaker is also an important element in the electrical network. In order to determine or to detect the abnormal conditions inside the circuit breakers, the powerful vibration techniques have been proposed for many years. Thus, vibration technique by analyzing the signal in time-frequency-domain was performed in this work under no-load switching operations with a commercially available high-voltage puffer-type circuit breaker without opening its major parts. Vibration of circuit breaker poles and operating mechanism as well as various monitored parameters were recorded under normal and variable operating conditions, which were the variations of auxiliary supply voltage, hydraulic oil pressure and SF_6 gas pressure. After that, a sensitivity of vibration method to the variable operating conditions was evaluated.**

I. Introduction

Up till now, the preventive maintenance is predominantly used to maintain circuit breakers after specific time interval or after specific number of operations. Even though nowadays, the reliability of the circuit breaker has been continuously improved by various measures in design and construction of the circuit breakers [1], [2], failures still exist and sometimes cause costly consequences. Therefore, maintenance is inevitably needed. However, this task is very costly, time-consuming and sometimes can incorporate unintentional defects due to excessively invasive maintenance.

The condition monitoring and diagnostic tests, especially with non-invasive techniques, have been developed with aiming to facilitate maintenance activity. Some techniques have been developed so far by many researchers, such as measurement of enclosure vibration to detect abnormal contact condition inside GIS [3], development of acoustic analysis by measuring vibration signals of circuit breaker in laboratory and in field test [4], [5], [6]. The idea is that mechanical malfunctions and abnormal behaviors should be detected as changes in the vibration signatures of the circuit breakers.

In this paper, the diagnostic method by analyzing the vibration signatures in time-frequency domain was presented. The tests were performed with a commercial 110kV SF_6 puffer-type circuit breaker, which is a free-standing pole model with 3-pole operating mechanism. At first, the vibration signature was recorded during no-load switching operations under normal operating condition as a reference fingerprint. After that, the signatures under variable auxiliary supply voltage, variable hydraulic oil pressure and SF_6 gas pressure variation were recorded. After comparison with the reference fingerprint, these intentionally variable operating conditions could be detected as changes in the analyzed vibration signatures.

II. Experimental Setup

This experiment was performed with a 110kV SF_6 puffer-type circuit breaker with hydraulic operating mechanism as shown in Fig. 1 for the experimental setup. The investigation was performed under no-load switching operations. The vibration signals of the free-standing poles and of operating mechanism were recorded under normal and variable operating conditions that could probably occur in service, e.g. variation of control voltage supplied from station service power source or battery from the secondary circuit, SF_6 pressure change due to leakage or over-filling and hydraulic oil pressure change caused by seal and gasket aging.

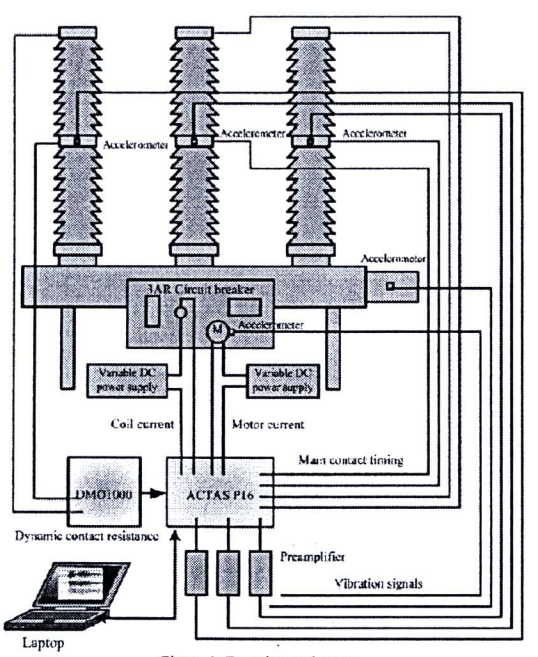

Figure 1. Experimental setup

During each no-load switching operation, other parameters such as close and trip coil current, hydraulic pumping motor current and time, main contact timing, dynamic contact resistance, were also measured as shown in Fig. 2. The measured vibration signatures under normal operating condition were used as a reference base line. The signatures under variable operating conditions summarized in Table I were compared with the reference signature. The tests and measurements were performed in a laboratory because of the readily controlled testing conditions.

The main components of the test system and their details were described as follows:

- A 110kV, 1250A, and 31.5kA puffer-type SF_6 circuit breakers with three-pole-operated hydraulic operating mechanism
- 5 accelerometers type 4501 (B&K) mounted externally at the middle of each pole, hydraulic operating mechanism and pumping motor of the circuit breaker
- 3 preamplifiers type 2626 (B&K) for vibration signal conditioning with optical cable connection to accelerometer
- 1 circuit breaker testing device ACTAS P16[1].
- 1 dynamic contact resistance measurement device DMO1000[1]
- Measurement cables and coaxial cable for serial connection between notebook and measurement device
- 1 notebook as a control unit with ACTAS software program
- 2 variable DC or AC power supply for control circuit and pumping motor
- SF_6 storage and filling unit.

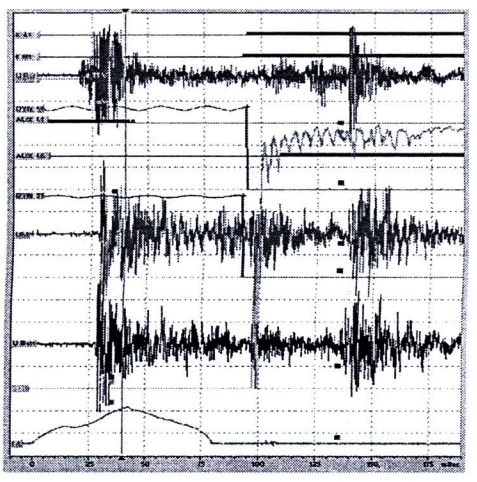

Figure 2. Vibration signals and other measured parameters recorded during closing operation

[1] KoCoS Meßtechnik AG, Südring 42, D-34497 Korbach, Germany

TABLE I
SUMMARY OF TESTING CONDITIONS

Test conditions	Voltage	Oil Pressure (bar)	SF_6 (bar)	Nr. of SW per test
Normal or rated operation	100%	320	6.5	15
Variable supply voltage	115%	320	6.5	15
	70%	320	6.5	15
Variable oil pressure	100%	280	6.5	15
	100%	250	6.5	15
Variable SF_6 pressure	100%	280	8	15
	100%	250	5.5	15

The vibration signals during closing and opening operations were recorded by using accelerometers and a data acquisition system. The vibration measurement consists of the following components:

1. Sensors: The piezoelectric accelerometer is used to measure the vibration signal propagating to the external structure via various parts of the internal mechanism and insulating medium. They were temporarily mounted with adhesive glue on circuit breaker enclosure surface. It produces a charge in proportional to the acceleration (pC/ms^{-2}).
2. Preamplifier and signal conditioner: These devices are needed in order to match the impedance and amplify the signal from accelerometer to reasonable value.
3. Data acquisition: The sampling rate was set at 10kHz. The total record time was set at 200ms for closing operation and 150ms for opening operation.

III. VIBRATION SIGNAL ANALYSIS

A. *Circuit breaker's Vibration Signal*

Vibration signal monitoring can refer to the movement of moving parts inside circuit breaker. The use of vibration signal can be compared with the hearth beating sound. Doctor can analyze the body health by the rhythm of beating. Like in circuit breaker condition assessment, the circuit breaker conditions can be acquired by vibration signal. Fig. 3 shows example signals of circuit breaker during opening and closing operations.

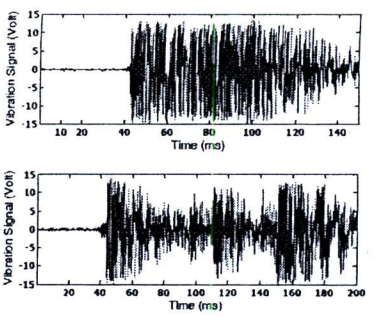

Figure 3. Opening (upper) and closing (lower) vibration signal.

Many sources of acoustic vibration are detected during the closing or opening operation such as the instant of solenoid coins, the impacted of arcing and main contacts. Each source of vibration will generate different vibration signature.

B. Wavelet transform

Wavelet Transform (WT) is a mathematical tool that transforms the signal in time domain to time-frequency domain. Its concept is similar to Short Time Fourier Transform (STFT). The STFT decomposes the original signal to a set of 'sinusoidal signals' with different frequencies. The coefficients of STFT are proportional to the correlation coefficients of the original signal with the unit complex sinusoidal in each frequency.

WT decomposes the original signal to a set of wave like signals, called 'wavelet'. These wavelet signals are the scaled (dilated) and shifted forms of the mother wavelet, as shown in Fig. 4.

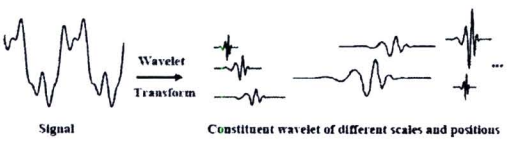

Figure 4. Signal decomposition using wavelet transformation [2]

The WT coefficient can be calculated by using the following expression.

$$C(a,b) = \int_{-\infty}^{\infty} f(t)\frac{1}{\sqrt{a}}\psi(\frac{t-b}{a})\,dt \qquad (1)$$

Where, ψ is the wavelet function and its shape varied by variables **a** (dilation) and **b** (position). Fig. 5 shows the example of the mother wavelet, dilated wavelet (a = 2) and position shifted wavelet (b = 10). The observation can be made that the smaller the dilation means the higher the frequency. The greater the position shifted means the longer the delay.

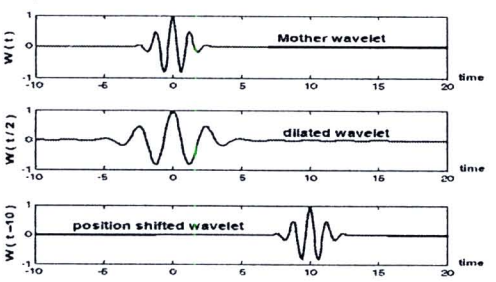

Figure 5. Mother wavelet, dilated wavelet *(a=2) and position shifted wavelet (b= 10)*

The great advantage of WT is the ability to decompose the selected frequency component at any time. Therefore it is suitable to analyze instant transient signals. Even a barely visible small discontinuity can still be detected [7].

The event extraction of time domain vibration signal as in Fig. 6 is not easy to perform by human eye, especially opening vibration signal. The Wavelet transform is applied to enhance the event detection. Wavelet transform is a mathematical tool that transforms a signal in time domain to time-frequency domain. For this resource, the complex morlet with 1 bandwidth parameter and 1.5 wavelet center frequencies is selected. Fig. 6 shows the comparison between opening vibration signal and its transformed signal.

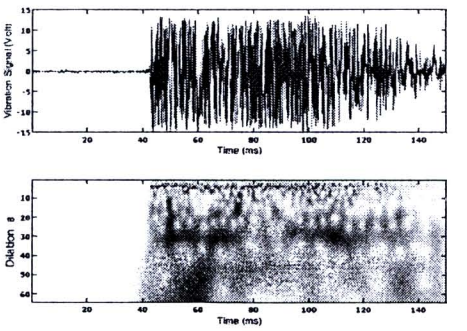

Figure 6. Time domain opening vibration signal (upper) and its wavelet transformed spectrogram (lower)

The wavelet transformed spectrogram in Fig. 6 shows the magnitude of signal in each frequency. At the vertical axis, the higher number of **a** (dilation) refers to the lower frequency signal. The value of horizontal axis is time in millisecond. Moreover, the darker color means the higher magnitude, e.g. the large magnitude low frequency signal (**a**=60) appears at 60ms.

C. Information Extraction from wavelet spectrogram

The wavelet transformed spectrogram contains a lot of information such as moving instant of solenoid armature and its speed, moving instant of moving contact. Fig. 7 shows the wavelet spectrogram of opening operation at normal operation as in table I compared with dynamic resistance (solid line) and delayed solenoid coil current signal (dash line).

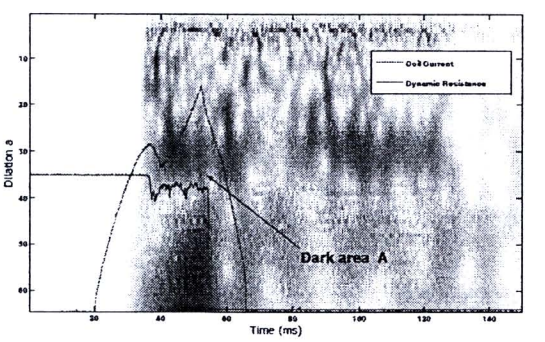

Figure 7. Spectrogram of normal condition closing operation compared with coil current (dash line) and dynamic resistance signal (solid line)

There are a lot of event signatures in the wavelet spectrogram shown in Fig. 7. The starting of shaded area of high frequency scale, at dilation = 1, relates to the starting movement of moving parts. The dark area A at scale of 30 refers to the scratching of arcing contact, and the arcing contact is fully separated at the end of this dark area. This result is confirmed by the comparison with dynamic resistance signal.

IV. Results

A. *Effect of control voltage to vibration signal*

Practically, the dedicate power supply is used to supply the power to every control device including trip circuit. The variation of this control voltage affects to electromechanical mechanism. Fig. 8 shows the comparison between transformed vibration signal of closing operations at 70%, 100% and 115% control voltage.

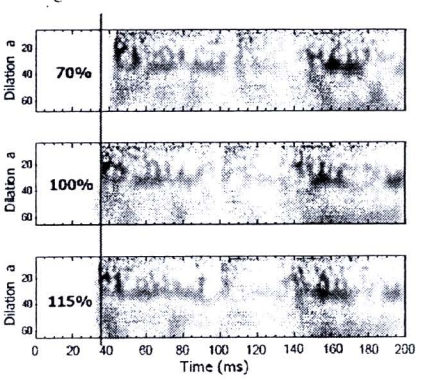

Figure 8. Spectrogram of vibration signal of circuit breaker closing operation which different control voltage

The higher the control voltage, the earlier appearance of the shaded zone of spectrograms occurs. However, the distance between signatures is still similar. Thus, there is no change of contact moving speed.

B. *Effect of hydraulic pressure to vibration signal*

Because the operation of puffer-type circuit break requires extremely high power and high speed, the hydraulic operating mechanism is selected. In the experiment, the hydraulic oil pressure is reduced from 320bar to 280bar and 250bar. The transformed signal is presented in Fig. 9. Each signature shows the same position of starting movement. For the higher hydraulic oil pressure, the faster moving occurs. Therefore, the event signature in this case occurs earlier and the signature becomes shorter, e.g. in Fig. 8, the arcing contact signature of closing operation at 320bar hydraulic oil pressure is much shorter than the others at 280bar and at 250bar.

C. *Effect of SF_6 pressure to vibration signal*

There is no significant effect of SF_6 pressure to the vibration signal. It is not easy to explicitly identify the event signature in the wavelet spectrogram.

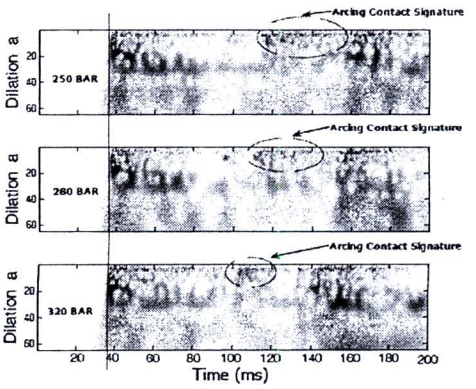

Figure 9. Spectrogram of closing vibration signal which different hydraulic oil pressure

V. Conclusion

The vibration signal analysis was performed in this work by using the wavelet transform in order to investigate the sensitivity of this method according to the variations of circuit breaker operating conditions. The variation of auxiliary supply voltage and hydraulic oil pressure results in reasonable changes in the transformed vibration signature. The variation of SF_6 gas pressure can not be detected by this method.

The changes in the transformed vibration signatures according to the variation of its operating conditions have been verified in this work. Thus, this vibration analysis can be used to observe the significant events occurring inside the circuit breaker. Therefore, further development of this method is recommended to use this as circuit breaker diagnostic tool.

Acknowledgment

The author would like to thank SIEMENS AG in Erlangen, Germany and Institute for High Voltage Technology, RWTH Aachen University, Germany for the cooperation and support.

References

[1] M. Pflaum, et al., "New aspects of the reliability of high voltage circuit breakers", *Cigre' Session Paper* Ref.13-07, published: 1978.

[2] C. A. Fawdrey, "The application of development and diagnostic techniques to circuit breaker reliability", *Cigre' Session Paper* Ref. 13-02, published: 1978.

[3] Y. Ohshita, A. Hashimoto, Y. Kurosawa, "A diagnostic technique to detect abnormal conditions of contacts measuring vibrations in metal enclosures of gas insulated switchgear", *IEEE transaction on power delivery*, vol. 4, pp. 2090-2094, October 1989.

[4] M. Runde, T. Aurud, L. E. Lundgaard, G. E. Ottessen, K. Faugstad, "Acoustic diagnosis of high voltage circuit breakers", *IEEE transaction on power delivery*, vol 7, no.3, pp 1306-1315, July 1992.

[5] M. Runde, G. E. Ottesen, B. Skyberg, M. Ohlen, "Vibration analysis for diagnostic testing of circuit breakers", *IEEE transaction on power delivery*, vol 11, no.4, pp 1816-1823, October 1996.

[6] T. Suwanasri, A. Schnettler, D. Fricke, A. Noack, "Non-invasive condition monitoring of a high voltage circuit breaker", *XIIIth International Symposium on High Voltage Engineering*, Netherlands, 2003

[7] M. Misiti, Y. Misiti, G. Oppenheim, J. Poggi, "Wavelet Toolbox for Use with MATLAB user guide", *MathWorks, Inc., 1996*

5. Experience on Stray Flux Interference of CT

(Case Study of A Power Plant in Thailand)

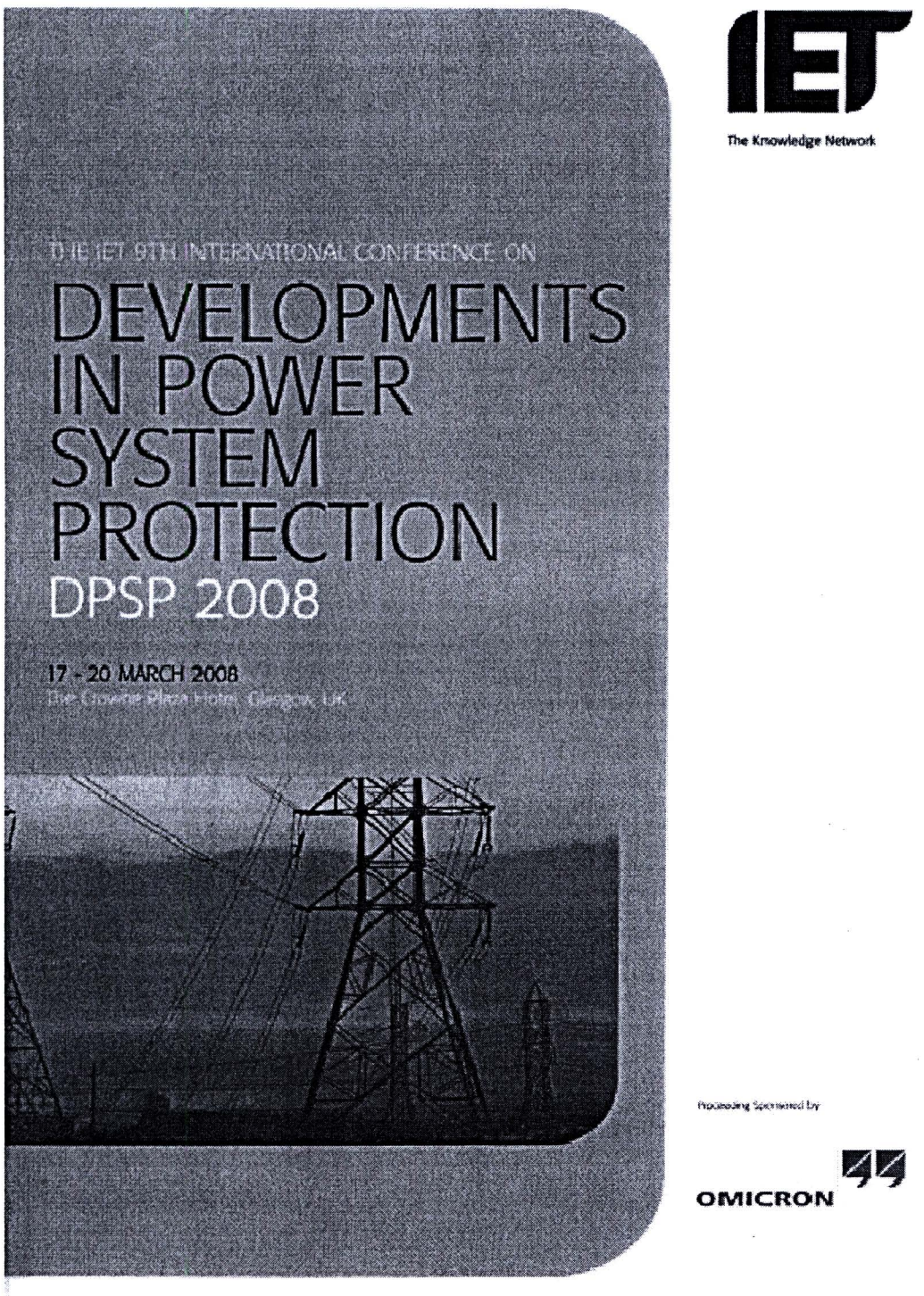

EXPERIENCE ON STRAY FLUX INTERFERENCE OF CT (CASE STUDY OF A POWER PLANT IN THAILAND)

N. Charbkaew*, T. Bunyagul*, Y. Chompusri†

* Department of Electrical Engineering
† Department of Industrial Electrical Technology

Faculty of Engineering, King Mongkut's University of Technology North Bangkok, Bangkok, Thailand

(noppadolc@kmitnb.ac.th , teratam@kmitnb.ac.th, ycps@kmitnb.ac.th)

Keywords: Generator protection, Current Differential Relay, Current Transformer, Stray Flux

Abstract

A current differential protection protects the winding of a generator. The relay must not operate on the occurrence of external fault. There is a power plant in Thailand where the generators were tripped by external fault. The tripping of generator results in severe stability problem. The case study shows single line to ground external fault on a transmission line. The fault current wave shapes were distorted from sinusoidal. This causes generator current differential relay mis-operate. The paper presents the investigation of external faults tripping of the differential relay. By looking into the current signal, the investigation shows that CT saturation might not be the cause of the distortion. The study also simulates a simple magnetic field model using finite element software to investigate the possibility of stray flux interference between CTs.

1 Introduction

In a power system, generator is a very importance unit. It must be run reliably. The high capacity generator has to be protected by several protection relays [1,4,7,9,10]. If an abnormal event occurs in the generator, the generator has to be separated from the power system before it causes more damage. On the other hand, if there is nothing wrong with the generator, it must run without any interruption.

In the middle of Thailand, a power plant was constructed in the surrounding of rice fields. In the summer, farmers burn their fields to prepare the paddy fields. The burning smoke under the transmission line leads to the breakdown of the air from the transmission line to the ground. Most of the fault occurs on phase C. This is because the phase C was installed at the lowest height. The fault should have tripped only the transmission line but the generator was also tripped by the current differential relay. Unnecessary tripping causes several problems, for example power system instability.

1.1 Current differential relay

The current differential relay is used to protect generators which its capacity is higher than 5 MVA [6]. The protection *principle based on Kirchhoff's Current Law. The internal fault can be detected by monitoring of current that flow in and* out from the stator winding [1,4,7,9,10], as shown in Fig. 1. If the current I_{out} is not equal to I_{in}, there must be a leakage of the current in the stator winding. This is called internal fault. Then the protection relay sends trip signal to isolate the generator from the power system.

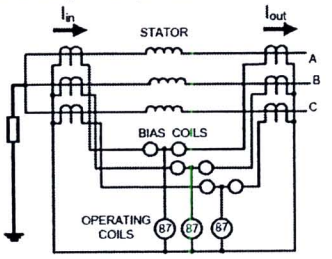

Fig. 1 Current differential protection

As mentioned above, differential current relay works by detect the difference between incoming and outgoing current. There fore, the error of current measurement may affect the operation of the relay. Especially during high current through fault, the error of measurement system is high. To reduce the effects of measurement error and CT saturation, the biased differential relays have been introduced. Their characteristics are shown as in Fig.2.

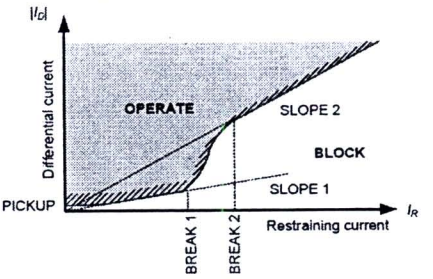

Fig. 2 characteristic of biased differential relay

PICKUP value in Fig. 2 defines the minimum differential current required for tripping operation.

SLOPE1 defines the ratio of differential to restraint current. If the operating point is at above the line, relay will operate. This slope is used to stabilize the relay due to the CT transformation error of a load current. The transformation error is proportional to the input current of CT. The higher the load current leads the higher the CT error. [1,4,7,9,10] The higher the SLOPE1 the relay gains more tolerance to the CT transformation error. [1,4,7,9,10]

SLOPE2 is applicable for restraint currents above the BREAK POINT2. This slope is set to ensure stability under heavy external fault conditions that could lead to high differential currents as a result of CT saturation. [1,4,7,9,10]

BREAK POINT1 defines the end of the Slope1 region. It should be set just above the maximum normal operating current level of the generator. [7]

BREAK POINT2 is setting that defines the start of the Slope 2 region. It should be set to the level at which any of the protection CTs are expected to begin saturation. [7]

Previously the biased differential relay in the case study was set as follow

PICKUP = 0.25 A SLOPE1= 7%

BREAK POINT1 – 5 A SLOPE2– 20%

BREAK POINT2= 15 A

2 Generator current during the external fault at phase C

In the case study, most of transmission line faults occurred on phase C. These faults were on the external zone of the generator protection. But the generator protection relay alerted that the cause of tripping came from phase B of the generator. Fig.3 shows the recorded data from the digital relay. The effects of the fault current to the generator have been investigated.

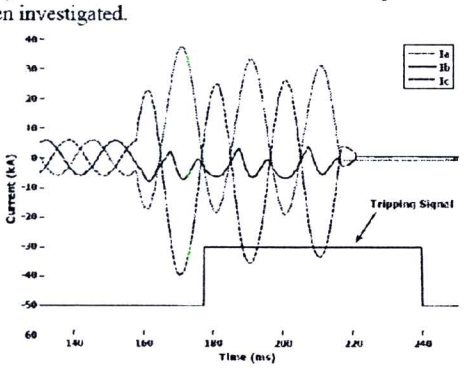

Fig. 3 Recorded current signal

2.1 The generator configuration and the model

Fig. 4 shows the model used for the simulation. The generator is connected with the delta side of delta/wye step up transformer. At the wye side of transformer, the sending end of 230 kV transmission line is connected. The 200 MVA load is supplied at the receiving end of transmission line. The phase C single line to ground fault is applied at the 500 m of transmission line.

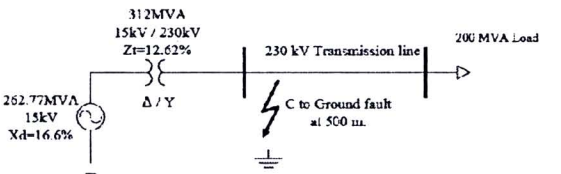

Fig. 4 Simulation Model

The fault current acquired form the simulation is shown in Fig. 5. The fault current appears only on phase C of the transmission line.

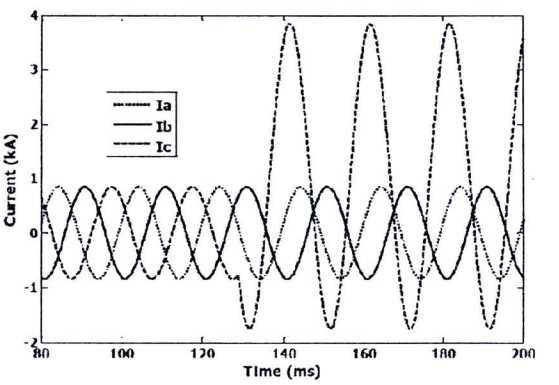

Fig. 5 The simulated fault current (C to ground fault)

The fault current in phase C causes the high current at the other side of the transformer (delta side) as shown in Fig. 6

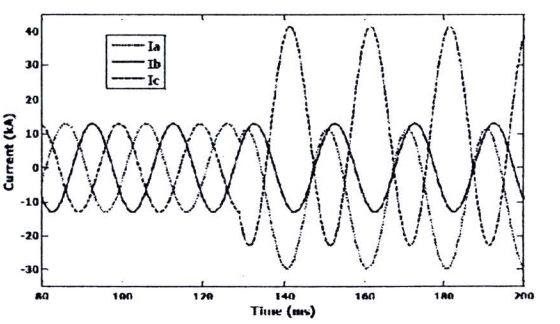

Fig. 6 Generator's current during fault

At the delta side of transformer, the current signals of phase A and C are higher than of phase B. This is because phase C

fault current at high voltage side (wye side) is transformed to phase A and C currents at the delta side. The fault has no effect to phase B current, as shown in Fig.7. Where $I_{a(Y)}$, $I_{b(Y)}$ and $I_{c(Y)}$ are currents at wye side in each phase. $I_{a(\Delta)}$, $I_{b(\Delta)}$ and $I_{c(\Delta)}$ are line currents at the delta side and n is the turn ratio of the transformer. It is importance to note that $I_{a(\Delta)}$ and $I_{c(\Delta)}$ are nearly in the opposite direction.

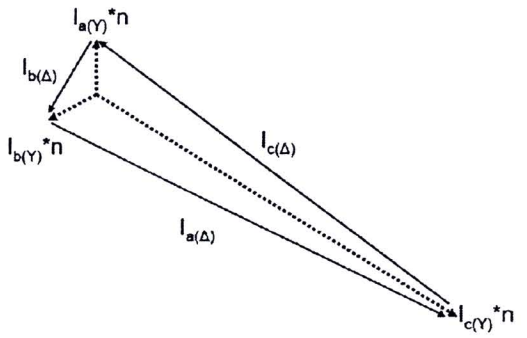

Fig. 7 Phasor of generator's currents during the fault

3 Distortion of the current signal

On the occurrence of external faults, the current differential relay has incorrectly tripped the generator. The relay setting was modified for getting more stability. The increasing of the SLOPE1 and SLOPE2 gains the relay achieves more immunity to the CT error. The setting of relay is shown as below

PICKUP = 0.5 A SLOPE1= 15%,

BREAK POINT1 = 5 A SLOPE2= 25%

BREAK POINT2= 15 A

Although, there have been several attempts to change the setting of the differential relay, the unwanted tripping of the generator still occurred. To find the root of the problem, the power plant engineers have started recording the current waveforms of the secondary side of the CTs. The current signals from the terminal ends and neutral ends of the generator were compared. There are significantly different in the current waveforms of phase B as illustrated in Fig. 8. It is obvious that the current at the terminal ends are heavily distorted during the fault. In the case of the external fault, this contradicts with the fact that the current of both ends must be the same. Then the differential current from the terminal ends and neutral ends should be zero.

3.1 Investigation into incorrect tripping

The investigation was started by recording the signal during the fault. There are twelve events of incorrect tripping which were recorded. One of them is shown in Fig. 8.

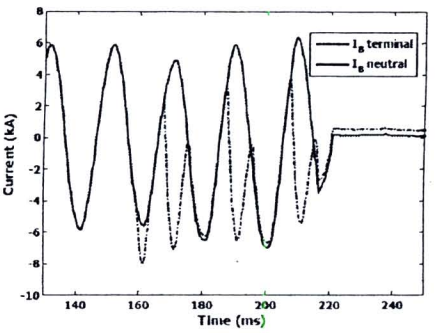

Fig. 8 Comparison of output currents of CT at the terminal and neutral sides of the generator

The recorded signals were then mapped into the setting of the biased differential current characteristic. The result shown in Fig. 9 indicates that the stabilized setting can not solve the problem. This is because the high differential current of phase B appears in the low restraining current region. Even we increased SLOPE1 or SLOPE2, it still can not block the trip.

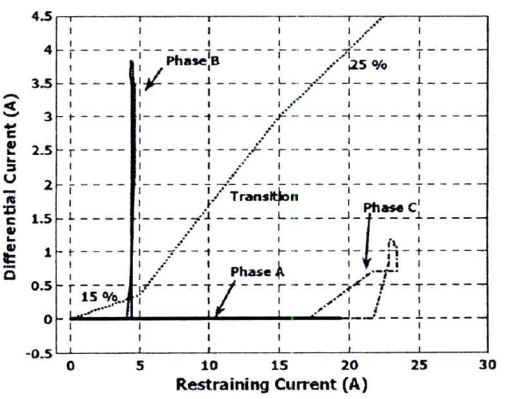

Fig. 9 Differential and restrain current mapped into the biased characteristic

The dot line represents the biased differential relay setting. The locus of phase A lies on zero differential current. This is because there is no distortion in phase A. The difference is always zero. In phase C, the graph is also lies on the zero line. And at about 20 A of restraining current, there is some different current. Although there is differential current, it is not enough to trip the circuit breaker. The differential current of B phase appears at the low restraining region. The locus is exceeds the operating region. This leads to the tripping of the generator.

3.2 Analysis of recorded signal

As mentioned above, the generator was tripped by the external faults. The relay alerted that the faults occurred at phase B, even though the fault currents did not affect phase B currents. The signals recorded by the relay were analysed in this section. Fig. 10 shows the RMS value of the differential current between the terminal side and the neutral side of the generator during the fault. The differential current of phase B is the highest and there is no differential current in the phase A. On the other hand, the restrain current of phase B is the lowest comparing with other phases as shown in Fig. 11.

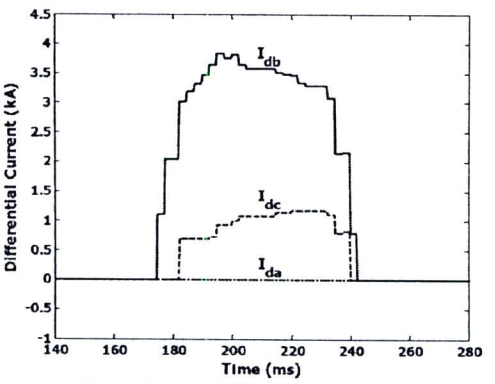

Fig. 10 Differential current in each phase

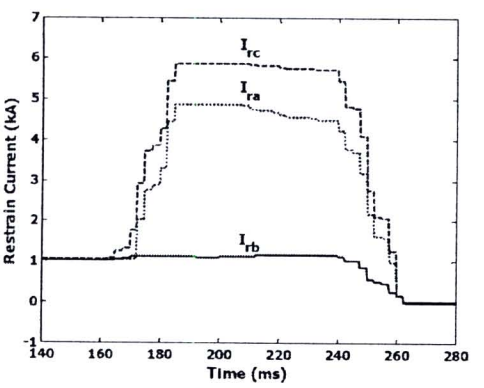

Fig. 11 Restrain current in each phase

The biased parameter (SLOPE1) of the relay is set at 15 percent and the pickup current is 0.5 A. So the tripping decision can be calculated by equation (1) and (2). Where I_{diff} and I_{rest} are differential and restrain current respectively.

$$\text{Operating Current} = (I_{diff} - I_{rest} * 0.15) - 0.5 \quad (1)$$

$$\text{Tripping Decision} = 1 = \text{Trip, if Operating Current} > 0 \quad (2)$$

The result is shown in Fig. 12. At about 177 ms, the operating current of B phase is positive. Then the trip signal is activated.

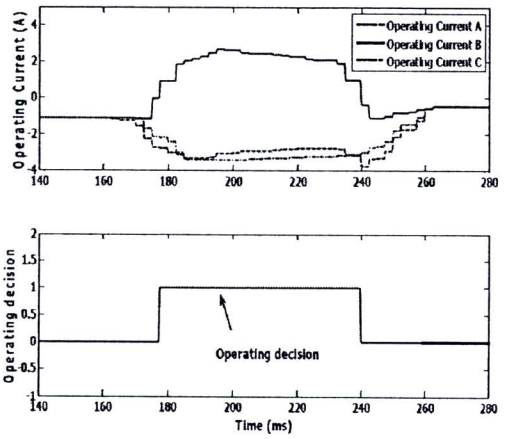

Fig. 12 Tripping decision of biased differential relay

3.3 Why CT saturation is not the cause of signal distortion

At the beginning of the study, saturation of current transformer is suspected. After the current signals were analysed, there are some other reasons that against the assumption.

The first reason, the RMS value of saturated CT signal is never greater than the healthy one. The recorded signal of fault current, the instantaneous and RMS value of the distorted signal are greater than the healthy one, as shown in Fig. 13 and Fig. 14 respectively. Therefore it is not CT saturation.

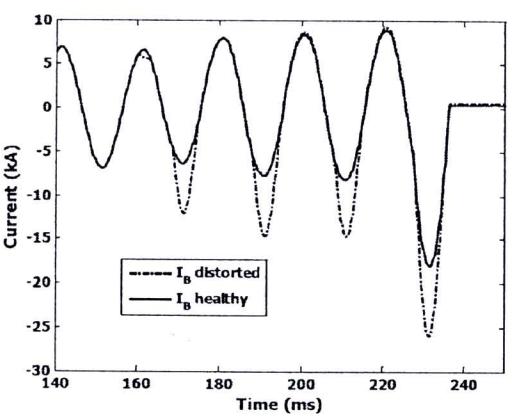

Fig. 13 Recorded current signals

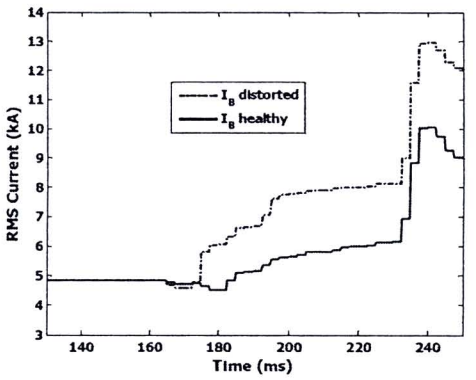

Fig. 14 RMS Value Recorded current signal

The second reason, the fault at transmission line on phase C causes the high current and DC offset only in phase A and C of the generator, there is no effect on phase B. If any saturation could happen, it could have been on phase A and C. The CT of phase B which has lower current then lower magnetic flux should not be saturated as shown in Fig. 15.

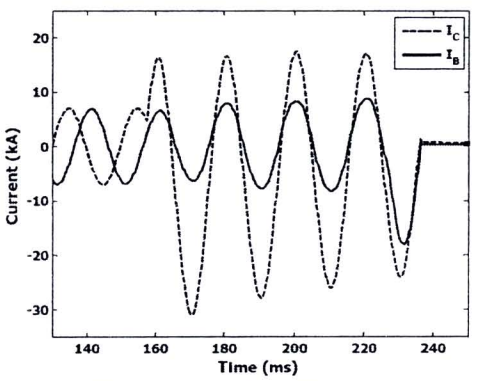

Fig. 15 Comparison of C and B phase current

The third reason, the CTs are 15,000/5 A, C800 class. This means that measurement of 20 times of rated current (300 kA), 8 ohm burden, the error is less than 10 percent [5, 8]. The current less than 10 kA without DC offset and low impedance burden should not cause saturation.

4. Suspected stray flux interference

At the generator terminals, CTs were installed for the protection purpose. During the external fault, the current obtained from CT at the terminal side was distorted. Fig.16 shows that CT of each phase was located very close to each other. The position of phase B's CT is in the middle between phase A and phase C.

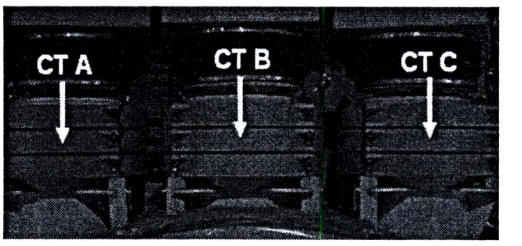

Fig. 16 CT of generator at line side

The fault is C phase to ground fault type. Fig.6 shows that the generator currents at phase A and C are very high. And phasor of phase A current is nearly in the opposite direction to phase C. This situation leads to very strong flux density at the CT of phase B because the magnetic flux which produced by phase A and C are in phase at the location of phase B, as shown in Fig.17.

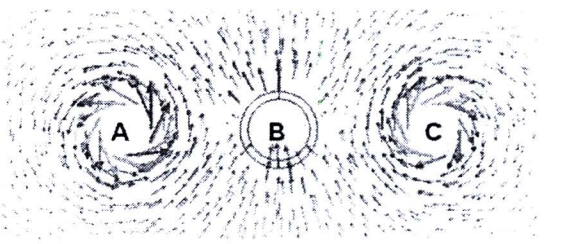

Fig. 17 magnetic flux plot of CTs

To find the relationship of the current in phase A and C to the error of phase B, I_a-I_c signal is compared with the differential current as shown in Fig.18. It shows that there is similarity between them. The error occurs only at the peak point of I_a-I_c signal.

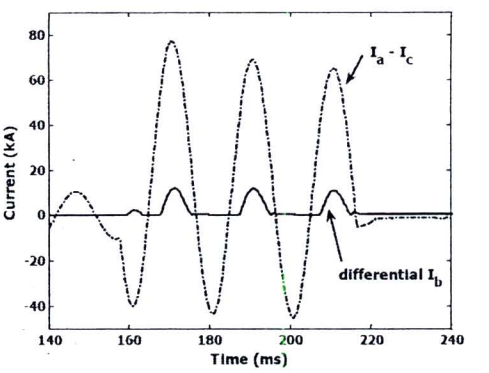

Fig. 18 Comparison between signal I_a- I_c and error I_b

To study more details about the magnetic field, a finite element simulation would be a proper tool [2,3]. The

simplified CTs and conductors were modeled. The fault currents were injected to each conductor. The acquired flux density is shown in Fig. 19. It indicates that the magnetic flux can pass through the magnetic shield of the CT. This interferes in the measurement of phase B current. This should be the reason of the distortion of the phase B current signal.

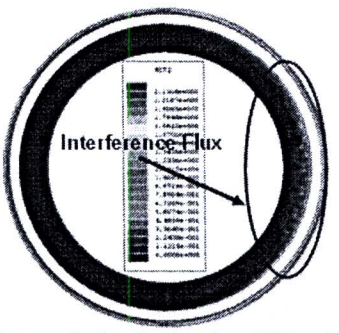

Fig. 19 magnetic flux density plot of CTs at B phase

5. Conclusion

The investigation shows that the burning smoke leads to the fault on the transmission line. And these through faults affect the biased differential relay causing unnecessary tripping of the generator. The analysis of the recorded signals indicates that the CT saturation is not the cause.

During the fault, the currents at phase A and C were very high and their phasors were nearly in the opposite direction. The magnetic field simulation indicates that these two currents generate the magnetic flux that might interfere phase B CT. This results in the differential current in phase B, then the generator is tripped.

The further work must study on magnetic flux model. Then the experiment can be set up to shield the flux between each CT. This is to ensure the correct assumption about the flux interference. The incorrect tripping can then be prevented from the external fault.

6. References

[1] Gerhard Ziegler, "Numerical Differential Protection, Principle and Applications", Siemens ,Publicis Corporate Publishing

[2] J.A. Guemes, M. Postigo, A. Ibero. "Influence of leader shields in the electric field distribution in current transformers", 10th Mediterranean Electrotechnical Conference. pp.958-961

[3] M. V. Mathis, C. S. Burns, V. M. Khalin. "In-service testing of generator current transformer – A new predictive maintenance tool for electric generation station"

[4] P.M. Anderson, "Power System Protection", McGraw-Hill

[5] Y. C. Kang, U. J. Lim, S. H. Kang, P. A. Cossley. "Compensation of the Distortion in the Secondary Current Caused by Saturation and Remanence in a CT" , IEEE TRANSACTIONS ON POWER DELIVERY, VOL. 19, NO. 4, OCTOBER 2004, pp. 1642-1649

[6] "Application Notes on Generator Protection Schemes", Siemens AG, 6/11/2002

[7] "G60 Generator Management Relay UR Series Instruction Manual", GE Multilin, 2004

[8] "IEEE standard Requirements for Instrument Transformers", IEEE Std. C57.13-1993 (R2003)

[9] "Multifunctional Machine Protection 7UM62 V4.6 Manual", Siemens AG, 2005

[10] "Numerical generator protection REG316*4", ABB Switzerland Ltd

6. Mechanical Defect Detection of SF6 High Voltage Circuit Breaker Using Wavelet Based Vibration Signal Analysis

International Conference on Electrical Engineering/Electronics, Computer, Telecommunications and Information Technology, ECTI-CON 2008, 14-17 May 2008, Thailand

Mechanical Defect Detection of SF6 High Voltage Circuit Breaker Using Wavelet Based Vibration Signal Analysis

N. Charbkeaw[1], T. Suwanasri[2], T. Bunyagul[1]
[1] Electrical Engineering Department, Faculty of Engineering
[2] The Sirindhorn International Thai-German Graduate School of Engineering
King Mongkut's University of Technology North Bangkok, Bangkok, 10800, Thailand

***Abstract*-High voltage circuit breaker is a device that requires frequent maintenance. This leads to high cost and time consuming. If the internal component of circuit breaker can be inspected without any disassembly. The period of the maintenance can be extended. This paper proposes the method of indirect internal component inspection.**

The experiment was applied with 110kV SF_6 puffer-type circuit breaker with hydraulic operating mechanism. The defect circuit breakers were tested. Then the vibration signals were recorded. The analyzing of vibration signal in time domain is difficult for the detection of small defect. Using wavelet transform, the detection of small defect can be performed. This detection reduces the risk of the failure in operation of circuit breaker.

I. INTRODUCTION

High voltage circuit breaker (CB) is a switching device that is generally used in substation. In the normal situation, CBs are used for circuit switching purpose. In the abnormal situation, when fault or emergency event occurs. CB is a protection device that separates the fault part from the power system. The fail operation of circuit breaker leads to sever damage of power system device. CB must operate with high reliability. Therefore circuit break needs frequent maintenance. Every 6 to 12 months, CBs have to be inspected even though the fault never happen [1]. This leads to high cost. Especially the internal inspection, CB must be disassembled so it consumes long time for maintenance. The frequency of internal inspection depends on experience and statistic. For the lower than 230kV CB, internal inspection has to be applied after 10 times fault interruptions or less [1]. And the time between each internal inspection must be never longer than 4 years [1]. It is possible that the fail operation occurs before the detection of defect element.

The research attempts to find the method to detect the internal defect part without disassembling the CB before the occurrence of fail operation. There are several signals that can be monitored such as operating coil current, contact timing, vibration of CB, etc.[2,3,4,5,6]

In this paper, the information extraction from vibration signal is focused. Vibration signal monitoring can refer to the movement of moving parts inside circuit breaker. The use of vibration signal can be compared with the heart beating sound. Doctor can analyze the body health by the rhythm of beating. Similarly, circuit breaker condition assessment, the circuit breaker conditions can be acquired from vibration signal. Fig. 1 shows example signals of circuit breaker during opening and closing operations.

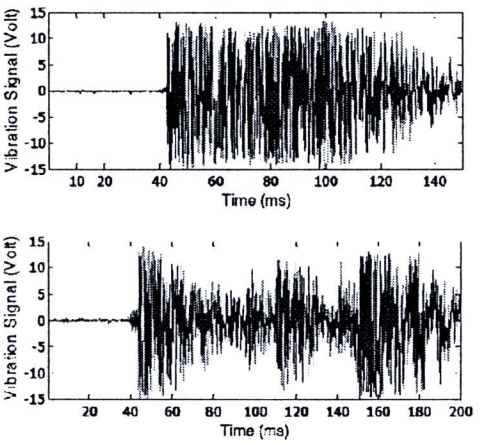

Figure 1. Opening (upper) and closing (lower) vibration signals.

Several sources of acoustic vibration are detected during the closing or opening operation such as the instant of solenoid coin movement, the impact of arcing and main contacts. Each source of vibration will generate different vibration signature.

II. THE EXPERIMENTAL SETUP

The experiment was performed with a 110kV SF_6 puffer-type circuit breaker with hydraulic operating mechanism as shown in Fig. 2 for the experimental setup. The investigation was performed under no-load switching operations. The vibration signals of the free-standing poles and of operating mechanism were recorded under normal operating conditions The operating environments were kept constantly at the normal condition such as the rated 110 VDC control voltage supplying from station service power source or battery from the secondary circuit, 6.5 bar SF_6 pressure and 320 bar hydraulic oil pressure.

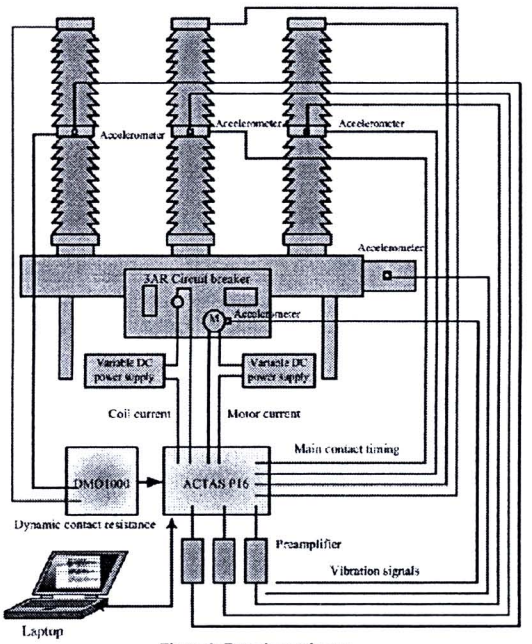

Figure 2. Experimental setup

During each no-load switching operation, other parameters such as close and trip coil current, hydraulic pumping motor current and time, main contact timing, dynamic contact resistance, were also measured as shown in Fig. 2. The measured vibration signatures under normal operating condition were used as a reference base line. The tests and measurements were performed in a laboratory because of the readily controlled testing conditions.

The artificial defects such as bush defect, damaged fix contact of pole B, cut rod and removed rod as shown in Fig. 3 were incorporated. Then, various measured parameters were evaluated and compared with those before defects. The arrangement of defective severity and the number of switching per test (both close and open operations) are also listed in Table I.

TABLE I
SUMMARY OF SIMULATED DEFECTS

Simulated defects	Severity of defect	No. of switching Per test
No defect (reference)	-	20
Remove bush of the rod	low	5
Fix contact damage	high	5
Cut connecting rod	very high	5
Remove connecting rod	extremely high	5

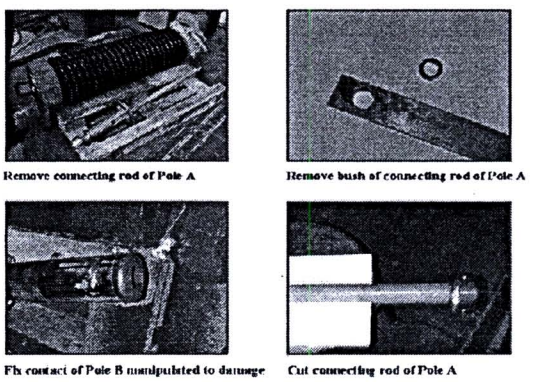

Figure 3: Incorporated artificial defects

The vibration signals during closing and opening operations were recorded by using accelerometers and a data acquisition system. The vibration measurement consists of the following components:

1. Sensors: The piezoelectric accelerometer is used to measure the vibration signal propagating to the external structure via various parts of the internal mechanism and insulating medium. They were temporarily mounted with adhesive glue on circuit breaker enclosure surface. It produces a charge in proportional to the acceleration.
2. Preamplifier and signal conditioner: These devices are needed in order to match the impedance and amplify the signal from accelerometer to reasonable value.
3. Data acquisition: The sampling rate was set at 10kHz. The total record time was set at 200ms for closing operation and 150ms for opening operation.

III. VIBRATION SIGNAL ANALYSIS

A. Time Domain Analysis

After the vibration signals of all cases were acquired. They were analyzed in time domain. The comparison of vibration signal is shown in Fig.4.

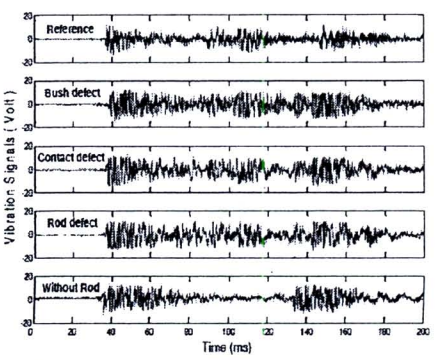

Figure 4: Comparison of vibration signal in time domain

Fig.4 shows that the difference between reference signal and the extremely high severity of defect is clearly seen. At about 100 ms of without rod, the vibration signal is very low. This is because the fix and the moving contact did not hit together at that time. But for the other signal, they are not clearly different.

The aim of research, the detectable of defect at low severity level by time domain analysis still can not achieve. The wavelet transform which gives the transformed information in both time and frequency is applied.

B. Wavelet (Time-Frequency) Domain Analysis

Wavelet Transform (WT) is a mathematical tool that transforms the signal in time domain to time-frequency domain. Its concept is similar to Short Time Fourier Transform (STFT). The STFT decomposes the original signal to a set of 'sinusoidal signals' with different frequencies. The coefficients of STFT are proportional to the correlation coefficients of the original signal with the unit complex sinusoidal in each frequency.

WT decomposes the original signal to a set of wave like signals, called 'wavelet'. These wavelet signals are the scaled (dilated) and shifted forms of the mother wavelet, as shown in Fig. 5.

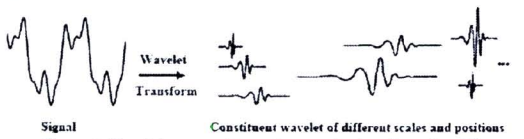

Figure 5. Signal decomposition using wavelet transformation [2]

The WT coefficient can be calculated by using the following expression.

$$C(a,b) = \int_{-\infty}^{\infty} f(t)\frac{1}{\sqrt{a}}\psi(\frac{t-b}{a})\,dt \qquad (1)$$

Where, ψ is the wavelet function and its shape varied by variables **a** (dilation) and **b** (position). Fig. 6 shows the example of the mother wavelet, dilated wavelet (a = 2) and position shifted wavelet (b = 10). The observation can be made that the smaller the dilation means the higher the frequency. The greater the position shifted means the longer the delay.

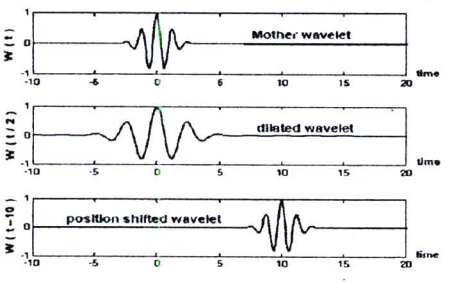

Figure 6. Mother wavelet, dilated wavelet *(a=2) and position shifted wavelet (b= 10)*

The great advantage of WT is the ability to decompose the selected frequency component at any time. Therefore it is suitable to analyze instant transient signals. Even a barely visible small discontinuity can still be detected [7].

The event extraction of time domain vibration signal as in Fig. 6 is not easy to perform by human eye, especially opening vibration signal. The Wavelet transform is applied to enhance the event detection. Wavelet transform is a mathematical tool that transforms a signal in time domain to time-frequency domain. For this resource, the complex morlet with 1 bandwidth parameter and 1.5 wavelet center frequencies is selected. Fig. 7 shows the comparison between opening vibration signal and its transformed signal.

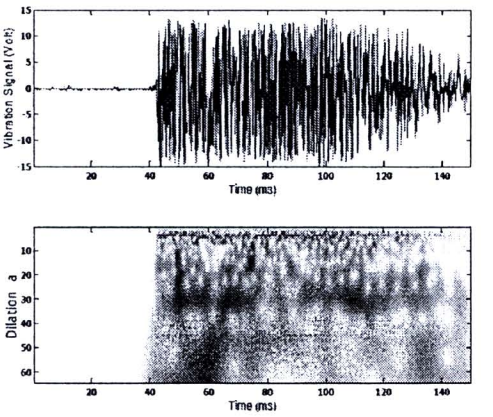

Figure 7. Time domain opening vibration signal (upper) and its wavelet transformed spectrogram (lower)

C. The Result of Reference Signal Transformation

Fig. 8 shows the result of closing operation. There are three bright zones, at about 45, 120 and 150 ms. The bright zones are in lump shape.

Fig. 9 shows the transformed signal of bush defect closing operation. Comparing with the reference, there are clear differences in signatures. Such as the defect has a lot of small red dot. And every bush defect signal has a big red dot at about 45 ms and dilation is about 20.

The reference opening is illustrated in Fig. 10. At dilation of 30, there is lined with bright area. And this bright area is in the lump shape. This differs from Fig. 11, the transform of bush defect vibration signal that the bush defect has many small dots at dilation is 10-20.

By use of these differences, the low severity defect, bush defect, can be detected. Every defect type such as damage contact, defect rod has its own signature.

Not only the mechanical defect can be detected, the environment condition, hydraulic pressure, battery voltage also can be monitored by use this method.[8]

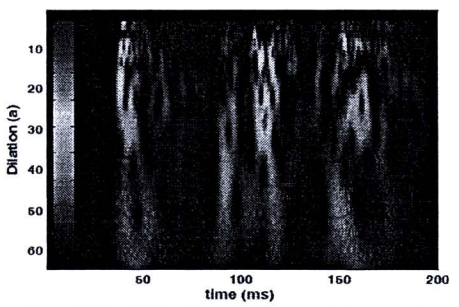

Figure 8. Wavelet transform of reference closing operation

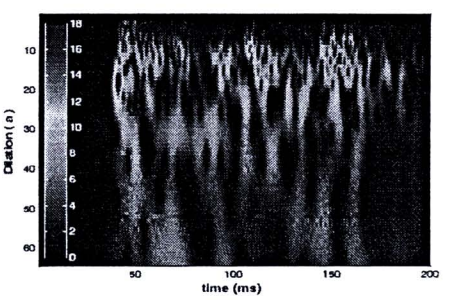

Figure 9. Wavelet transform of bush defect closing operation

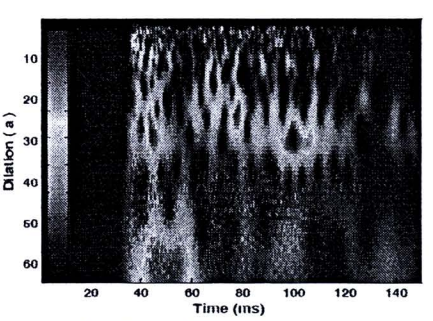

Figure 10. Wavelet transform of reference opening operation

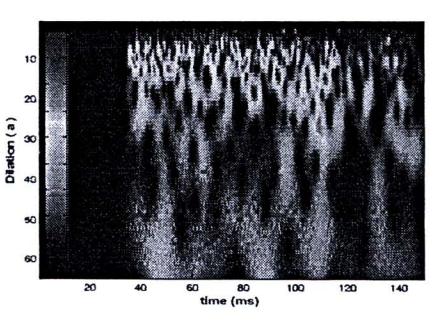

Figure 11. Wavelet transform of bush defect opening operation

IV. Conclusion

The frequency of circuit breaker maintenance can be optimized if the internal part of CB can be inspected without any disassembly. The vibration signals during opening and closing operation were used. In the time domain, there is difficulty to distinguish between the healthy signal and the low severity signal. This experiment shows that the healthy and each defect type can be classified by using the wavelet transform.

If the non-severe defect is detected, the CB needs to be repaired in order to prevent the fail operation. So the frequent in maintenance can be subsequently minimized.

Acknowledgment

The author would like to thank King Mongkut's University of Technology North Bangkok (KMUTNB) for the financial support and thank to SIEMENS AG in Erlangen, Germany and Institute for High Voltage Technology, RWTH Aachen University, Germany for the cooperation.

References

[1] Hydroelectric Research and Technical Service Group "Facilities Instructions, Standards and Technique 3-16T 3-16, Maintenance of Power Circuit Breaker", , US Department of the interior Bureau of Reclamation, d Colorado,1999

[2] Y. Ohshita, A. Hashimoto, Y. Kurosawa, "A diagnostic technique to detect abnormal conditions of contacts measuring vibrations in metal enclosures of gas insulated switchgear", *IEEE transaction on power delivery*, vol. 4, pp. 2090-2094, October 1989.

[3] C. A. Fawdrey, "The application of development and diagnostic techniques to circuit breaker reliability", *Cigre' Session Paper* Ref. 13-02, published: 1978.

[4] M. Runde, T. Aurud, L. E. Lundgaard, G. E. Ottessen, K. Faugstad, "Acoustic diagnosis of high voltage circuit breakers", *IEEE transaction on power delivery*, vol 7, no.3, pp 1306-1315, July 1992.

[5] M. Runde, G. E. Ottesen, B. Skyberg, M. Ohlen, "Vibration analysis for diagnostic testing of circuit breakers", *IEEE transaction on power delivery*, vol 11, no.4, pp 1816-1823, October 1996.

[6] T. Suwanasri, A. Schnettler, D. Fricke, A. Noack, "Non-invasive condition monitoring of a high voltage circuit breaker", *XIIIth International Symposium on High Voltage Engineering*, Netherlands, 2003

[7] M. Misiti, Y. Misiti, G. Oppenheim, J. Poggi, "Wavelet Toolbox for Use with MATLAB user guide", *MathWorks, Inc., 1996*

[8] T. Suwanasri, N. Charbkaew, T. Bunyagul, "Vibration Signal Analysis for Condition Monitoring of High Voltage Circuit Breakers", ECTI2007, Chaingrai, Thailand, May 2007

[9] T. Suwanasri, "Investigation on No-load Mechanical Endurance and Electrical Degradation of a Circuit Breaker Model under Short Circuit Current Interruption",Doctoral Thesis, RWTH Aachen , Germany, Feb 2006

ประวัติผู้วิจัย

ชื่อ : นายนพดล ฉาบแก้ว

ชื่อวิทยานิพนธ์ : อัลกอริธึมของการป้องกันแบบผลต่างเพื่อเสริมความทนทานต่อการผิดเพี้ยนของสัญญาณกระแส

สาขาวิชา : วิศวกรรมไฟฟ้า

ประวัติ

นายนพดล ฉาบแก้ว สำเร็จการศึกษาวิศวกรรมศาสตรบัณฑิต (วิศวกรรมไฟฟ้า) จากคณะวิศวกรรมศาสตร์ สถาบันเทคโนโลยีพระจอมเกล้าพระนครเหนือเมื่อปี พ.ศ. 2544 หลังจากนั้นได้ศึกษาต่อในระดับปริญญาโทในหลักสูตร Master of Engineering in Elektro-und Informations-technik ที่ Rosenheim University of Applied Sciences สหพันธ์สาธารณรัฐเยอรมนี หลังจากที่สำเร็จการศึกษาในปี 2546 ได้รับการบรรจุเข้าเป็นอาจารย์ประจำภาควิชาวิศวกรรมไฟฟ้า คณะวิศวกรรมศาสตร์ สถาบันเทคโนโลยีพระจอมเกล้าพระนครเหนือ

นายนพดล ฉาบแก้วได้มีส่วนร่วมในโครงการวิจัยหลายโครงการซึ่งมีส่วนช่วยในการแก้ปัญหาและส่งเสริมประสิทธิภาพการปฏิบัติงานของภาคอุตสาหกรรมดังนี้

2548 นักวิจัยในโครงการ “วิจัยหุ่นยนต์สำรวจท่อร้อยสายไฟฟ้าใต้ดิน” (ทุนสนับสนุนจากการไฟฟ้านครหลวง)

2549 นักวิจัยในโครงการ “แนวทางการเพิ่มประสิทธิภาพการใช้พลังงานไฟฟ้าของเครื่องทำอากาศแห้ง” (ทุนสนับสนุนจากการไฟฟ้าฝ่ายผลิตแห่งประเทศไทย)

2552 นักวิจัยในโครงการ “การวิจัยเบื้องต้นเพื่อหาแนวทางการพัฒนาระบบเฝ้าตรวจภาระของหม้อแปลงจำหน่าย” (ได้รับทุนสนับสนุนจากการไฟฟ้านครหลวง)

2553 นักวิจัยในโครงการ “การวิจัยและพัฒนาชุดตรวจวัดและเปรียบเทียบความแตกต่างของเฟสเซอร์แรงดัน” (ทุนสนับสนุนจากการไฟฟ้าฝ่ายผลิต)